FLUID FLOW AND HEAT TRANSFER IN U-BENDS

By

MAHMOOD MOSHFEGHIAN

Bachelor of Science
Oklahoma State University
Stillwater, Oklahoma
1974

Master of Science
Oklahoma State University
Stillwater, Oklahoma
1975

Submitted to the Faculty of the Graduate College
of the Oklahoma State University
in partial fulfillment of the requirements
for the Degree of
DOCTOR OF PHILOSOPHY
May, 1978

FLUID FLOW AND HEAT TRANSFER IN U-BENDS

Thesis Approved:

Thesis Adviser

Dean of the Graduate College

PREFACE

The effect of 180^{o} bend on heat transfer to a single phase fluid in tube was studied. The test fluids were distilled water, Dowtherm G and ethylene glycol. A Reynolds number range from 55 to 31,000 was investigated for four 180^{o} bend with curvature ratios 4.84 to 25.62. Each test section was heated electrically by passing DC current through the tube wall.

I would like to extend my appreciation to my adviser, Dr. K. J. Bell, for his expert guidance and much valued counsel during the course of my study. I am also grateful to my Advisory Committee which consisted of Drs. J. H. Erbar, R. L. Robinson, Jr., and J. D. Parker, for their very helpful criticism and suggestions. I would like to thank Drs. M. N. Farukhi, S. P. N. Singh, and C. B. Panchal for providing me the computer program and their assistance.

I thank the School of Chemical Engineering of Oklahoma State University for providing me financial assistance during the course of my study. I also thank the Atomic Energy Organization of Iran for awarding me their scholarship for one year during the course of my doctoral program.

I am grateful to Mr. E. E. McCroskey, Storeroom Manager, and the graduate students of the School of Chemical Engineering for their assistance in the fabrication of some of the minor equipment needed

for the completion of the experimental phase of the research program. I also thank Mrs. D. Behrens and Mr. M. Neshan for their professional typing and drawing of this work.

On a more personal note, I thank all of my family, especially my father, Mr. A. A. Moshfeghian, for encouraging and providing me financial support throughout my education. I also thank my wife Sedigheh for her patience, support, and help during the course of this study.

TABLE OF CONTENTS

Chapter		Page
I.	INTRODUCTION.	1
II.	LITERATURE SURVEY	4
III.	EXPERIMENTAL EQUIPMENT.	10
	Description of Individual Units.	10
	Test Sections	10
	Fluid Bath.	13
	Pumps	13
	DC Power Source	14
	Heat Exchanger.	15
	Measuring Devices.	15
	Thermocouples	15
	Conax "Con-o-clad" Thermocouples.	16
	Insulated Wire Thermocouples.	16
	Manometer	20
	Rotameters.	21
	DC Ammeter and Voltmeter.	21
	Mercury-in-glass Thermometers	22
	Numatron.	22
	Auxiliary Equipment.	23
	Rotameter Calibration and Fluid Flow Rate Measurement Equipment	23
	Numatron Calibration Equipment.	24
IV.	EXPERIMENTAL PROCEDURE.	25
	Calibration Procedure.	25
	Thermocouple Calibration.	25
	Manometer Calibration	26
	Rotameter Calibration	26
	Numatron Calibration.	27
	Start-Up Procedure	27
	Data Gathering	28
V.	DATA REDUCTION.	31
	Calculation of the Error Percent in Heat Balance . . .	32
	Calculation of the Local Inside Wall Temperature and the Inside Wall Radial Heat Flux	33
	Calculation of the Local Heat Transfer Coefficient . .	34
	Calculation of the Relevant Dimensionless Numbers. . .	34

Chapter Page

VI. RESULTS AND DISCUSSION OF RESULTS 36

General Discussion 36
Peripheral Distribution of Heat Transfer Coefficients. 38
Curvature Ratio and Reynolds Number Effect. . . . 47
Negative Heat Transfer Coefficient. 51
Reynolds Number Effect on the Interaction Between Secondary and Tertiary Flows. 58
Comparison with Straight Tube Under Similar Flow Conditions 60
Testing of Literature Correlations. 67
Development of Correlation. 69

VII. CONCLUSIONS AND RECOMMENDATIONS 85

BIBLIOGRAPHY 88

APPENDIX A - EXPERIMENTAL DATA 90

APPENDIX B - CALIBRATION DATA. 107

APPENDIX C - PHYSICAL PROPERTIES 113

APPENDIX D - NUMERICAL SOLUTION OF WALL TEMPERATURE GRADIENT WITH INTERNAL HEAT GENERATION 118

APPENDIX E - SAMPLE CALCULATIONS 129

APPENDIX F - CALCULATED RESULTS. 144

APPENDIX G - ERROR ANALYSIS. 184

LIST OF TABLES

Table		Page
I.	Specification of the Four Test Sections	12
II.	The Value of X_i as Shown in Figure 3, m	18
III.	Rotameter Specifications	21
IV.	Peripheral Heat Transfer Coefficient at Station 5, BTU/HR-FT^2-^{o}F	57
V.	Test Results of Literature Correlations Fitted to Experimental Data for the Turbulent Flow Regime	68
VI.	Calibration Data for Rotameter 1 for Distilled Water	108
VII.	Calibration Data for Rotameter 2 for Distilled Water	109
VIII.	Calibration Data for Calibration of Outside Surface Thermocouples (Test Section B)	110
IX.	Calibration Data for Inlet and Outlet Thermocouples During In-situ Calibration of Surface Thermocouples on the Test Section B	111
X.	Calibration Data for Heat Loss from Test Section B	112
XI.	Calculated Wall Thickness in the Bend	129
XII.	Run 420 - Outside Surface Temperatures, ^{o}F	134
XIII.	Run 420 - Calculated Inside Surface Temperatures, ^{o}F	135
XIV.	Run 420 - Radial Heat Flux for Inside Surface, BTU/(HR-FT^2)	136
XV.	Peripheral Heat Transfer Coefficient at Station 11	137

LIST OF FIGURES

Figure		Page
1.	Sketch of the Secondary Flow Pattern in a Curved Tube	2
2.	Heat Transfer Loop.	11
3.	Location of Thermocouple Stations and Pressure Taps Along Test Sections	17
4.	Identification of Test Points in U-Bend Tests	19
5.	Peripheral Distribution of Heat Transfer Coefficients, Run 252	39
6.	Peripheral Distribution of Heat Transfer Coefficients, Run 252	40
7.	Peripheral Distribution of Heat Transfer Coefficients, Run 252	41
8.	Peripheral Distribution of Heat Transfer Coefficients, Run 515	44
9.	Peripheral Distribution of Heat Transfer Coefficient, Run 515	45
10.	Peripheral Distribution of Heat Transfer Coefficient, Run 515	46
11.	Effect of Curvature Ratio and Reynolds Number on Peripheral Distribution of Heat Transfer Coefficient at Station 3.	48
12.	Effect of Curvature Ratio and Reynolds Number on Peripheral Distribution of Heat Transfer Coefficient at Station 5.	49
13.	Effect of Curvature Ratio and Reynolds Number on Peripheral Distribution of Heat Transfer Coefficient at Station 7.	50
14.	Temperature Profile Between Two Parallel Planes	54

Figure Page

15. Peripheral Distribution of Inside Wall Heat Flux and Inside Wall Temperature at Station 5. 55

16. Peripheral Distribution of Inside Wall Heat Flux and Inside Wall Temperature at Station 5. 56

17. Effect of Reynolds Number on the Interaction Between Secondary and Tertiary Flows. 59

18. Comparison of Peripheral Average Heat Transfer with that Predicted by Sieder-Tate Equation. 63

19. Comparison of Peripheral Average Heat Transfer with that Predicted by Eagle-Ferguson Equation 64

20. Comparison of Experimental Heat Transfer Coefficient with that Predicted by Morcos-Bergles Equation. 65

21. Comparison Between Predicted and Experimental Heat Transfer Coefficients in a Straight Pipe Preceded by a 180^{o} Bend 72

22. Comparison Between Predicted and Experimental Heat Transfer Coefficients in a 180^{o} Bend. 73

23. Idealized Secondary and Tertiary Flow Patterns Downstream from the U-Bend. 75

24. Comparison Between Predicted and Experimental Heat Transfer Coefficients in a Straight Section Preceded by 180^{o} Bend 77

25. Flow Map for a Straight Pipe (Station 2). 80

26. Flow Map for a Straight Pipe Preceded by 180^{o} Bend (Station 7, $X^{*}/d_{i} = 0$) 81

27. Flow Map for a Straight Pipe Preceded by 180^{o} Bend (Station 8, $X^{*}/d_{i} = 7.7$) 82

28. Flow Map for a Straight Pipe Preceded by 180^{o} Bend (Station 9, $X^{*}/d_{i} = 15.5$). 83

29. Flow Map for a Straight Pipe Preceded by 180^{o} Bend (Station 10, $X^{*}/d_{i} = 23.3$) 84

30. Division of Tube Wall Thickness 120

31. Interior Element. 121

Figure Page

32. Cross-Section for Straight Tube 127

33. Cross-Section for Curved Tube 127

NOMENCLATURE

A - heat transfer area, ft^2 or m^2

A_c - cross-sectional area of the tube based on the tube inside diameter, ft^2 or m^2

AAPD - average absolute percent deviation

C_p - specific heat of the fluid, $Btu/lb_m\text{-}^oF$ or $J/kg\text{-}K$

D_c - U-bend diameter, inches or mm

De - Dean number, $Re\sqrt{d_i/D_c}$

d_i - inside diameter of the tube, inches or mm

D_c/d_i - curvature ratio

d_o - straight tube outside diameter, inches or mm

G - mass velocity of the fluid, $lb_m/hr\text{-}ft^2$ or $kg/hr\text{-}m^2$

g - gravitational acceleration, ft/hr^2 or m/hr^2

g_c - conversion factor, $lb_m\text{-}ft/lb_f\text{-}sec^2$

Gr - Grashof number, $g\, d_i^3\, \rho^2 \beta\, (\overline{T}_{w_i} - T_b)/\mu^2$

h_θ - local heat transfer coefficient, $Btu/hr\text{-}ft^2\text{-}^oF$ or $W/m^2\text{-}^oC$

$\overline{h}$ - peripheral average heat transfer coefficient, $Btu/hr\text{-}ft^2\text{-}^oF$ or $W/m^2\text{-}^oC$

H_1 - peripheral average heat transfer coefficient, defined by Equation (6-1), $W/m^2\text{-}^oC$ or $Btu/hr\text{-}ft^2\text{-}^oF$

H_2 - peripheral average heat transfer coefficient, defined by Equation (6-2), $Btu/hr\text{-}ft^2\text{-}^oF$ or $W/m^2\text{-}^oC$

I - current in the test section, amperes

J_H, J_X - heat transfer parameter, $Nu/Pr^{0.4}(\mu_b/\mu_w)^{0.14}$

k - thermal conductivity, Btu/hr-ft-^oF or W/m-^oC

l - length of the heated portion of the test section, inches or m

L - total length of test section, inches or m

Nu - Nusselt number, $\bar{h}\, d_i/k$

Pr - Prandtl number, $C_p\mu/k$

Q - heat flow rate, Btu/hr or W

$\dot{q}$ - heat flow rate, Btu/hr or W

$\dot{q}'' = Q/A$ - heat flux rate, Btu/hr-ft^2 or W/m^2

(r,θ,Z) - cylindrical coordinates with the origin at the center of the tube cross-section

r_i - inside radius of tube, inches or mm

Ra - Rayleigh number, GrPr

R_c - bend radius, measured to the tube axis, inches or mm

R_c/r_i - curvature ratio

Re - Reynolds number, $d_i\, G/\mu$

t - tube wall thickness, inches or mm

T_b - bulk fluid temperature, ^oF or ^oC

T_{w_i} - inside wall temperature, ^oF or ^oC

$\bar{T}_{w_i}$ - peripheral average inside wall temperature, ^oF or ^oC

V - fluid velocity, ft/sec or m/sec; voltage drop in test section, volts

W - mass flow rate of fluid, lb_m/hr or kg/hr

X_i - distance between thermocouple stations, inches or mm

X^* - distance measured from the exit of the bend (thermocouple station 7), inches or mm

X - distance measured from the inlet of the bend (thermocouple station 3), inches or mm

(X/d_i) - nondimensional distance from the inlet of the bend (thermocouple station 3)

Greek Letters

β - coefficient of volume expansion of the fluid, $1/^oF$ or $1/^oC$

μ - fluid viscosity, Ns/m^2 or $lb_m/hr\text{-}ft$

ρ - fluid density, kg/m^3 or lb_m/ft^3

θ,ϕ - angular position, degree or radian

Subscripts

avg - average

b - bulk fluid

c - calculated

cr - critical

DB - Dittus-Boelter

EF - Eagle-Ferguson

e - experimental

E - experimental

i - inside of tube, or index

in - test section inlet

MB - Morcos-Bergles

O - outside of tube

out	- test section outlet
s	- straight tube
ST	- Sieder-Tate
w	- wall
x	- local value

CHAPTER I

INTRODUCTION

U-tubes (two lengths of straight tube joined by 180^{o} bend at one end) are commonly used in large variety of tublar heat exchangers, e.g., a continuous length of tubing may be bent back and forth across a duct. U-tubes are also used in shell-and-tube heat exchangers having entry and exit headers at the same end.

When a fluid moves through a straight tube, the fluid velocity near the centerline is higher than that near the wall. The effect is especially pronounced in laminar flow but is true for turbulent flow, too. When the tube is coiled or bent 180^{o}, all fluid elements experience a centrifugal force radially outward which is proportional to the square of the element velocity and inversely proportional to the radius of the curvature. Therefore, the more rapidly moving elements near the centerline tend to move towards the outside, displacing the slower elements, which in turn move back toward the bend axis. The effect is to superimpose a "secondary" flow pattern upon the primary flow pattern (which is itself somewhat different from the flow pattern of the straight tube.) A highly idealized diagram of the secondary flow pattern is shown in Figure 1.

Due to the existence of the secondary flow, the heat transfer is higher in a curved tube than in an equivalent straight tube under

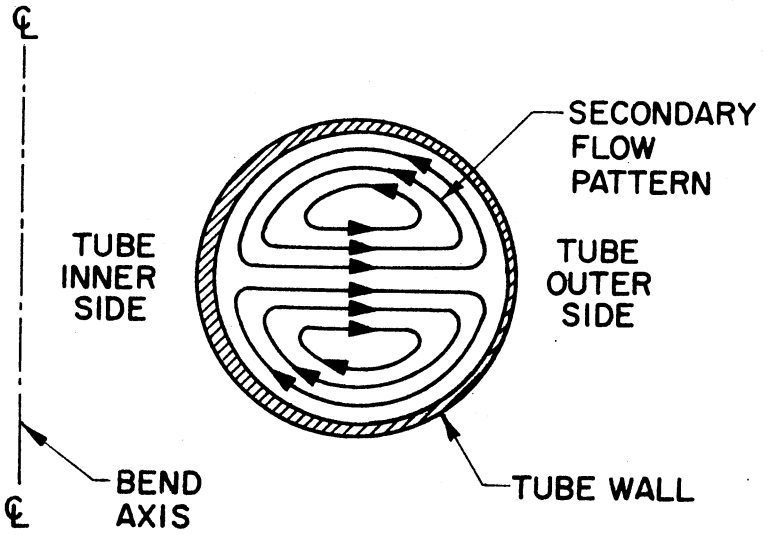

Figure 1. Sketch of the Secondary Flow Pattern in a Curved Tube

similar fluid flow conditions and the heat transfer mechanism is more complicated.

The present investigation was undertaken to study the effect of a 180^{o} bend on heat transfer to a single phase fluid in tubes and to obtain a better and more quantitative insight into the heat transfer process that occurs when a fluid flows in a U-bend tube.

Experiments were made with water, Dowtherm G®, and ethylene glycol flowing through an electrical-resistance-heated tube. The emphasis was to explore the effect of the secondary flow on heat transfer and the variation of local tube-to-fluid transfer coefficient in the U-bend and downstream from it. Using apparatus which allows the local temperature to be measured and local heat fluxes to be calculated, the author has obtained heat transfer coefficients around the periphery of tube which should be useful in understanding the mechanism of the flow. The study has covered Reynolds numbers from 55 to 31,000 and Prandtl number from 4 to 270. Four different bends have been studied. The bend radius (measured to the tube centerline) to tube inside radius ratios ranged from 25.62 to 4.84.

CHAPTER II

LITERATURE SURVEY

Despite the wide-spread application of U-bends in industry, there is only a limited number of investigations reported in the literature. This chapter presents the summary of these investigations.

Lis and Thelwell (1) investigated the turbulent heat transfer in a vertical pipe, with upwards flow, preceded by a 180^{o} bend. Based on their experimental findings on the entry effects of 180^{o} bends under uniform heat-flux boundary condition (electrical heating) with large wall-to-bulk water temperature difference, they reported the following conclusions:

1. The local heat transfer parameter, $J_X = NuPr^{-0.4}(\mu_b/\mu_w)^{-0.14}$, in the entrance region of the heated tube depends on the distance downstream from the bend, X^*/d_i, ratio of bend radius to tube radius, R_c/r_i, and the Reynolds number. The dependence of J_X on both X^*/d_i and R_c/r_i diminishes with increase of Reynolds number. For a given X^*/d_i and Reynolds number the parameter J_X increases as the ratio of bend to tube radii decreases.

2. The peripheral distribution of heat transfer coefficient, h_θ, at positions up to twelve diameters downstream of the bend is not uniform. The minimum value of h_θ occurs invariably on the inside of the tube with respect to the bend.

3. For the range of variables covered, the following correlation was obtained for the straight section downstream from the bend.

$$J_X = \frac{Nu}{Pr^{0.4}(\mu_b/\mu_w)^{0.14}} = 0.0239\ Re^{0.826}(X^*/d_i)^{-0.064}(R_c/r_i)^{-0.062} \qquad (2\text{-}1)$$

where X^* is the distance measured from the exit of the 180^o bend.

Equation (2-1) is valid for:

$$10{,}000 \leqslant Re \leqslant 94{,}000$$

$$5.5 \leqslant Pr \leqslant 9.7$$

$$2 \leqslant R_c/r_i \leqslant 15$$

$$1 \leqslant X^*/d_i \leqslant 15$$

Ede (2) studied the effect of a 180^o bend on heat transfer to water in a tube. Both the straight sections and the 180^o bend were positioned in a horizontal plane. Heat was generated in the wall of the tube by passing a direct current through the wall of the tube. He explored the nature of the variation in local heat transfer coefficient in and near a bend. Actually, due to nonuniform wall thickness and nonuniform heat generation in the bend, Ede did not measure the local heat transfer coefficient in the bend. He merely measured a number of temperature distributions in the bend.

Ede found the flow mechanism to be complex, except at high Reynolds numbers. He reported the disturbance due to a 180^o bend produces higher heat transfer coefficients than a straight tube not preceded by a 180^o bend. Ede concluded further that the velocity of the liquid near the outside of the bend becomes much higher than that near the inside, and a secondary circulation develops; these conditions may extend for a considerable distance downstream from the

bend. This secondary circulation gives rise to higher heat transfer coefficients than normal on the outside of the bend and lower on the inside, the average effect being an increase. With laminar flow the effects are accentuated and, in addition, if the temperature profile upstream of the bend is markedly nonuniform, very large coefficients can be obtained in and downstream of the bend. For Reynolds numbers in the neighborhood of 5000 to 10,000, Ede suggests the possibility that an incipient laminar flow may develop and tentatively advances this as an explanation of the production of unusually low heat heat transfer coefficients. This finding is in accordance with the Ito's (3) empirical correlation for determining the critical Reynolds number for fluid flow in curved pipes. In the range of $15 < R_c/r_i < 860$ Ito's correlation is given as follows:

$$Re_{critical} = 20{,}000\ (r_i/R_c)^{0.32} \qquad (2\text{-}2)$$

Ede's test ranges were as follows:

$$700 \lll Re \lll 42{,}000$$

$$4 \lll R_c/r_i \lll 22.$$

Tailby and Staddon (4) also investigated experimentally the influence of 90^o and 180^o pipe bends on heat transfer from an internally flowing gas stream, with the straight sections and the bend positioned in a horizontal plane. The test section was immersed in water which acted as a heat sink. Hot air was blown through the test section and Reynolds numbers in the range 10,000 to 50,000 were studied. Local heat transfer coefficients were computed from a knowledge of local heat flux values along the test section.

They reported the following conclusions:

1. In comparison with Ede's (2) findings: when a fluid is being heated, the heat transfer coefficient on the outside of the bend are greater than when the fluid is being cooled, with corresponding decrease in the coefficient on the inside of the bend.

2. For the ranges studied ($10{,}000 \leqslant Re \leqslant 50{,}000$, $4 \leqslant R_c/r_i \leqslant 14$), Reynolds number has no effect on the distribution of the peripheral mean coefficient during and after the bend.

3. With decreasing curvature ratio, R_c/r_i, the secondary flow effect increases.

4. The effect of the pipe bend is barely noticeable upstream of the bend, and in all cases the peripheral mean coefficients return to straight pipe values within 30 pipe diameters from the beginning of the bend.

5. For the ranges of variables covered, the following correlation was obtained for the straight section downstream of the 180^o bend.

$$\frac{Nu}{Pr^{0.4}} = 0.0341\ Re^{0.82}\ (R_c/r_i)^{-0.11}\ (X/d_i)^{-0.04} \qquad (2\text{-}3)$$

where X is the distance measured from the beginning of the 180^o bend.

Equation (2-3) is valid for:

$$10{,}000 \leqslant Re \leqslant 50{,}000$$

$$7 \leqslant X/d_i \leqslant 30$$

$$4 \leqslant R_c/r_i \leqslant 14.$$

For air, the turbulent heat transfer rate and wall temperature distribution in rectangular ducts (aspect ratio 10- aspect ratio is

defined as the ratio of the width to depth of the duct cross section) with a 180^{o} bend were studied experimentally by Yang and Liao (5). They also reported higher heat transfer coefficients at the outer wall than at the inner wall of the bend.

More recently, Moshfeghian (6) studied the effect of a 180^{o} bend on turbulent heat transfer in a pipe. The bend and the two straight sections were positioned in a vertical plane with fluid flowing horizontally in the straight sections. Moshfeghian reported the following conclusions:

1. The peripheral heat transfer is far from uniform in the bend, being much higher on the outside and somewhat lower on the inside of the bend, resulting in a higher mean heat transfer coefficient as compared to a straight tube under similar conditions.

2. At any cross section in the bend, the distribution of peripheral heat transfer coefficient is almost symmetrical about a plane containing the longitudinal axis of the tube and the radius of the bend.

3. Along the straight section downstream of the bend, the distribution of peripheral heat transfer coefficient is symmetrical about the plane of the bend. Also, the peripheral heat transfer coefficient is highest at the outside wall of the bend and lowest at the inside wall. The nonuniform heat transfer coefficient results in a higher mean heat transfer coefficient as compared to a straight section under similar conditions without the bend. The nonuniform behavior of the local heat transfer coefficient disappears as fluid flows further down the tube.

In addition to 180^{o} bends, coiled tubes have been studied intensively by many workers. Singh (7) gives a complete literature survey on helical coils. He also compared the literature heat transfer correlations to his own extensive data. On this basis, he found the best set of correlations over the entire range of flow rates is due to Schmidt (8). Furthermore, Singh proposed the following correlation for laminar flow heat transfer:

$$N_{hc} = \left\{0.224 + 1.369\ (d_i/D_c)\right\}\ \left\{Re^{[0.501\ +\ 0.318\ (d_i/D_c)]}\right\}$$
$$X\ \left\{1+4.8\ [1-e^{-0.00946\ (Gr/Re^2)(D_c/d_i)}]\right\}$$
$$X\ \left\{Pr^{1/3}\right\}\ \left\{(\mu_b/\mu_w)^{0.14}\right\} \qquad (2\text{-}4)$$

The physical properties of the fluid used in Equation (2-4) were evaluated at the bulk fluid temperature except μ_w which was evaluated at the average inside wall temperature at the thermocouple station.

Equation (2-4) is valid for:

$$6 \leqslant Re \leqslant Re_{cr}$$
$$1 \leqslant De \leqslant 1.7 \times 10^3$$
$$2.3 < Pr < 250$$
$$241 < Gr < 9.22 \times 10^5.$$

CHAPTER III

EXPERIMENTAL EQUIPMENT

Liquid phase heat transfer was studied in four 180° bend tubes using distilled water, Dowtherm G® and ehtylene glycol. A sketch of the experimental set-up is shown in Figure 2. Since the experimental set-up and equipment used was essentially the same as that used by Farukhi (9) and Singh (7), some parts of this chapter and the following chapters are taken from their Ph.D. theses (7) (9).

Description of Individual Units

Test Sections

Four test sections with different bend radii were used. Two of the test sections were fabricated from initially-straight Inconel 600 tubing 22.22 mm (7/8 inch) o.d. x 1.32 mm (0.052 inch) wall thickness. The other two test sections were fabricated from initially-straight Type 304 seamless stainless steel tubing 19.05 mm (3/4 inch) o.d. x 1.65 mm (0.065 inch) wall thickness. Dimensions of the four test sections are summarized in Table I.

The test sections were thermally insulated by wrapping them with several layers of bonded fiberglass tape and two inches (5.1 cm) of fiberglass sheets. The outside surface of insulation was then wrapped with aluminum foil so the radiation losses would be minimized.

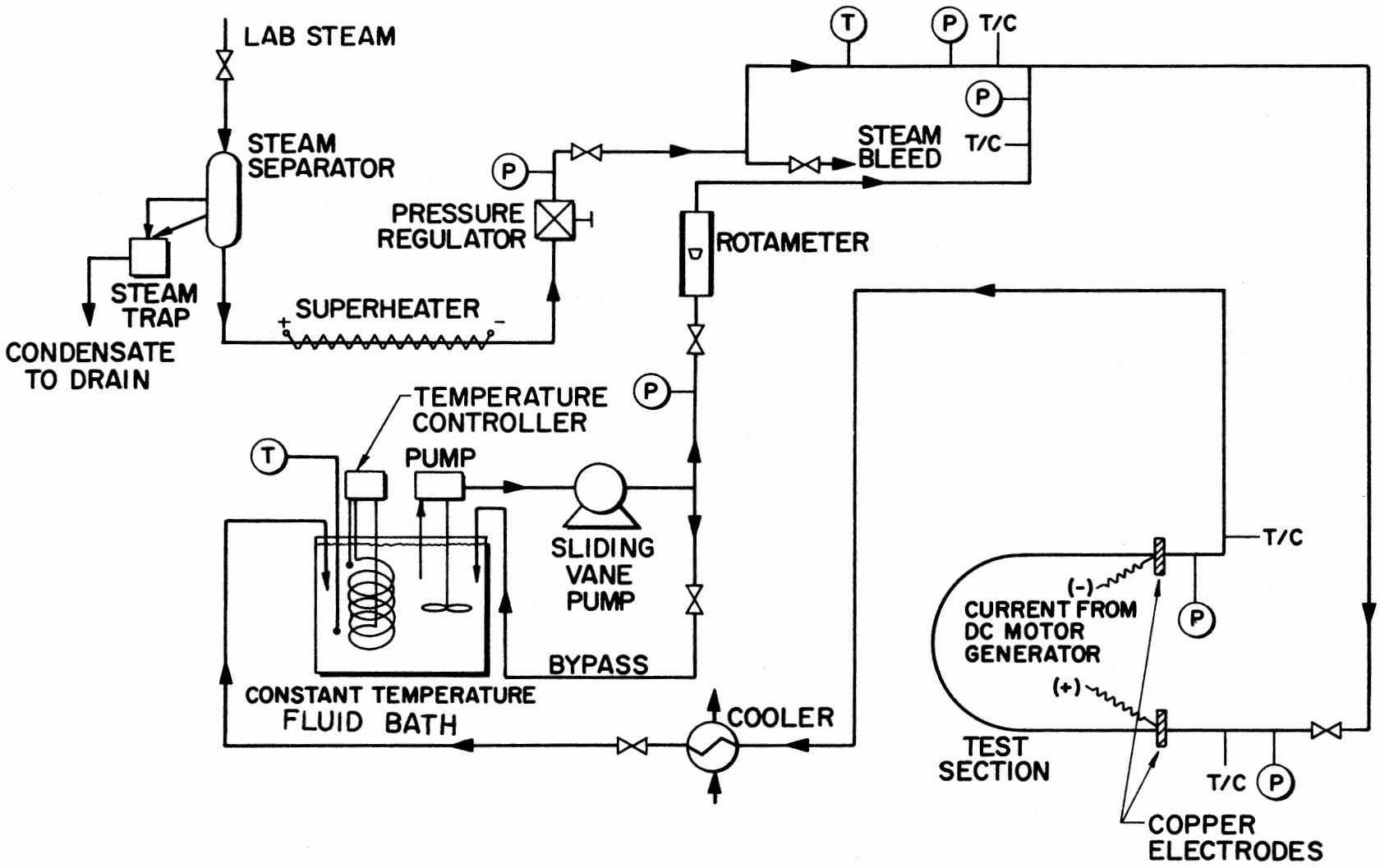

Figure 2. Heat Transfer Loop

TABLE I

SPECIFICATION OF THE FOUR TEST SECTIONS

Tube ID	Material	Bend Radius mm	Bend Radius (in.)	Outside Tube Diameter mm	Outside Tube Diameter (in.)	Inside Tube Diameter mm	Inside Tube Diameter (in.)	Straight Section Length m	Straight Section Length (in.)	Curvature Ratios R_c/r_i
A	Seamless Inconel 600	251	(9.875)	22.22	(0.875)	19.58	(0.771)	1.651	(65)	25.62
B	Seamless Inconel 600	121	(4.750)	22.22	(0.875)	19.58	(0.771)	1.778	(70)	12.32
C	Seamless Stainless Steel 304	60	(2.375)	19.05	(0.750)	15.75	(0.620)	3.480	(137)	7.66
D	Seamless Stainless Steel 304	38	(1.500)	19.05	(0.750)	15.75	(0.620)	3.480	(137)	4.84

Each test section was also electrically isolated from the loop by connecting it with a short piece of neoprene tubing at each end.

Four pressure taps with 1.59 mm (1/16 inch) holes were silver-soldered to each test section. The location of the pressure taps are shown on Figure 2. The taps were electrically isolated from the recording instrument by connecting them with silicone rubber tubing.

Each test section was heated by passing DC current through its wall. Two thick copper bars were silver-soldered to each test section to serve as electrodes for connection to the motor generator.

Experiments were performed with the U-bend in the vertical plane, with the test fluid entering at the bottom and exiting at the top.

Fluid Bath

A "Colora" type "Ultra-Thermostat" vessel was used as the fluid bath. The bath has a capacity of 4.1 gallons and is equipped with thermostat, a 500 and a 1,000 watt immersion-type electric heaters, a centrifugal pump and an impeller mounted on a common shaft and driven by an electric motor. The model number of the bath is NB-33279. The temperature of the bath fluid was controlled by adjusting the set point on the thermostat and the bath temperature was measured by means of a Brooklyn P-M mercury-in-glass thermometer having a range from 20 to 300^{o}F and graduated in 2^{o}F intervals.

Pumps

A sliding vane pump and a turbine pump were used to pump fluid through the experimental loop depending upon the fluid flow rate to be investigated.

The sliding vane pump was manufactured by Eastern Industries, Inc. The pump model number is VW-5-A. The pump is a positive displacement pump having a rated maximum capacity of 1.2 gpm (0.273 m^3/hr) of water and capable of developing a head of 138 feet (42 m).

The turbine pump was manufactured by Roy E. Roth Co. The pump model number is ISCU1131-AB. The pump has a rated capacity of 10 gpm (2.271 m^3/hr) of water and is capable of developing a head of 300 feet (91.4 m).

DC Power Source

A Lincolnweld SA-750 AC motor-driven DC generator was used to generate the DC current, which was fed to the test section tube through two copper bars silver-soldered to the tube. Resistance heating, due to the passage of DC current through the tube wall, provided the heat to the fluid. All experimental runs were conducted under approximately constant wall heat flux conditions. The DC power generator has a maximum rated output power of 30 kilowatts.

DC resistance heating was chosen over AC because:

1. Complex AC induction and skin effects are avoided.

2. AC heating may cause cyclic temperature variations in the test section whereas DC heating provides a constant heat source.

3. Possible thermal stresses in the test section caused by the cyclic nature of the AC are avoided.

4. The cyclic nature of the electrical forces in AC may induce vibrations in the test section. These vibrations do not exist when DC is used.

5. AC, because of its cyclic nature, may induce spurious emfs in the thermocouple wires resulting in erroneous readings.

A motor-generator was used as opposed to a rectifier because:

1. It was available.

2. Its power output is relatively smooth and free from large magnitude superimposed sine waves.

3. It is more resistant to overload than rectifiers.

4. It is not as susceptible to transient voltage peaks that occur in switching the unit on and off.

Heat Exchanger

A 1 shell-pass-4-tube-pass heat exchanger was used to cool the test fluid from the test section. The heat exchanger is a size 502, 'BCF' type exchanger manufactured by the Kewanee-Ross Corporation (10). Water was used to cool the test fluid. The test fluid was in the shell and water was in the tubes.

Measuring Devices

Thermocouples

Two different types of thermocouples were used to measure temperature in the experiment:

1. Conax "Con-o-clad" thermocouples to measure the bulk fluid temperature.

2. Insulated wire thermocouples to measure the outside wall temperature of test section tube.

Conax "Con-o-clad" Thermocouples

Two Iron-Constantan type ungrounded "Con-o-clad" thermocouples, manufactured by the Conax Corporation, were used to measure the bulk fluid temperature at the inlet and exit of the test section. Ungrounded thermocouples are manufactured such that the thermocouple is sealed inside a metal sheath (usually 316 stainless steel) but does not contact the metal sheath. Sheathed ungrounded thermocouples were used to measure the bulk fluid temperature because:

1. The sheath protects the thermocouple from corrosion by the fluid.

2. The ungrounded thermocouples are immune to any stray emfs that may be produced by the DC heating.

The above-mentioned thermocouples will hereafter be referred to as the "Conax thermocouples".

The Conax thermocouples were calibrated in-situ by using low pressure saturated steam. Details of the calibration procedure are presented in Chapter IV.

Insulated Wire Thermocouples

The outside wall temperatures of the test section tube were measured using thermocouples made from fiberglass-insulated, 30 B & S gauge Iron-Constantan thermocouple wire. The thermocouples were fabricated in the laboratory by using the thermocouple welder. These thermocouples will hereafter be referred to simply as "thermocouples".

Thermocouples were placed at eleven stations on the tube wall along the test section. The position of each station along the test

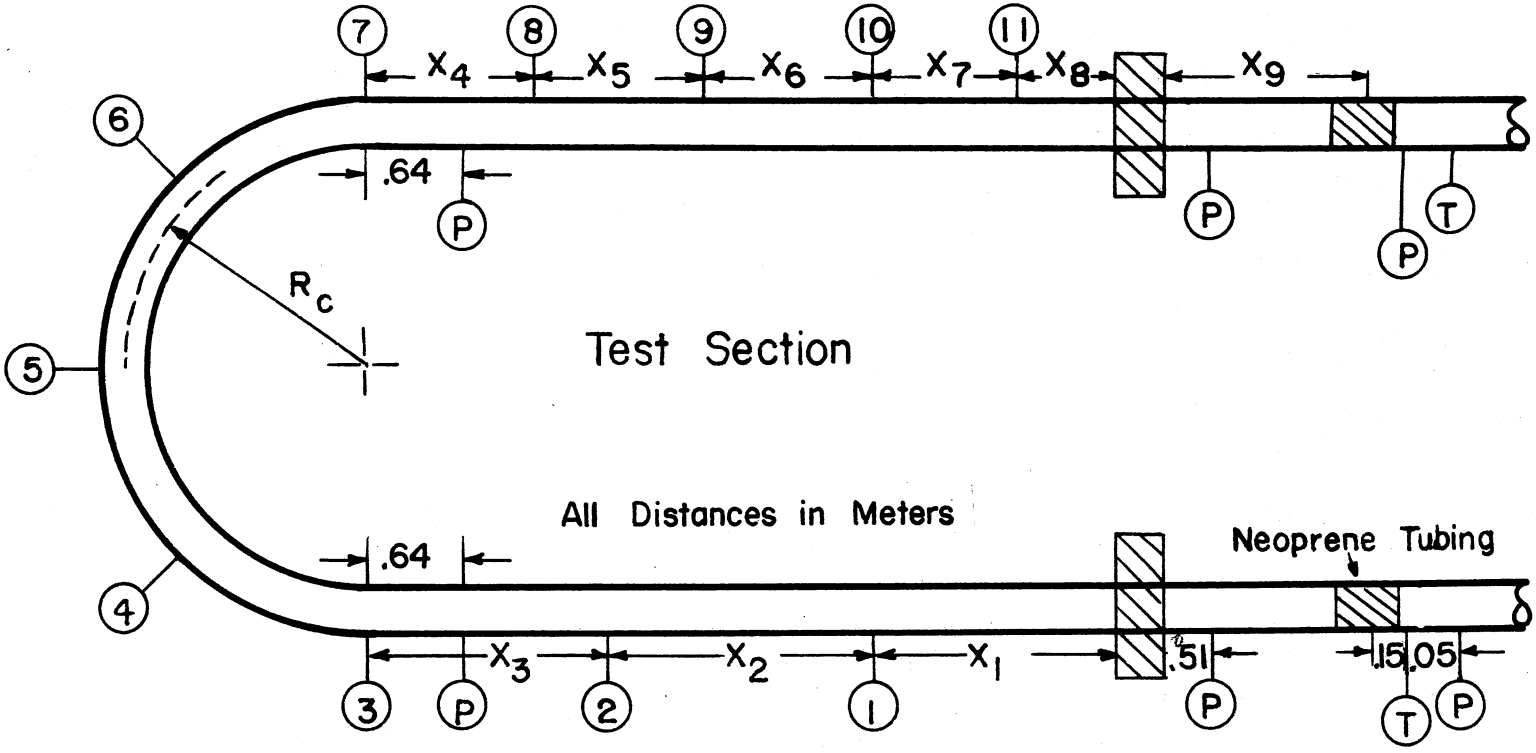

Figure 3. Location of Thermocouple Stations and Pressure Tops Along Test Sections

section is shown in Figure 3 and Table II. At each station, eight thermocouples were placed 45 degrees apart on the tube periphery. Figure 4 is a sketch of the thermocouple layout at each station.

TABLE II

THE VALUE OF X_i AS SHOWN IN FIGURE 3, m

Tube ID	R_c/r_i	X_1	X_2	X_3	X_4	X_5	X_6	X_7	X_8	X_9
A	25.62	0.102	0.889	0.152	0.152	0.152	0.152	0.584	0.102	0.508
B	12.32	0.102	1.219	0.152	0.152	0.152	0.152	0.914	0.102	0.305
C	7.66	1.219	1.143	0.381	0.381	0.381	0.762	0.762	0.457	0.737
D	4.84	1.219	1.143	0.381	0.381	0.381	0.762	0.762	0.457	0.737

The thermocouple beads were fixed on the tube surface with Sauereisen cement. In order to electrically insulate the thermocouple beads from the heating current, a thin layer of Sauereisen cement was first placed at the intended thermocouple location and allowed to set before cementing the thermocouple bead to its intended location. The thermocouple wires from the thermocouple beads were held in place about 1/2-inch from the thermocouple beads by means of a layer of asbestos paper tape and a flexible hose clamp. The asbestos paper tape was

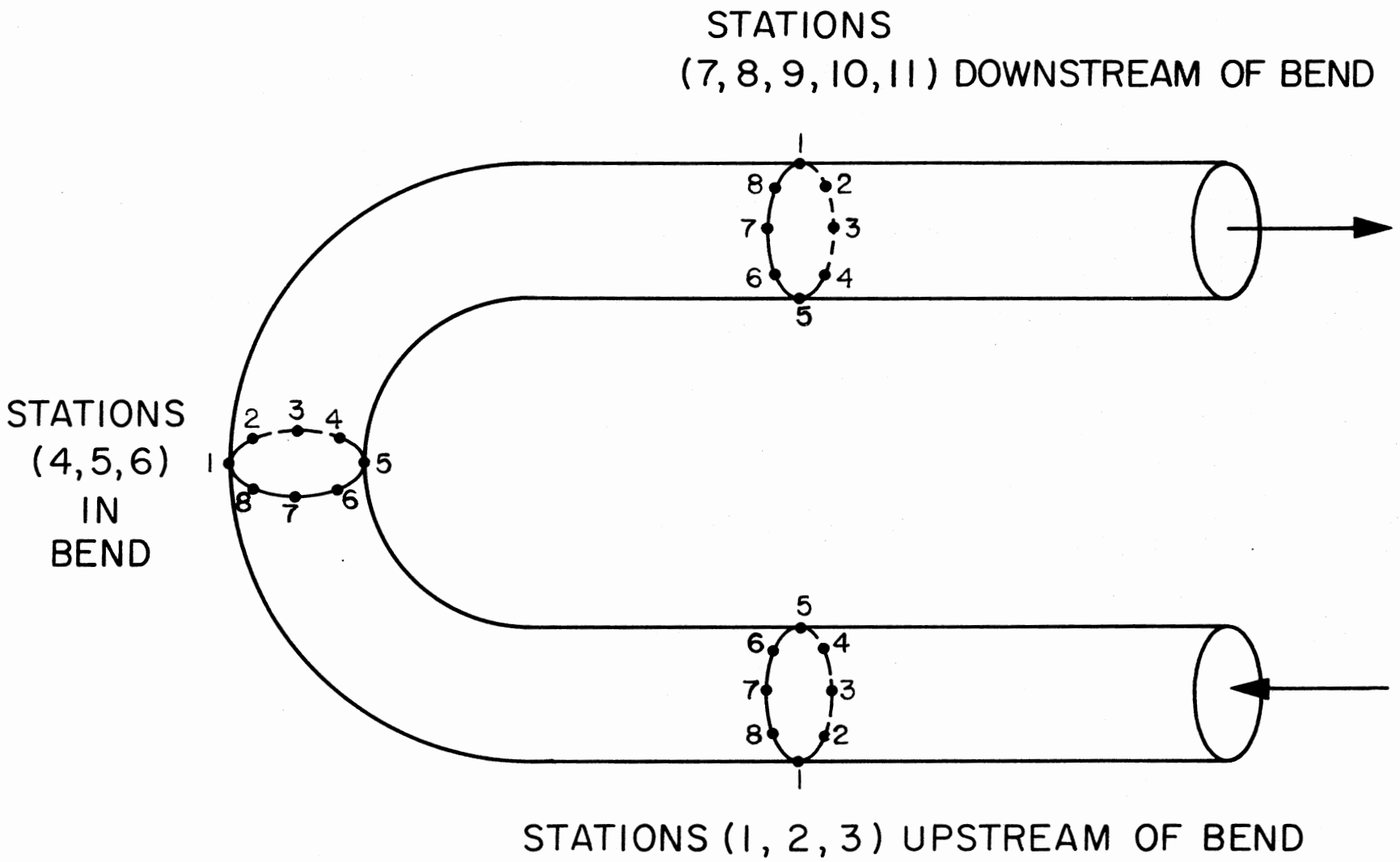

Figure 4. Identification of Test Points in U-Bend Tests

placed between the clamp and the thermocouple wires to prevent any accidental short-circuiting of the thermocouple wires due to the sharp edges of the metal hose clamp. The thermocouple wires were then placed along the test section for about two inches and clamped again to the tube before being led off to the thermocouple selector switch-board.

All the surface thermocouples were connected to an array of barrier strips which in turn were connected to 11 rotary switches. The terminal lugs used on the barrier strips were made of either iron or constantan and this feature eliminated any problems associated with creation of new thermocouples due to variation in room temperature. The rotary switches were mounted on a panel and the connections were enclosed in a constant temperature box. The outputs from the rotary switches were brought to a master rotary switch which was connected to a Leeds and Northrup Numatron. The Numatron incorporated a reference junction compensator and output was displayed in digital form in degrees Fahrenheit.

For all four test sections, the thermocouples were calibrated in-situ by bleeding low pressure saturated steam through the test section. Details of the calibration procedure are given in Chapter IV.

Manometer

The six pressure taps, as shown in Figure 3, were connected to a manifold by a series of Whitey valves. The switching system was connected in such a manner that any of the six taps could be activated and read on a Meriam U-type manometer against atmospheric pressure.

Rotameters:

Two Brooks "Full-View" rotameters were used to indicate and measure the fluid flow rate. The rotameter specifications are given in Table III.

TABLE III

ROTAMETER SPECIFICATIONS

Item	Rotameter 1	Rotameter 2
Rotameter model number	1110-08H2B1A	10-110-10
Rotameter tube number	R-8M-25-4	R-10M-25-3
Float number	8-RV-14	10-RV-64
Maximum water flow rate, gpm	1.45	6.28

DC Ammeter and Voltmeter

The power input to the test section was measured by a DC ammeter and a voltmeter.

The current flowing through the test section was measured by a Weston model 931 DC ammeter in conjunction with a 50 millivolt shunt. The ammeter has a 0-750 amperes range.

The 50 millivolt shunt was connected in the line carrying the current to the test section. The ammeter was connected across the shunt.

To voltage drop across the test section was measured by a Weston model 931 DC voltmeter. The voltmeter has a 0-50 volt range. The voltmeter was connected to the two copper bars.

The ammeter and the voltmeter were calibrated by the manufacturer and were guaranteed to be accurate to within one percent of their full range, that is $\pm$ 7.5 amperes and $\pm$ 0.5 volts, respectively.

Mercury-in-glass Thermometers

Mercury-in-glass thermometers were used to measure the bath fluid temperature and the room temperature. A Brooklyn "P-M" 20 to 300^{o}F thermometer was used to measure the bath fluid temperature. The thermometer was graduated in 2^{o}F intervals. A 23-inch long, 65 to 90^{o}F ASTM Calorimeter Thermometer was used to measure the room temperature.

Numatron

The thermocouple outputs were measured on the Numatron. The Numatron is Leeds and Northrup Company's trade name for a voltmeter with a digital readout. The Numatron is also equipped with the circuitry that converts a thermocouple emf fed to the instrument into its corresponding temperature reading. The reading is displayed directly in degrees Fahrenheit on the digital readout panel in the Numatron.

The Numatron has the following stated accuracies: $\pm$ 0.26^{o}F for the 0 to 300^{o}F temperature range; 10 microvolts $\pm$ 1 digit for the 0.01 volt range; and, 1 millivolt $\pm$ 1 digit for the 10 volt range. Further details regarding the Numatron may be obtained from the Numatron Operations Manual (11).

Auxiliary Equipment

Auxiliary equipment was used for the calibration of the measuring devices. All measuring devices were calibrated except the DC ammeter and voltmeter which had been previously calibrated by the School of Electrical Engineering Laboratories at Oklahoma State University. The description of the auxiliary equipment consists of two sections:

1. Rotameter calibration and fluid flow rate measurement equipment.
2. Numatron calibration equipment.

Rotameter Calibration and Fluid Flow Rate Measurement Equipment

The rotameter calibration and fluid flow measurement equipment consisted of the following:

1. Stop Watch: A 60 minute stop watch with a main dial range of 60 seconds was used to time the fluid flow rate. The stop watch has a precision of 0.2 seconds.

2. Weighing Equipment: A 5 kilogram capacity Ohaus Pan Balance was used to weigh the amount of fluid collected for fluid flow rates below 1.0 gpm. The balance has a sensitivity of 0.5 grams. A set of calibrated weights was used in conjunction with the balance.

For fluid flow rates greater than 1.0 gpm, a single-beam platform weighing scale was used to weigh the amount of fluid collected. The weighing scale has a capacity of 300 lbs and an accuracy of 0.125 lb. The beam is graduated in pounds and ounces.

3. Fluid Collecting Vessels: The fluid collecting vessels consisted of various capacity beakers and cylindrical jars. The vessels were used to collect the fluid for a given time interval, so that the mass flow rate could be determined.

Numatron Calibration Equipment

A Leeds and Northrup model 8687 volt potentiometer was used for the calibration of the Numatron. The potentiometer used has a maximum stated accuracy of $\pm$ (0.03% of reading + 30 microvolts) (12). The Numatron was also checked against ice water temperature and was adjusted to give 32.0^{o}F reading.

CHAPTER IV

EXPERIMENTAL PROCEDURE

This chapter presents: (1) Calibration procedure; (2) Start-up procedure; (3) Data gathering procedure.

Calibration Procedure

Thermocouple Calibration

All surface thermocouples were calibrated in-situ by using saturated steam as the reference temperature. Low pressure laboratory steam was allowed to go through a steam separator and liquid water was trapped out of the stream. Then saturated dry steam at atmospheric pressure was sent to the test section and the thermocouple outputs, inlet and exit steam pressure, room temperature and atmospheric pressure were recorded after a run time of approximately eight hours. In addition, the steam condensate flow rate and steam pressure at four more points along the test section were measured.

Knowing the absolute pressure of the saturated steam at the inlet and exit of the test section, the steam temperature was determined from steam tables and hence the deviation indicated by the thermocouples was determined. As shown in Table VIII, in Appendix B, the deviations are small. The steam temperature was assumed to drop

linearly along the length of the test section. Knowing the condensate flow rate, the steam temperature in the test section, the room temperature and the total outer surface area of the test section, the average heat loss flux and the heat loss at calibration conditions was determined. Thermocouple calibration data are presented in Appendix B.

The thermocouple calibrations and the heat loss information obtained were incorporated into the computer programs for calculating heat balance and the inside wall temperatures.

Manometer Calibration

The reading of the U-type manometer was verified to be zero for the condition of no flow through the test section. Liquid mercury was used as the indicator fluid in the manometer.

Rotameter Calibration

Both rotameters used in the course of the experiments were calibrated for distilled water. Both rotameters were calibrated from 10 percent to 100 percent of maximum flow in 10 percent increments. Each rotameter was calibrated with the flow rate increasing up to the maximum and then decreasing to the minimum flow rate.

The calibration procedure consisted of the following steps:

1. The fluid flow rate was adjusted to the desired float setting on the rotameter.

2. After operating for some time at the desired float setting, the fluid flowing in the system was collected in a previously weighed empty container for a predetermined interval of time. The time

interval ranged from 30 seconds up to 3 minutes, depending upon the flow rate being calibrated.

3. The bath fluid temperature was recorded and taken to be the temperature of the fluid in the rotameter.

4. The vessel containing the fluid collected was weighed to determine the weight of the fluid collected.

The above mentioned procedure was repeated twice for each float setting on the rotameter.

For Dowtherm G and ethylene glycol as test fluids, the rotameters were used as guides to set the flow rate and the mass flow rate was measured (by the procedure outlined above) at the time of execution of the data run.

Calibration data for both rotameters are presented in Appendix B.

Numatron Calibration

The Numatron was calibrated periodically. The calibration procedure is detailed in section 14 of the Numatron Operations Manual (11).

Start-Up Procedure

Experimental data were obtained for four different diameter bend test sections.

After one of the test sections was installed in the fluid flow loop and the thermocouple wires were connected to the switches on the thermocouple selector switchboard, the fluid flow loop was tested for possible leaks by flowing fluid at the anticipated maximum flow rate through the loop. Any leaks detected were eliminated. The fluid

flow loop was then insulated with fiberglass tape and fiberglass wool insulation and prepared for obtaining experimental data.

The above operation was performed every time the test section was changed.

The following step-by-step procedure was followed to gather experimental data for each run:

1. The impeller and the heater in the fluid bath were activated and the fluid in the bath was brought to the desired operating temperature ($60^{o}F$ to $90^{o}F$).

2. The DC generator was started, with the polarity switch in the "Off" position, and allowed to warm up for 30 minutes.

3. Cooling water was started to the heat exchanger located downstream of the test section.

4. The Numatron was activated.

5. The pump was started and the fluid was allowed to circulate in the by-pass line.

6. The flow control valve located upstream of the rotameter was opened and the fluid was allowed to flow through the test section.

7. After about five minutes, the polarity switch was thrown to the "Electrode Negative" position thereby causing the DC current to flow through the test section.

Data Gathering

The data gathering procedure consisted of the following steps:

1. The fluid flow rate was adjusted to the desired value by means of the flow control valve.

2. The DC current was adjusted to the desired value by varying the output control switch on the control box of the generator. Fine control of the current was accomplished by adjusting the external rheostat connected to the generator.

3. The cooling water flow rate to the heat exchanger was adjusted so that the bath fluid temperature remained constant.

4. The experimental set-up was then operated for at least one and half hours to allow the system to achieve steady state. Minor adjustments were made to the current, the fluid flow rate and the cooling water flow rate, as was deemed necessary.

5. After about two hours of operation, the following experimental data were taken:

   a. The test section surface temperatures (indicated by the insulated wire thermocouples cemented on the test section).
   b. The inlet and exit bulk fluid temperature (indicated by the Conax thermocouples).
   c. The fluid flow rate indicated by the rotameter.
   d. The DC current flowing through the test section and the voltage drop across the test section.
   e. The room and bath fluid temperature.
   f. The six pressures along the test sections, as indicated by the U-type manometer.

All of the thermocouple outputs were measured on the Numatron.

6. The entire set of data, as indicated in step 5 above was measured again to ascertain if steady state had been achieved. The time span between the two sets of measurements was approximately half an hour.

7. Steady state was deemed to have been achieved if the two sets of temperature measurements agreed within $\pm$ 0.3^{o}F.

If steady state had not been achieved, steps 5 and 6 were repeated after about one hour of continued operation.

Except for a few data cases, steady state was achieved when data were measured after about two hours of operation for a given set of fluid flow rate and current settings.

The fluid flow rate and/or the current was changed to a new set of conditions and the entire Data Gathering Procedure was repeated for the new set of input conditions.

For the Dowtherm G and ethylene glycol runs, the mass flow rate of the fluid was measured, after obtaining the temperature and pressure data as indicated in step 5 and 6 of the Data Gathering Procedure section, before proceeding to a new set of input conditions. Since the fluid temperature became highly nonuniform at the exit of the test section, for the Dowtherm G and ethylene glycol runs, the exit bulk fluid temperature as measured by Conax thermocouples was in error. Therefore, the exit bulk fluid temperature was calculated from the measured inlet bulk fluid temperature and the net amount of electrical heat input.

The distilled water used in experiments was changed frequently to minimize the buildup of solid content in the water.

CHAPTER V

DATA REDUCTION

Experimental data were obtained for four test sections using distilled water, Dowthern G and ethylene glycol. A total of 90 runs were made using water, 33 runs were made using Dowtherm G and 26 runs were made using ethylene glycol as the working fluid. The raw experimental data are presented in Appendix A. Computer programs which were originally written by Farukhi (9) were modified to reduce the experimental data using the IBM 370/158 computer. Computer program flow charts and listing are essentially the same as that presented in Moshfeghian's M.S. thesis (6).

The physical quantities measured for each experimental run are listed under item 5 in the Data Gathering Procedure in Chapter IV. The outer surface temperatures were measured at 88 locations along the length of the test section. The locations of the thermocouples are given in Chapter III.

The physical properties of the fluid were evaluated at the bulk fluid temperature at each thermocouple station. The bulk fluid temperature was assumed to increase linearly along the axial length of the test section, starting from inlet electrode.

Average bulk fluid temperature for the entire test section, for each data run, was taken to be the arithmetic average of the inlet and

exit bulk fluid temperatures. To correct for wall effects, the fluid viscosity was also determined at the average inside wall temperatures so that the viscosity correction factor could be evaluated.

The regression correlations, developed by Singh (7), were used to evaluate the physical properties of the distilled water and Dowtherm G. For ethylene glycol, physical properties were evaluated by the regression correlations presented by Curme (13). Thermal conductivity and electrical resistivity of Inconel 600 and stainless stell were evaluated by the regression correlations developed by Singh (7) and Farukhi (9). These correlations and the original source of these physical properties are presented in Appendix C and are incorporated into the computer programs used for the data reduction.

Data reduction consisted of the following steps:

1. Calculation of the error percent in heat balance.
2. Calculation of the local inside wall temperature and the inside wall radial heat flux.
3. Calculation of the local heat transfer coefficient.
4. Calculation of the relevant dimensionless numbers. Details regarding the above mentioned steps follow.

Calculation of the Error Percent in Heat Balance

The error percent in the heat balance for each data run was calculated as follows:

$$\dot{q}_{input} = (3.41213)(I)(V) - \dot{q}_{loss} \qquad (5\text{-}1)$$

where

I = current in test section, amperes;

V = voltage drop across test section, volts;

$\dot{q}_{loss}$ = heat loss; Btu/hr (calculated from calibration data).

Heat output rate, Btu/hr = $\dot{q}_{output}$

$$\dot{q}_{output} = WC_p[(T_b)_{out} - (T_b)_{in}] \tag{5-2}$$

where

W = mass flow rate of fluid flowing through test section, lb_m/hr;

C_p = specific heat of the fluid at the average bulk fluid temperature in the test section, Btu/lbm-^oF;

$(T_b)_{in}$ = bulk fluid temperature at the test section inlet, ^oF;

$(T_b)_{out}$ = bulk fluid temperature at the test section outlet, ^oF.

$$\text{percent error in heat balance} = \left[\frac{\dot{q}_{input} - \dot{q}_{output}}{\dot{q}_{input}}\right](100)\ \%$$

The inlet and outlet bulk fluid temperature were measured by Conax thermocouples. These temperatures were corrected based on the thermocouple calibration given in Appendix B.

Calculation of the Local Inside Wall Temperature and the Inside Wall Radial Heat Flux

Computer programs originally written by Owhadi (22) and Crain (14) and later developed by Singh (7) and Farukhi (9) were modified to determine the inside wall temperatures from the measured otuside wall

temperatures. Appendix D presents the derivation of equations for numerical solution of wall temperature gradient with internal heat generation. Using the outside wall temperatures and the electrical heat input, the modified computer program computes the inside wall temperatures by a trial-and-error solution. The program also computes the inside wall radial heat flux at each thermocouple location on the test section. Details regarding the computer program are given in Reference (14). A flowchart and a listing of the modified computer programs are given in Moshfeghian's M.S. thesis (6).

Calculation of the Local Heat Transfer Coefficient

Knowing the inside wall temperature, the inside wall radial heat flux and the bulk fluid temperature, the local heat transfer coefficient was calculated as follows:

$$h_i = \frac{\dot{q}''_i}{[(T_w)_i - T_b]} \tag{5-3}$$

where

h_i = local inside heat transfer coefficient, Btu/(hr-ft^2-^{o}F);

$\dot{q}''_i$ = local inside wall heat flux, Btu/(hr-ft^2);

$(T_w)_i$ = local inside wall temperature, ^{o}F;

T_b = bulk fluid temperature at the thermocouple station, ^{o}F.

Calculation of the Relevant Dimensionless Numbers

The dimensionless numbers calculated at the bulk fluid temperature at each station were Reynolds and Prandtl numbers. The Nusselt number

was also calculated for each station using the circumferentially-averaged local heat transfer coefficient at each station. In addition, the Grashof number was calculated for each station using the circumferentially-averaged inside wall temperature and the bulk fluid temperature at each station.

All the experimental data gathered were reduced using the above procedure. Sample calculations for one data run are given in Appendix E.

To understand the mechanism of the heat transfer process in the bend and and downstream of the bend, the inside wall heat transfer coefficients were calculated for each thermocouple location on the test section and were digitally plotted for the eight thermocouple locations on the tube periphery for each data run.

CHAPTER VI

RESULTS AND DISCUSSION OF RESULTS

For the four 180^{o}-bend test sections, experimental data were gathered for Reynolds numbers ranging from 55 to 31,000, Prandtl numbers ranging from 4 to 270, and curvature ratio (ratio of bend radius to inside radius of tube) numbers ranging from 4.84 to 25.62. The test fluids were water, Dowtherm G and ethylene glycol. Results of this study together with a discussion of the results are presented in this chapter.

General Discussion

Values of the average Reynolds, average Prandtl numbers, average values of the heat flux and the heat transfer coefficient for the inside wall were computed for each thermocouple location for each data run. These values are summarized in Appendix F for all of the experimental data runs.

The average heat transfer coefficient at a thermocouple station was defined as follows:

$$H_1 = \begin{matrix}\text{average heat} \\ \text{transfer coefficient}\end{matrix} = \frac{1}{8}\sum_{i=1}^{8}\left[\frac{(\dot{q}/A)_i}{(T_w)_i - T_b}\right] \qquad (6.1)$$

where i indicates the peripheral location on the tube cross section at a thermocouple station. The average heat transfer coefficient obtained

from Equation (6.1) was then used to determine the average Nusselt number for the thermocouple station. The physical properties of the fluid used in determination of the Reynolds, Prandtl and Nusselt numbers were evaluated at the bulk fluid temperature at the thermocouple station, T_b, calculated by a heat balance based upon the inlet and exit bulk fluid temperature and the heat input.

In addition to Equation (6.1) the average heat transfer coefficient at a thermocouple station may also be computed as follows:

$$H_2 = \begin{matrix}\text{average heat} \\ \text{transfer coefficient}\end{matrix} = \frac{(\overline{q/A})}{\overline{T}_w - T_b} \tag{6.2}$$

where $(\overline{q/A}$ and $\overline{T}_w$ were defined as follows:

$$(\overline{q/A}) = \frac{1}{8}\sum_{i=1}^{8} (q/A)_i \tag{6.3}$$

and

$$\overline{T}_w = \frac{1}{8}\sum_{i=1}^{8} (T_w)_i \tag{6.4}$$

where i in Equations (6.3) and (6.4) has the same definition as in Equation (6.1). In Appendix F, H_1 and H_2 represent the average heat transfer coefficient using Equations (6.1) and (6.2) respectively. H_1 and H_2 become equal if the peripheral distribution of inside wall temperatures is uniform; however, for the nonuniform distribution of inside wall temperatures H_1 becomes larger than H_2. For example the ratio of H_1/H_2 ranged from 1.0 to 1.18 and 1.0 to 2.49 for runs 515 and 252, respectively.

Peripheral Distribution of Heat Transfer Coefficients

Since heat transfer coefficients were almost symmetrical about a vertical meridional plane, arithmetic average heat transfer coefficients were calculated between locations 2 and 8, 3 and 7, and 4 and 6 for purposes of comparing secondary and tertiary flow effects.

Laminar Flow Regime

Figures 5 through 7 present the peripheral distribution of heat transfer coefficient for run 252. The average Reynolds number for this run was 1,240, and the average heat flux was 1,700 Btu/hr-ft^2 (5,584 W/m^2).

Straight Section Upstream of the Bend. Figure 5 indicates that as the fluid enters the straight section upstream of the bend the heat transfer coefficients are fairly uniform. However, as the fluid moves along this straight section the difference between heat transfer coefficients at the top and the bottom of the tube becomes larger (see station 3). This behavior was also observed by Morcos and Bergles (15) and could be explained by the fact that during heating, the fluid near the wall is warmer and, therefore, lighter than the bulk fluid in the core. As a consequence, two upward currents flow along the side walls, and, by continuity, the heavier fluid near the center of the tube flows downward. Hereafter, this natural convection flow pattern will be referred to as "tertiary" flow. The effect of tertiary flow is to cause the heat transfer coefficient to be higher at the bottom than at the top of the tube.

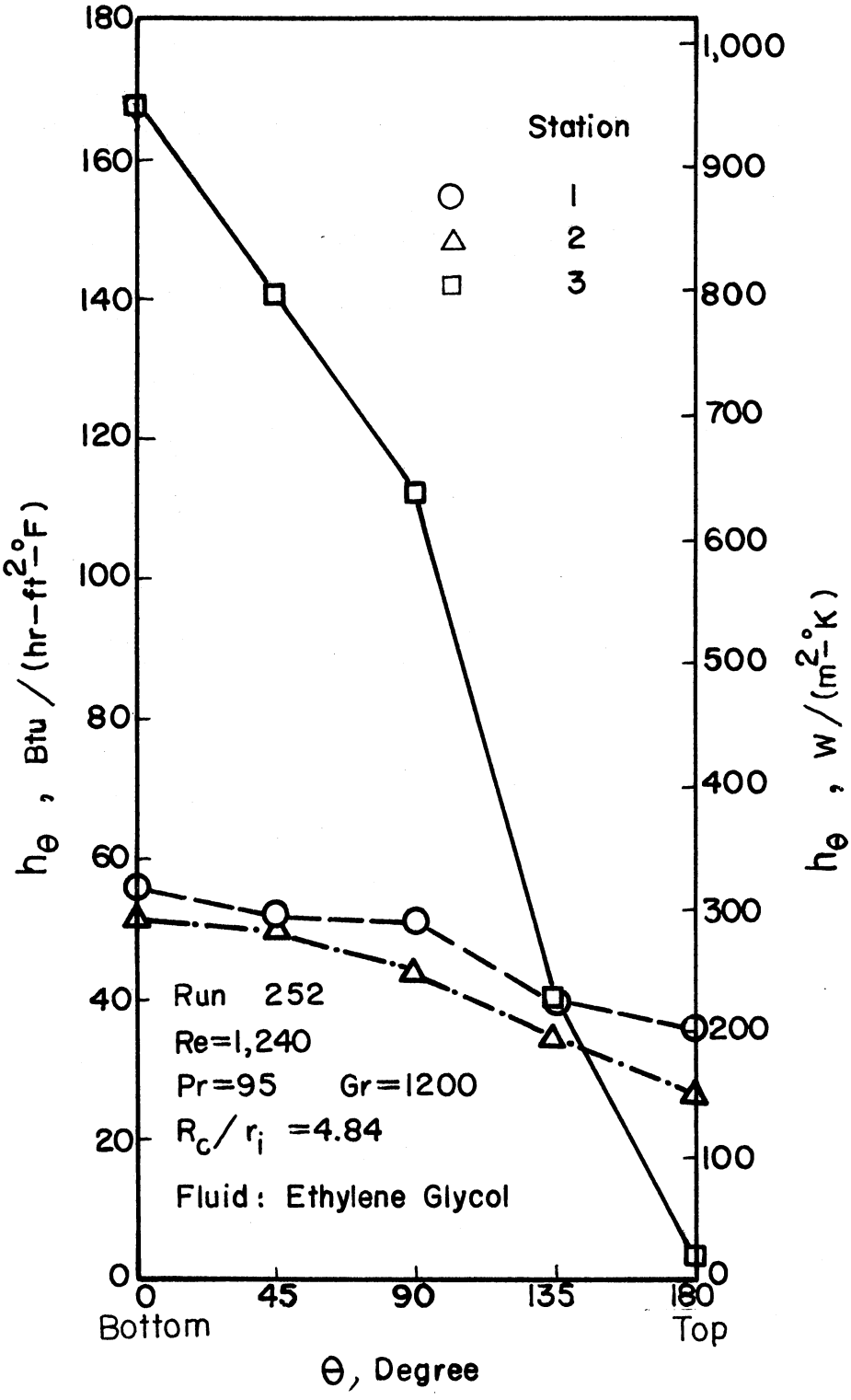

Figure 5. Peripheral Distribution of Heat Transfer Coefficients, Run 252

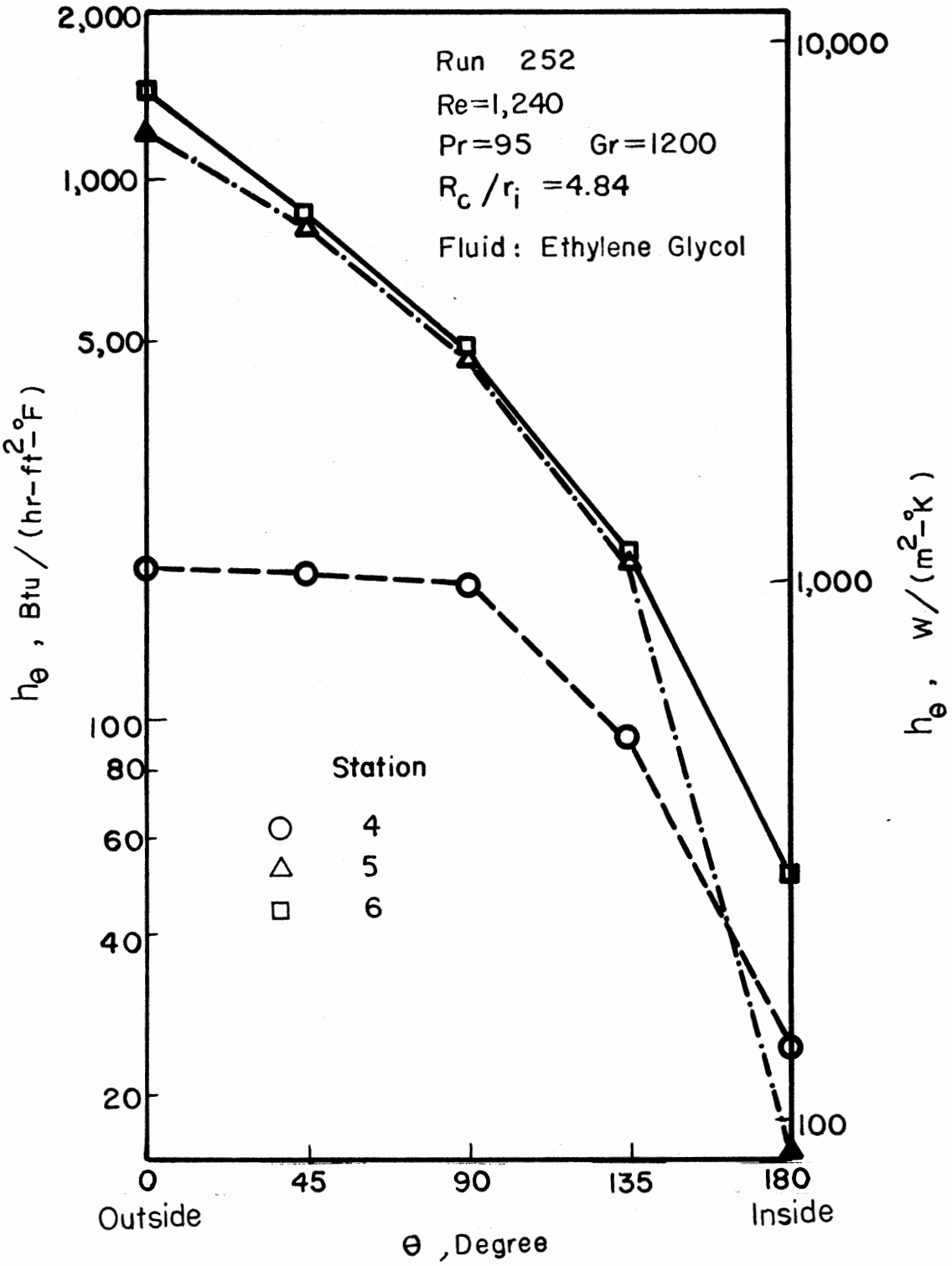

Figure 6. Peripheral Distribution of Heat Transfer Coefficients, Run 252

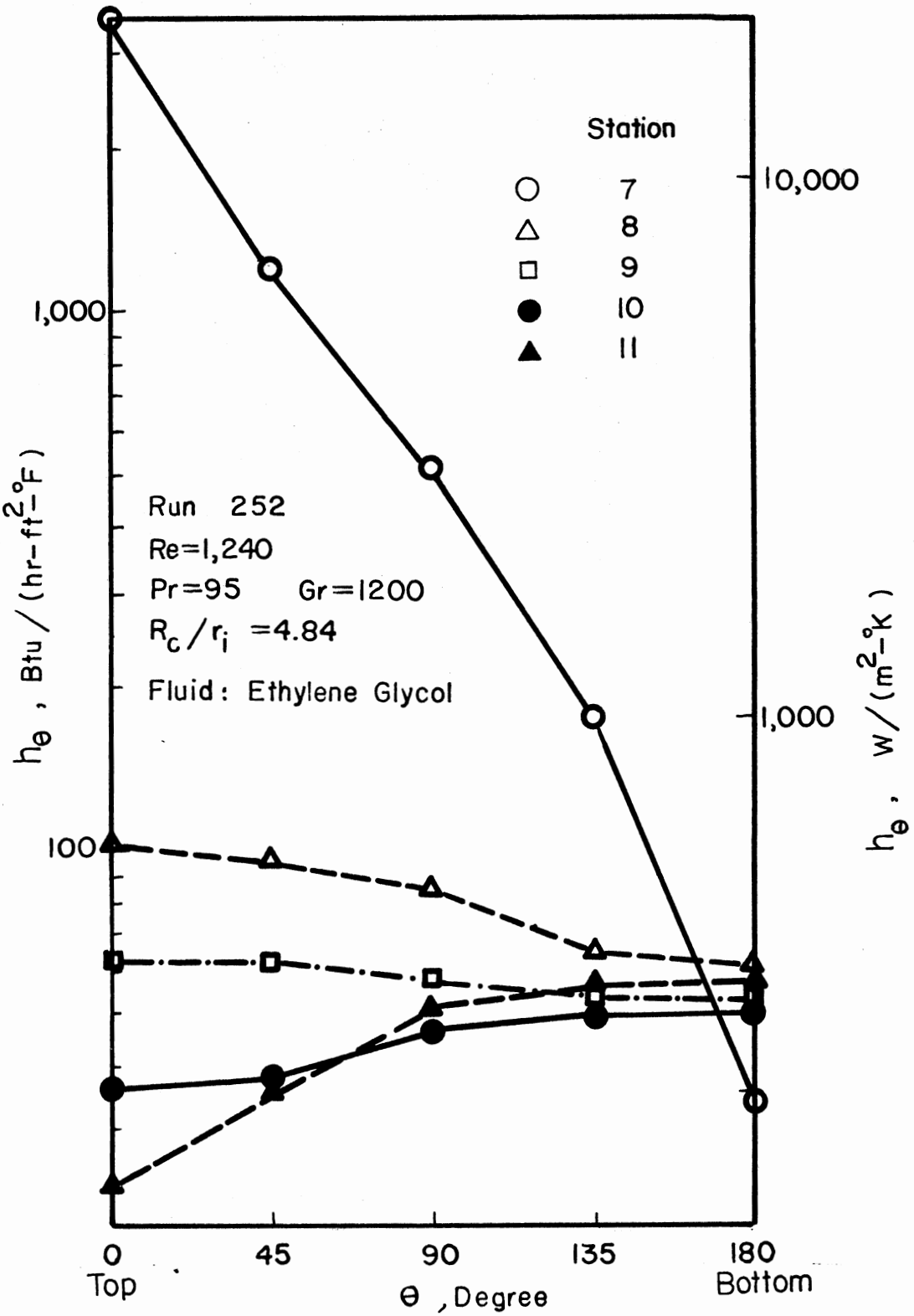

Figure 7. Peripheral Distribution of Heat Transfer Coefficients, Run 252

In the Bend. Figure 6 presents the peripheral distribution of heat transfer coefficients for stations 4, 5, and 6, which were located in the U-bend portion of the test section. As anticipated, higher heat transfer coefficients were obtained for locations on the outside wall of the bend than for locations on the inner wall of the bend. This fact has been known historically for helically-coiled tubes and has been indicated by earlier workers in the field (Singh (7) and Moshfeghian (6), to mention a few). It has been attributed to the presence of the superimposed secondary flow due to centrifugal action. The secondary flow causes the faster moving fluid elements to move toward the outer wall of the bend and the slower moving fluid elements to move toward the inner wall of the bend. Therefore, there are higher coefficients and more heat removal from the outer wall than the inner wall of the bend.

Straight Section Downstream from the Bend. As it is shown on Figure 7 (stations 7 and 8), when the fluid leaves the bend and enters the straight section downstream of the bend the heat transfer coefficients are higher at the top than at the bottom. However, as the fluid moves further away from the bend the peripheral distribution of heat transfer coefficients becomes uniform (station 9). Beyond station 9, as it is shown on Figure 7, the heat transfer coefficient at the top becomes smaller than that at the bottom. Examination of peripheral distribution of heat transfer coefficients at stations 7 through 11 indicates that as the fluid leaves the bend it carries the secondary flow effect some distance downstream of the bend. For this typical run the secondary flow is carried up to station 9. Beyond

station 9, as was explained for station 3 located upstream of the bend, the fluid elements experience tertiary flow (natural convection) superimposed on the primary flow.

Turbulent Flow Regime

Figures 8 through 10 present the peripheral distribution of heat transfer coefficients for run 515. The average Reynolds number for this run was 27,230, and the average heat flux was 17,900 Btu/hr-ft^2 (56,467 W/m^2).

Straight Section Upstream of the Bend. Figure 8 presents the peripheral distribution of heat transfer coefficient at stations 1, 2, and 3. The peripheral distribution of heat transfer coefficients at station 3 indicates that the tertiary flow is not as important as was the case for run 252 (Re = 1,240). The decrease in the tertiary flow (natural convection) for the turbulent flow regime (when compared to the laminar flow regime) may be due to the increased mixing of the fluid due to turbulent flow.

In the Bend. Peripheral distributions of heat transfer coefficients for stations 4, 5, 6 (located in the bend) are presented in Figure 9. As was the case for the laminar flow regime, the heat transfer coefficients are much higher at the outer wall of the bend than at the inner wall. Again the nonuniform heat transfer coefficient distribution is due to the secondary flow superimposed on the primary flow due to the presence of centrifugal force.

Straight Section Downstream from the Bend. The peripheral distributions of heat transfer coefficients for the straight section downstream of the bend (stations 7 through 11) are presented in Figure 10.

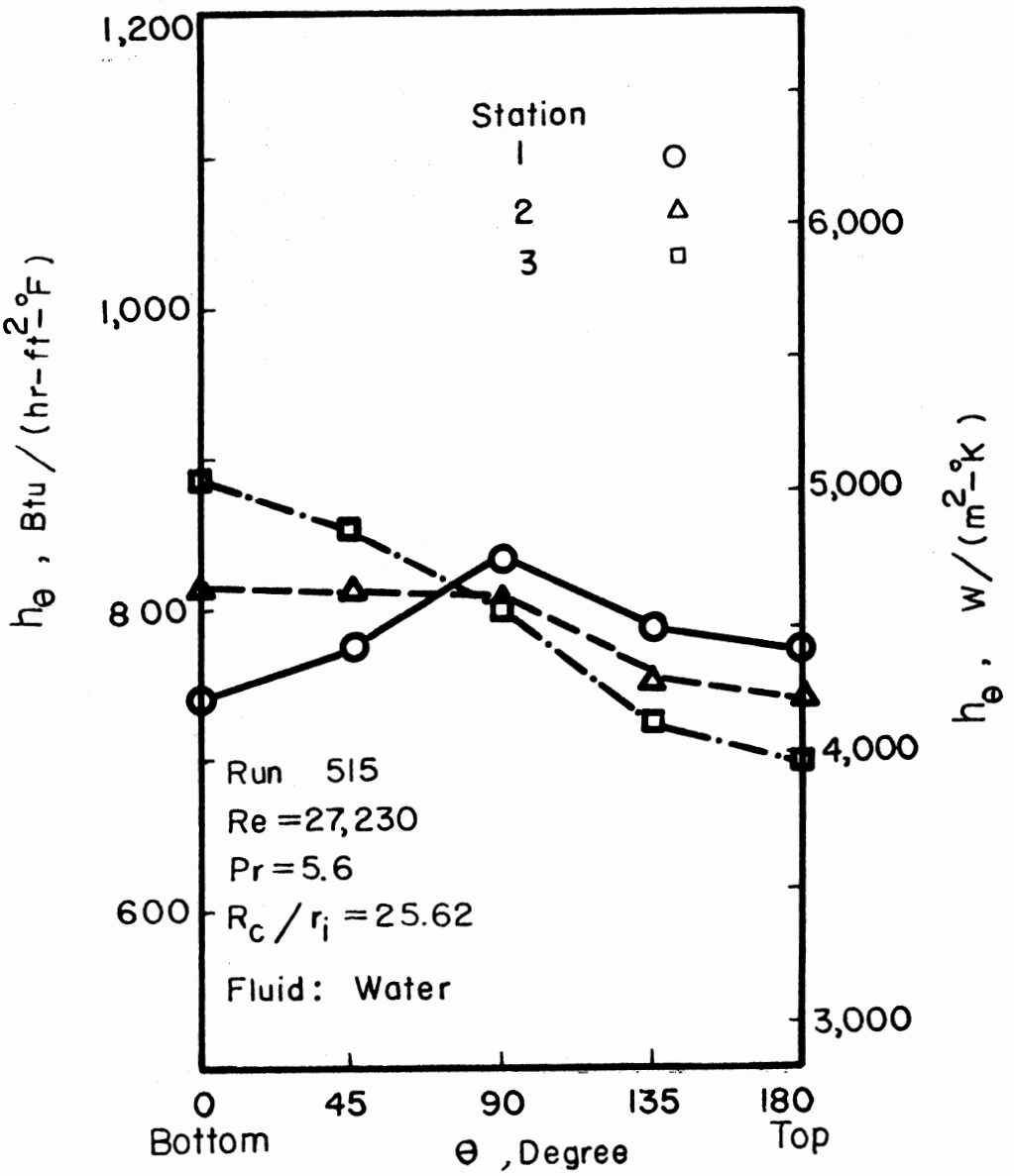

Figure 8. Peripheral Distribution of Heat Transfer Coefficients, Run 515

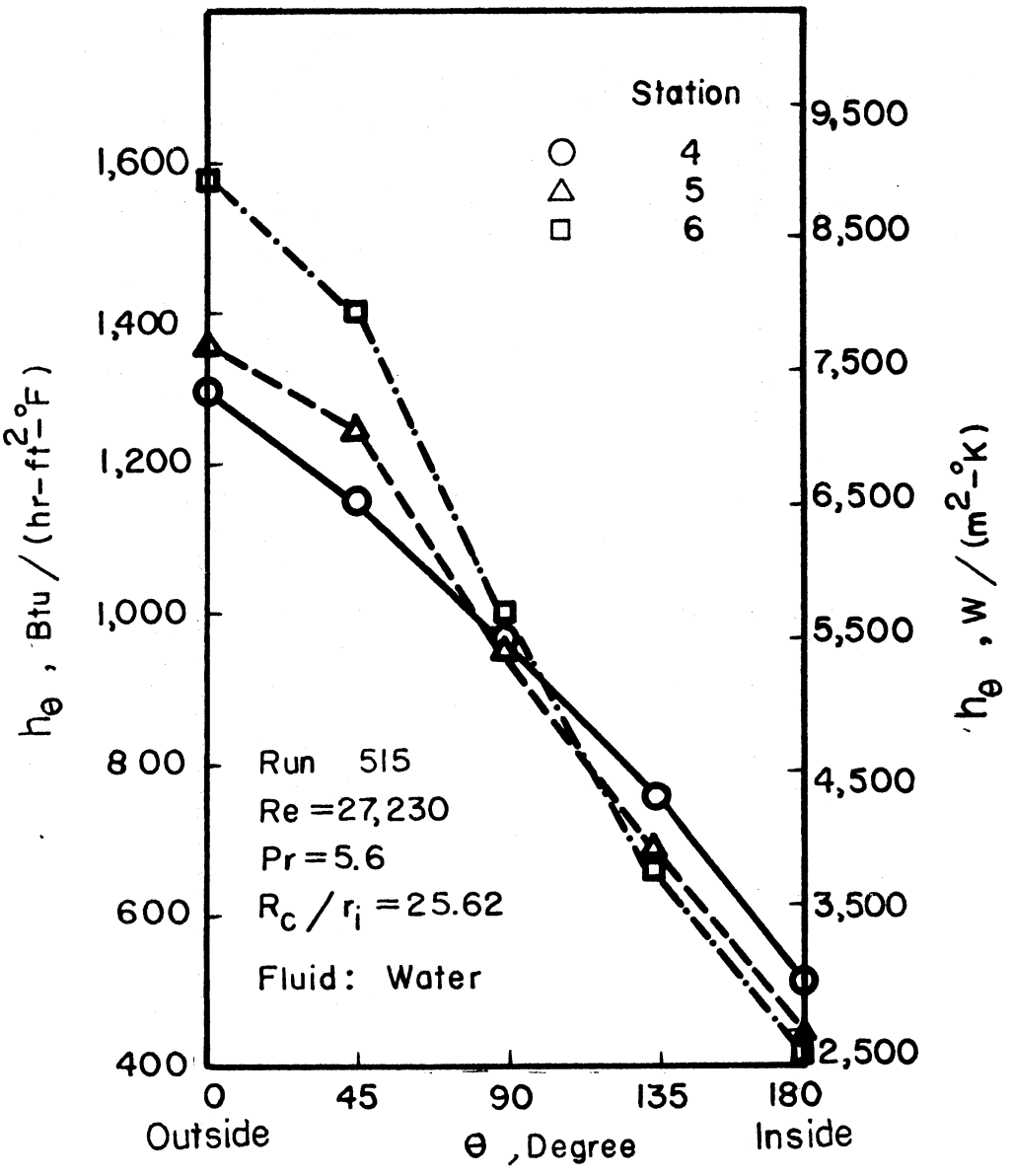

Figure 9. Peripheral Distribution of Heat Transfer Coefficient, Run 515

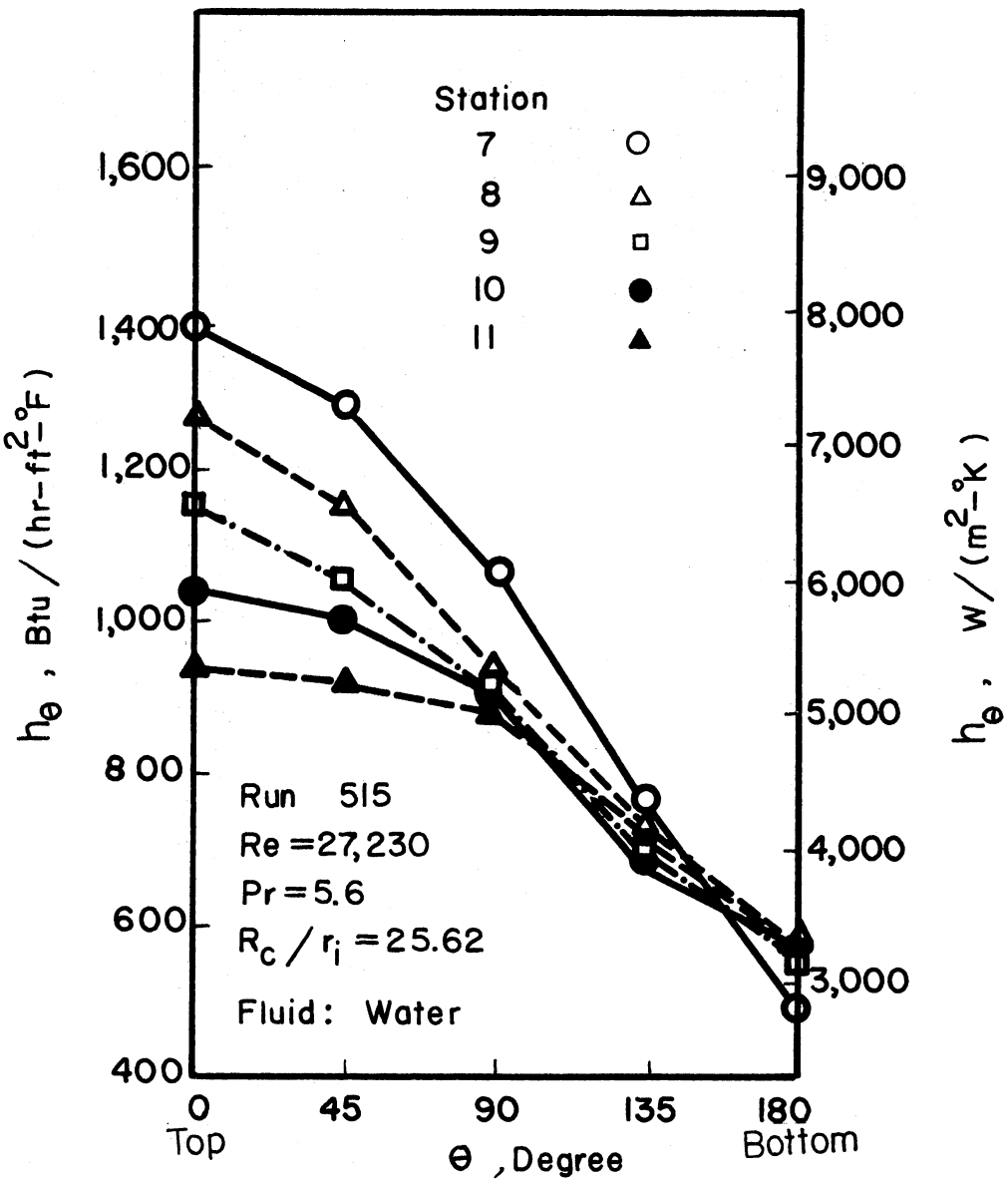

Figure 10. Peripheral Distribution of Heat Transfer Coefficient, Run 515

Figure 10 indicates that, as for the laminar flow regime, the secondary flow effect is carried to the straight section downstream of the bend, resulting in higher heat transfer coefficients at the top and lower heat transfer coefficients at the bottom of the tube. However, the tertiary flow does not become important at any of the measurement stations along the straight section downstream of the bend, and the secondary flow effect has not decayed out completely by station 11.

Curvature Ratio and Reynolds Number Effect

Peripheral distribution of heat transfer coefficients for runs 402, 419, 428, 514, 522, and 528 are presented in Figures 11 through 13. Runs 402 and 528 represent laminar regime; runs 428 and 522 represent transition regime, and runs 419 and 514 represent turbulent flow regime.

Figure 11 indicates that as the Reynolds number increases, from 765 to 23,890, the tertiary effect diminishes in the straight horizontal tube inlet. In other words, turbulent mixing destroys the tertiary flow pattern.

Figure 12 indicates that for the same Reynolds numbers, as the curvature ratio decreases, from 25.62 to 12.23, the heat transfer coefficient increases. This is due to the fact that the centrifugal force is inversely proportional to the curvature ratio: by decreasing the curvature ratio, the centrifugal force increases. Therefore, secondary flow becomes relatively stronger and causes higher heat

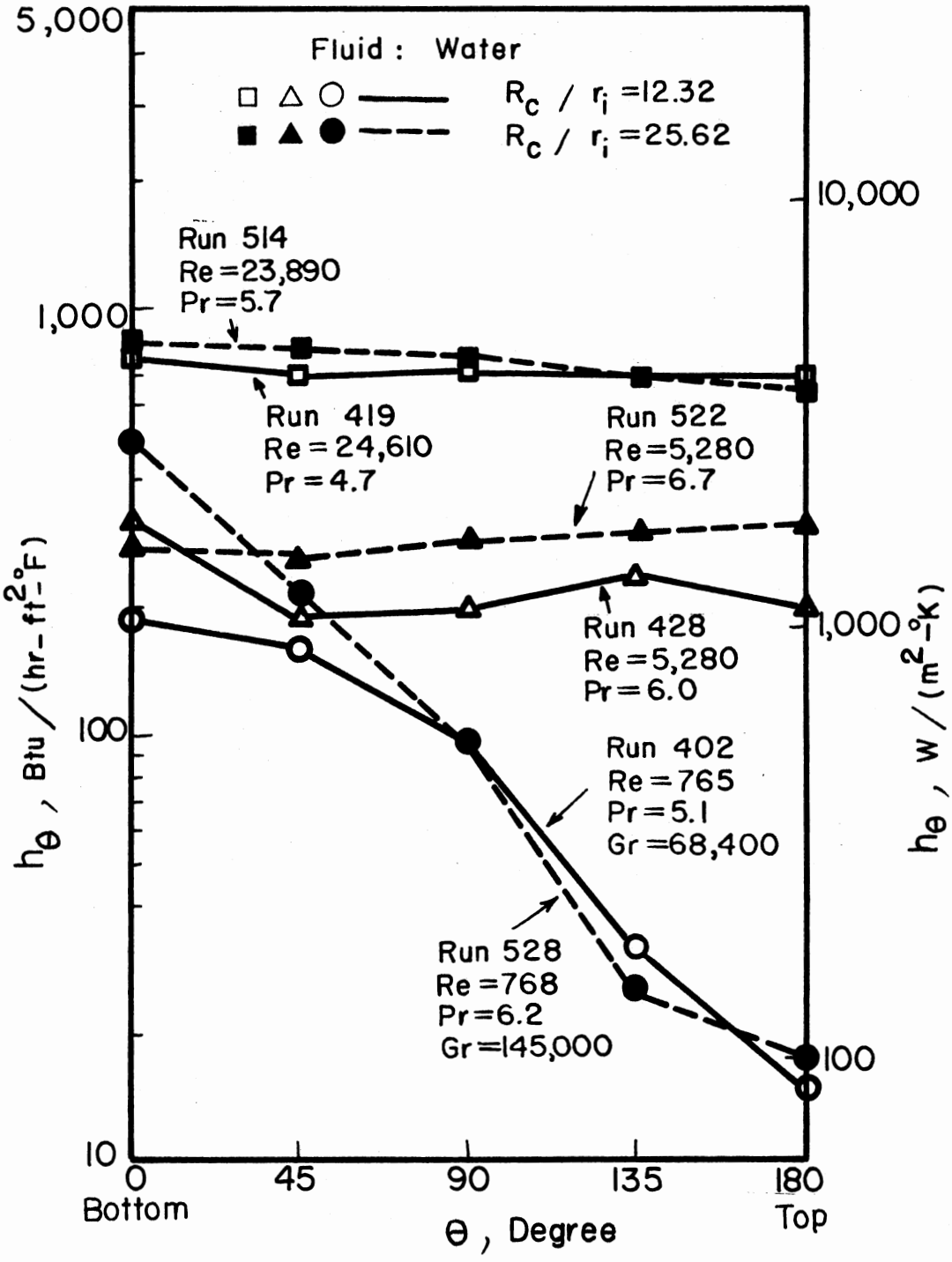

Figure 11. Effect of Curvature Ratio and Reynolds Number on Peripheral Distribution of Heat Transfer Coefficient at Station 3

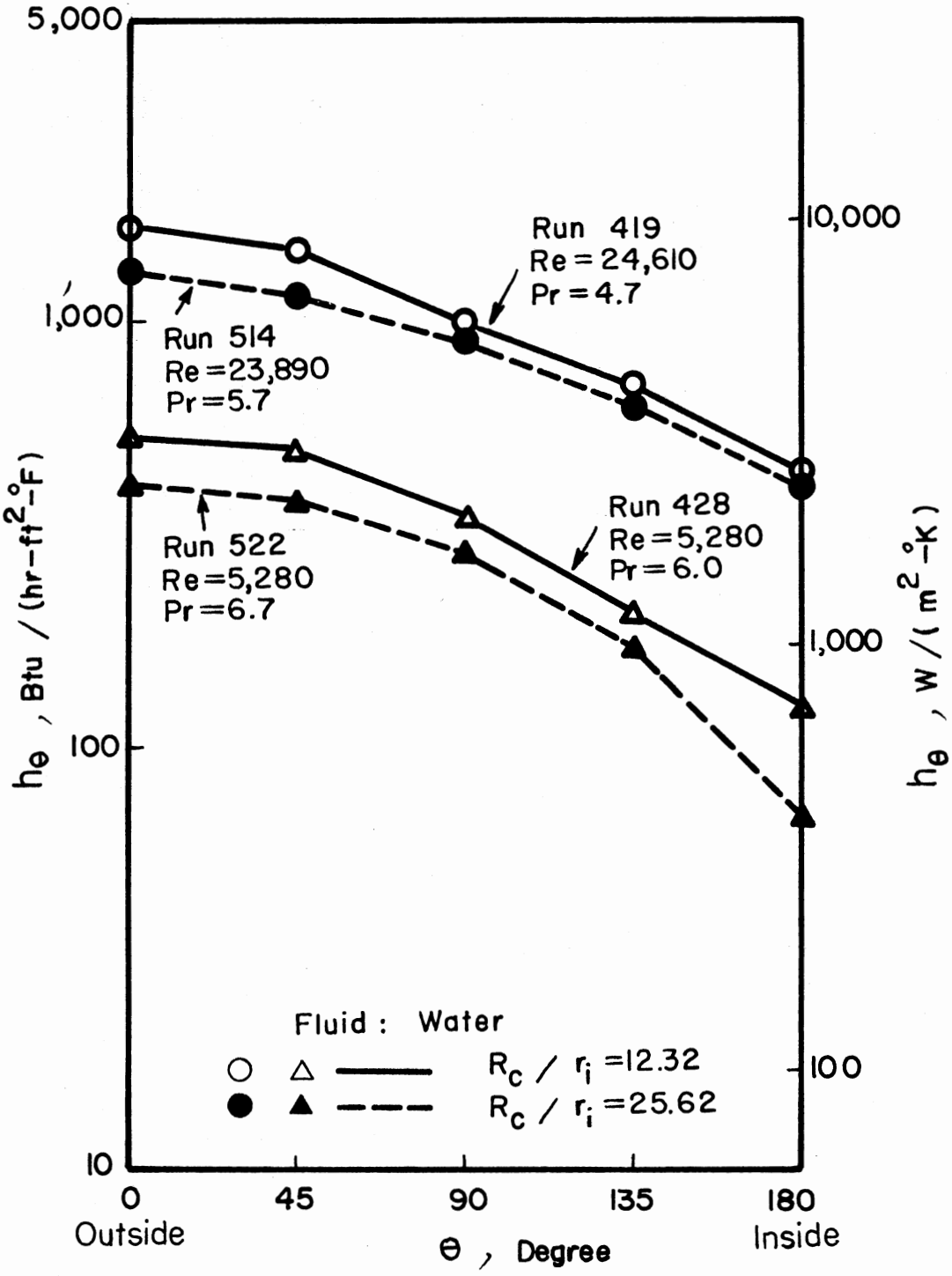

Figure 12. Effect of Curvature Ratio and Reynolds Number on Peripheral Distribution of Heat Transfer Coefficient at Station 5

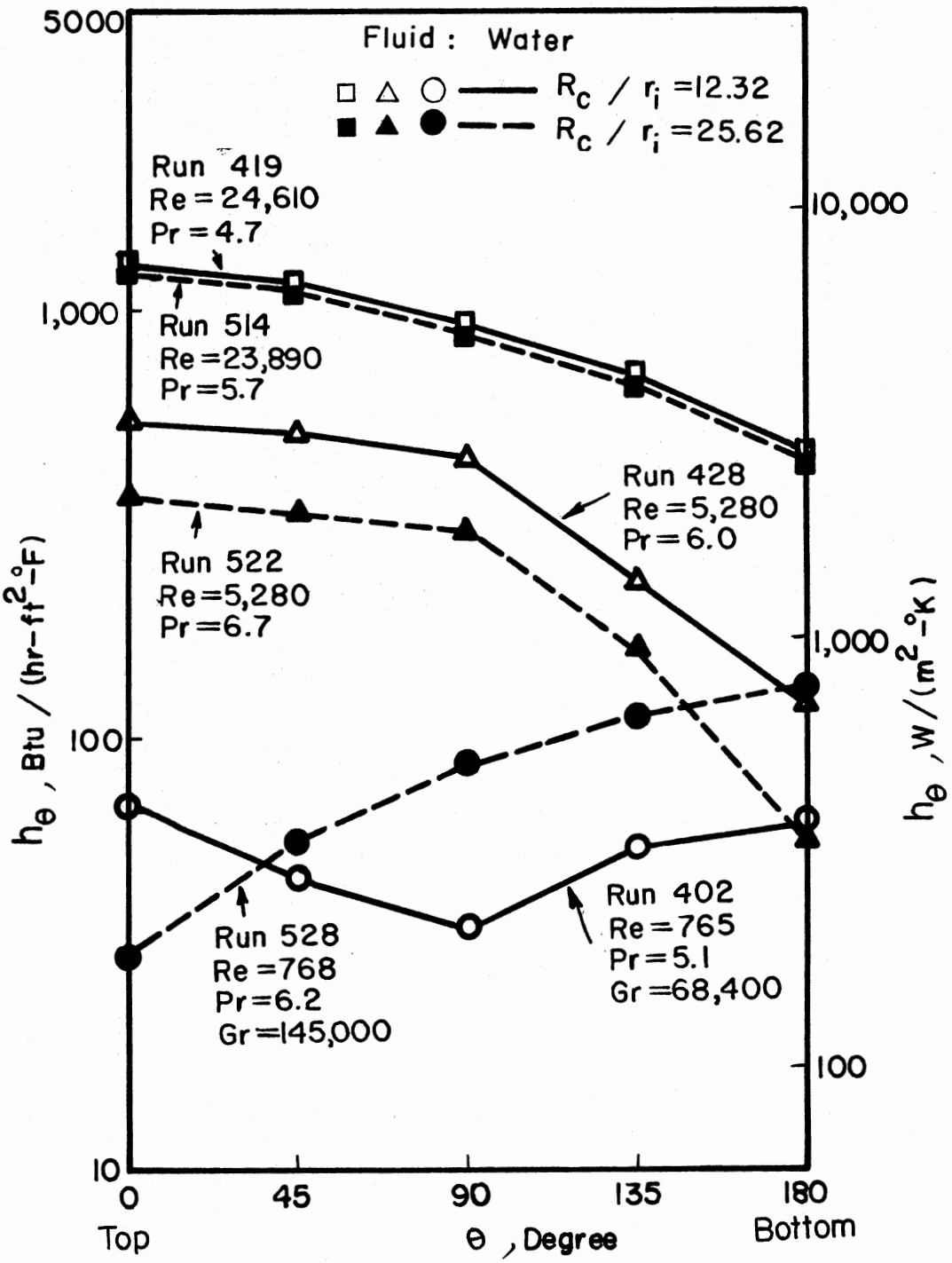

Figure 13. Effect of Curvature Ratio and Reynolds Number on Peripheral Distribution of Heat Transfer Coefficient at Station 7

transfer coefficients. The peripheral heat transfer coefficients for Reynolds numbers 765 and 768 are not shown on Figure 12 because at the outer wall of the bend the heat transfer coefficients were negative. "Negative heat transfer coefficients" are discussed in the following section of this chapter.

Figure 13 represents peripheral distribution of heat transfer coefficient at station 7. This figure indicates that for higher Reynolds number the secondary flow is carried to the straight section downstream of the bend. However, by decreasing the Reynolds number, from 5,280 to 765, the secondary flow becomes less important and the tertiary flow becomes important. Figure 13 also indicates that when the curvature ratio increases, from 12.32 (run 402) to 25.62 (run 528), the secondary flow diminishes; furthermore, the tertiary flow becomes more severe. Inspection of Figure 13 reveals also that, for the same Reynolds number, by decreasing the curvature ratio the heat transfer coefficient increases; however, for higher Reynolds number, e.g. turbulent flow regime, the curvature ratio becomes less significant.

Negative Heat Transfer Coefficient

As presented in Appendix F, some of the calculated heated transfer coefficients for the outer wall of the bend are negative. Analysis of these negative heat transfer coefficients indicates that they occur for the cases of low Prandtl number (water data) and in the laminar regime. These negative heat transfer coefficients could be attributed to the effect of peripheral heat flux variation.

Kays (16) has shown that if the peripheral variation of heat flux, for a circular pipe, can be represented by

$$\dot{q}''_\theta = \dot{q}''_a \ (1 + b \cos \theta) \tag{6.5}$$

then the energy equation for laminar fully developed flow, constant heat rate (axially) gives:

$$Nu_\theta = \frac{1 + b \cos \theta}{\frac{11}{48} + (b/2) \cos \theta} \tag{6.6}$$

If b=0, then Nusselt number becomes independent of θ and equal to 4.364 as would be expected.

Depending upon the magnitude of b the Nusselt number can vary in very strange ways. For example, if b = 0.458, the Nusselt number goes to infinity at $\theta=\pi$. Here an infinite Nusselt number merely means that the surface temperature is the same as the bulk fluid temperature and does not imply an infinite heat flux.

Similarly, for fluid flow between parallel planes, with $\dot{q}''_1$ and $\dot{q}''_2$ the heat fluxes through plane 1 and 2, the Nusselt number is given by the following expression (16):

$$Nu_1 = \frac{5.385}{1-0.346(\dot{q}''_1/\dot{q}''_2)} \tag{6.7}$$

If $\dot{q}''_2 = 0$, $Nu_1 = 5.385$, which is of course the solution for one side only heated. If both sides are heated equally, $\dot{q}''_2/\dot{q}''_1 = 1$, and then $Nu_1 = Nu_2 = 8.23$. Now note what happens if

$$0.346 \ (\dot{q}''_2/\dot{q}''_1) = 1 \tag{6.8}$$

In this case

$$Nu_1 = \infty \tag{6.9}$$

and

$$\dot{q}''_2/\dot{q}''_1 = 2.9 \qquad (6.10)$$

Again, this does not imply an infinite heat transfer rate; it implies that $T_{w_1} - T_b = 0$ because of the temperature profile shown in Figure 14.

If $\dot{q}''_2/\dot{q}''_1 < 2.9$ the apparent Nusselt number and the apparent heat transfer coefficient become negative.

As an example, peripheral distributions of inside wall heat flux and inside wall temperature at station 5 (middle of the bend) for runs 215 and 203 are shown on Figure 15 and 16, respectively. Table IV also gives the calculated heat transfer coefficients at station 5 for these two runs. For run 215, in which the peripheral distribution of wall heat flux is highly nonuniform, negative heat transfer coefficients have been obtained on the outer wall region of the bend. However, by increasing Reynolds number (e.g., from 1317 to 3600) all of the calculated heat transfer coefficients become positive. By increasing the Reynolds number, the effect of secondary flow due to centrifugal force in the bend is lessened due to increased mixing associated with a high Reynolds number. So, the secondary flow is more pronounced for low Reynolds numbers than for high Reynolds numbers. At the same time, analysis of the calculated values (see Appendix F) indicates that by increasing the Prandtl number, negative heat transfer coefficients become positive. This means that increasing the Prandtl number (diffusivity for velocity becomes greater than the diffusivity for heat) has the same qualitative effect as increasing the Reynolds number. Both changes indicate an increase in the mixing

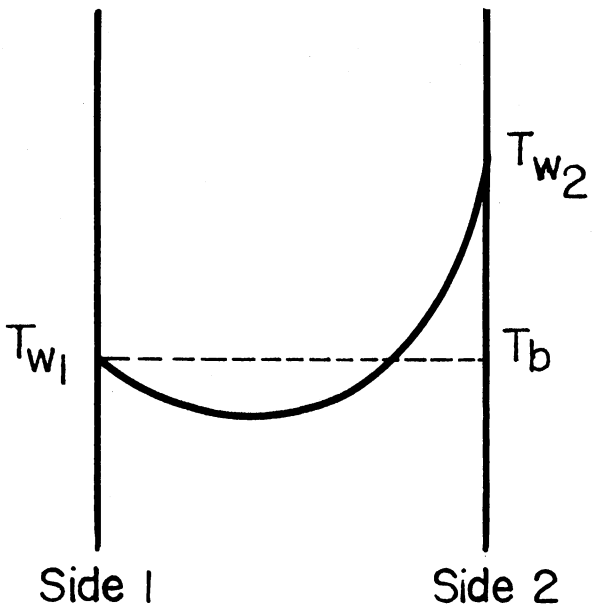

Figure 14. Tempeature Profile Between Two Parallel Planes

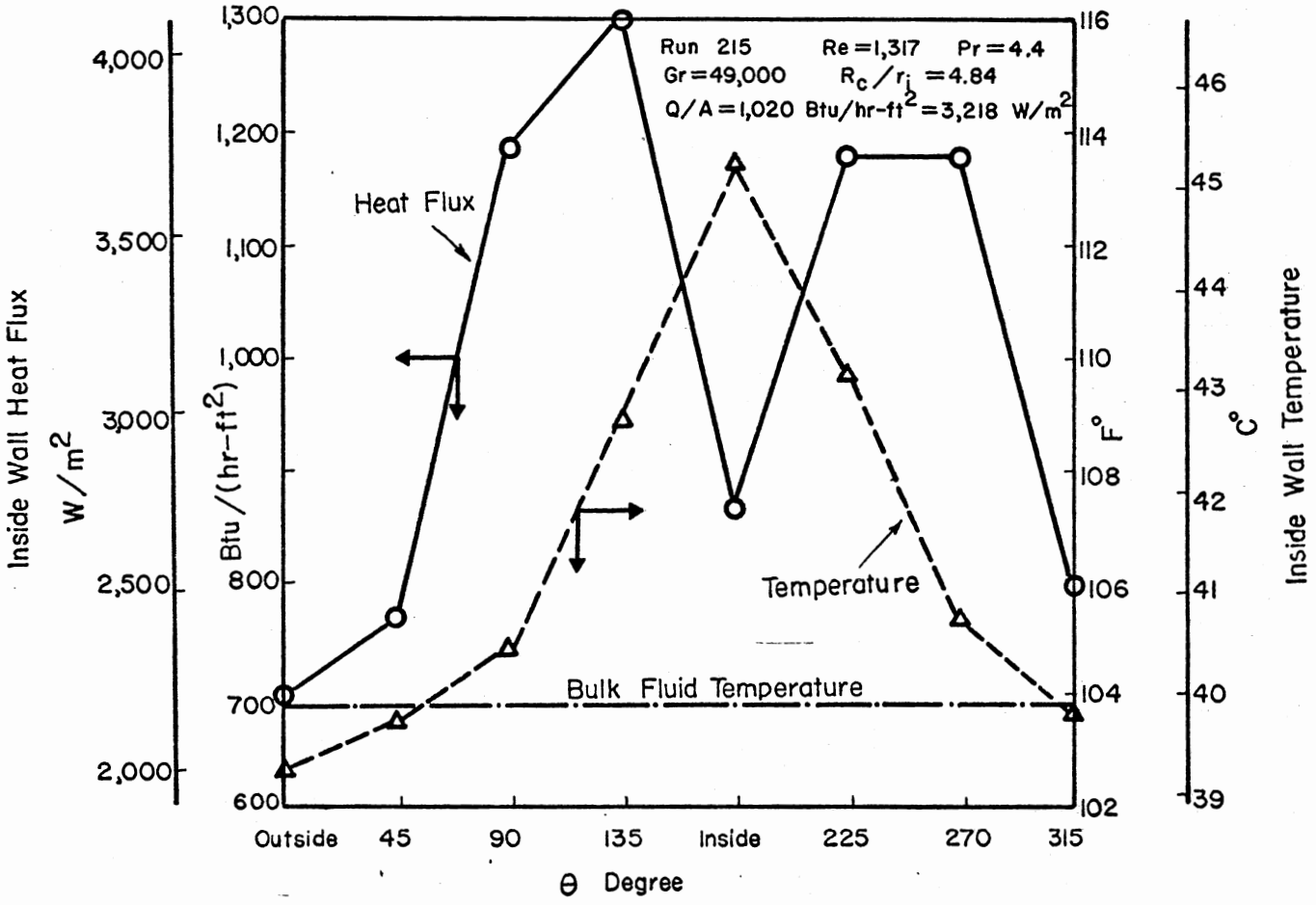

Figure 15. Peripheral Distribution of Inside Wall Heat Flux and Inside Wall Temperature at Station 5

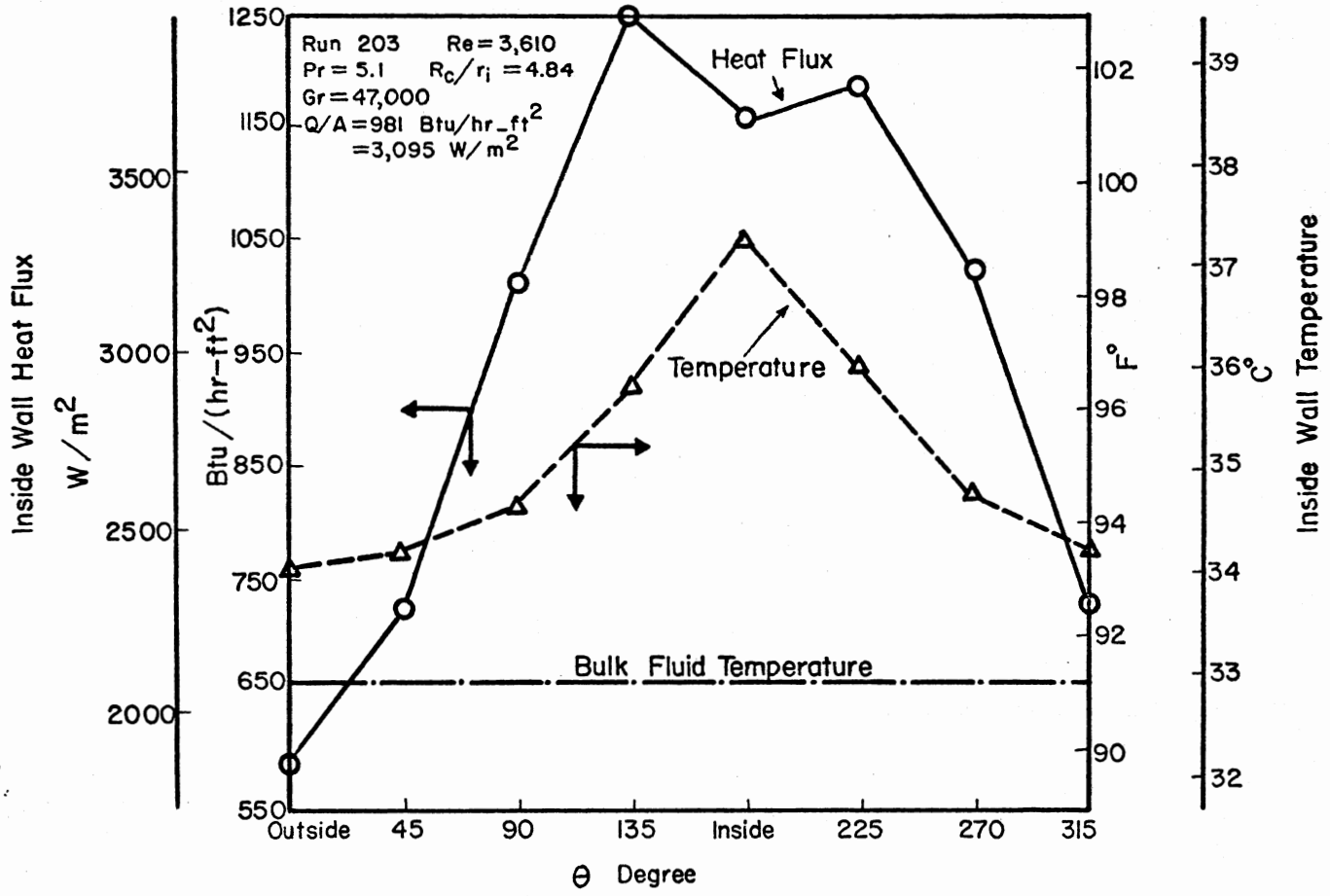

Figure 16. Peripheral Distribution of Inside Wall Heat Flux and Inside Wall Temperature at Station 5

TABLE IV

PERIPHERAL HEAT TRANSFER COEFFICIENT AT STATION 5, BTU/HR-FT^2-^{o}F

Run	Re	Pr	Peripheral Position, Degrees							
			Outside	45	90	135	Inside	235	270	315
215	1,317	4.4	-611(3,469)*	-2056(-11,675)	1204(6,836)	259(1470)	91(517)	201(1,141)	792(4,497)	-2828(-16,058)
203	3,600	5.1	290(1,647)	323(1,834)	332(1,885)	149(846)	212(1,203)	315(1,788)	315(1,788)	310(1,760)

* The numbers in parentheses are in SI units (W/m^2-K).

process, which lessens the relative importance of the secondary flow.

Reynolds Number Effect on the Interaction Between Secondary and Tertiary Flows

As mentioned in the preceding sections, when the fluid enters the straight section downstream of the bend it carries the effect of secondary flow to some distance along the test section. This distance depends mainly on the curvature ratio and the Reynolds number. In Figure 17 the ratios of the heat transfer coefficient at the top of the tube to the heat transfer coefficient at the bottom of the tube are plotted as a function of axial position and Reynolds number as a parameter. If this ratio is greater than one, it means secondary flow is dominating. On the other hand if the ratio of heat transfer coefficients is less than one, it indicates that the tertiary flow (natural convection) is dominating.

For Re = 184, the ratio of heat transfer coefficients is about 2 at station 7 located at the end of the bend. As the fluid moves along the straight section, downstream of the bend, the effect of the secondary flow diminishes. For example, somewhere between stations 7 and 8, the ratio becomes equal to unity. The value of unity for the ratio of heat transfer coefficients coulg be an indication that the secondary flow and the tertiary flow effects cancel each other since their flow directions are opposite to each other. Beyond station 8 (see Figure 17, for Re = 184), the tertiary flow is dominating.

The secondary flow action becomes stronger for higher Reynolds number. Therefore, the point where the value of unity for the heat

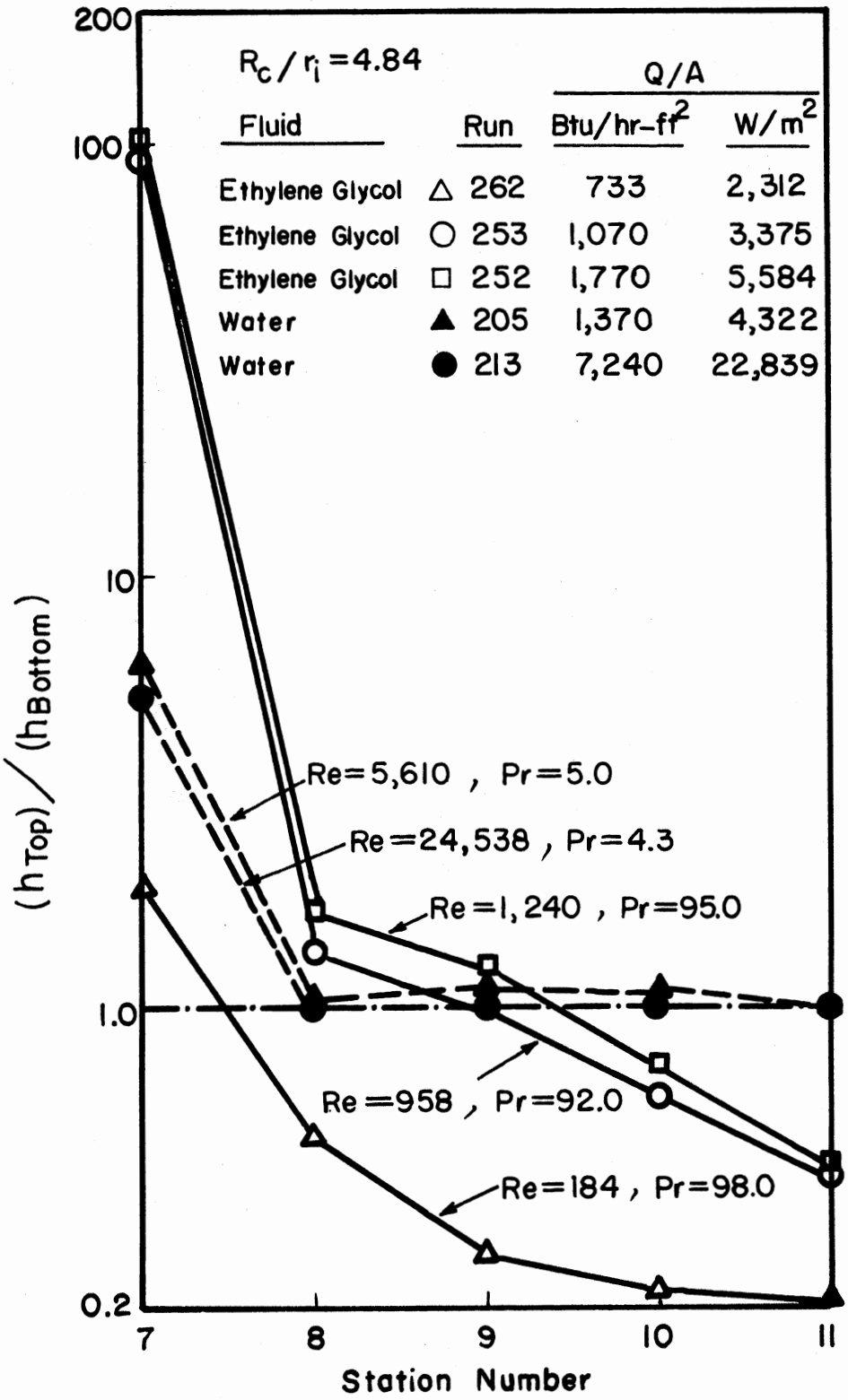

Figure 17. Effect of Reynolds Number on the Interaction Between Secondary and Tertiary Flows

transfer coefficients ratio occurs shifts further away from the bend. For example, when Reynolds number increases from 184 to 958 the position of equality of the heat transfer coefficients (top and bottom) shifts from between station 7 and 8 to station 9. In addition to Reynolds number dependence, this shift also depends on the magnitude of $\Delta T = \bar{T}_w - T_b$. Here $\bar{T}_w$ is the average inside wall temperature and T_b is the bulk fluid temperature at the thermocouple station.

In the turbulent flow regime, as shown in Figure 17, heat transfer coefficient at the top of the tube is greater than heat transfer coefficient at the bottom by a factor of 5 at station 7. However, the ratio approaches unity and remain at unity as the fluid moves away from the bend. This means as the fluid moves away from the bend the secondary flow effect diminishes and tertiary flow (natural convection) does not become significant at any point.

Comparison with Straight Tube Under Similar Flow Conditions

The peripheral average heat transfer coefficient at each station along the test section was calculated using Equation (6-1) and was compared to the following correlations:

Sieder-Tate (17); Re $>$2100

$$Nu = 0.023\ Re^{0.8}\ Pr^{0.333}\ (\mu_b/\mu_w)^{0.14} \qquad (6\text{-}11)$$

The reported mean absolute deviation for Equation (6-11) is 10.00 percent (water and Re $>$10,000).

Dittus-Boelter (18); $Re > 2100$

$$Nu = 0.023\ Re^{0.8}\ Pr^{0.4} \tag{6-12}$$

The reported root-mean-square error for Equation (6-12) is 16.66 percent ($3.16 < Pr < 10$ and $10{,}000 < Re < 32{,}000$).

Eagle-Ferguson (19) (for water only); $Re > 2100$

$$h = c\ (1.75\ T_b + 160)\ V^{0.80} \tag{6-13A}$$

where

$$c = 0.9109 - 0.4292\ \log\ (d_i) \tag{6-13B}$$

Morcos-Bergles (15); $Re < 2100$

$$Nu = \left\{(4.36)^2 + \left[0.055\left(\frac{GrPr^{1.35}}{P_w^{0.25}}\right)^{0.4}\right]^2\right\}^{1/2} \tag{6-14}$$

for

$$3 \times 10^4 < Ra < 10^6,\ 4 < Pr < 175 \text{ and } 2 < P_w < 66$$

where

$$P_w = \frac{hd_i^2}{k_w t} \tag{6-15}$$

Here t = tube wall thickness and k_w = thermal conductivity of tube wall. In Equation (6-14), the average heat transfer coefficient is defined as in Equation (6-2), therefore, for $Re < 2100$ the peripheral average coefficient was calculated by Equation (6-2).

Appendix F presents the comparison between the experimental and predicted heat transfer coefficient at each station along the test section for each experimental run.

Turbulent Flow Regime

In addition to Appendix F, Figure 18 presents the comparison of the experimental heat transfer coefficient with the heat transfer coefficient predicted by the Sieder-Tate correlation. At station 1, the experimental heat transfer coefficient is greater than that predicted by Sieder-Tate. This is attributed to entrance effects. However at station 2 and 3 (both located along the straight section upstream of the bend) the agreement is excellent.

At stations 4, 5, 6 (in the bend), and 7 (at the end of the bend) the experimental heat transfer coefficients are higher than those predicted by literature correlations for a straight tube under similar flow conditions. The higher heat transfer coefficients are attributed to the secondary flow due to the centrifugal action superimposed on the primary flow along the tube axis. As mentioned in the preceding section, the secondary flow effect is carried to the straight section downstream of the bend. That is why the heat transfer coefficients along the straight section downstream of the bend are higher, up to station 11, than those predicted for a straight tube which is not preceded by a 180^{o} bend. At station 11 the agreement between the experimental heat transfer coefficient and the predicted heat transfer coefficient is excellent because the secondary flow effect has decayed.

Figure 19 also gives the comparison between experimental heat transfer coefficients and those predicted by the Eagle-Ferguson correlation.

Laminar Flow Regime

Figure 20 presents the comparison between the experimental heat

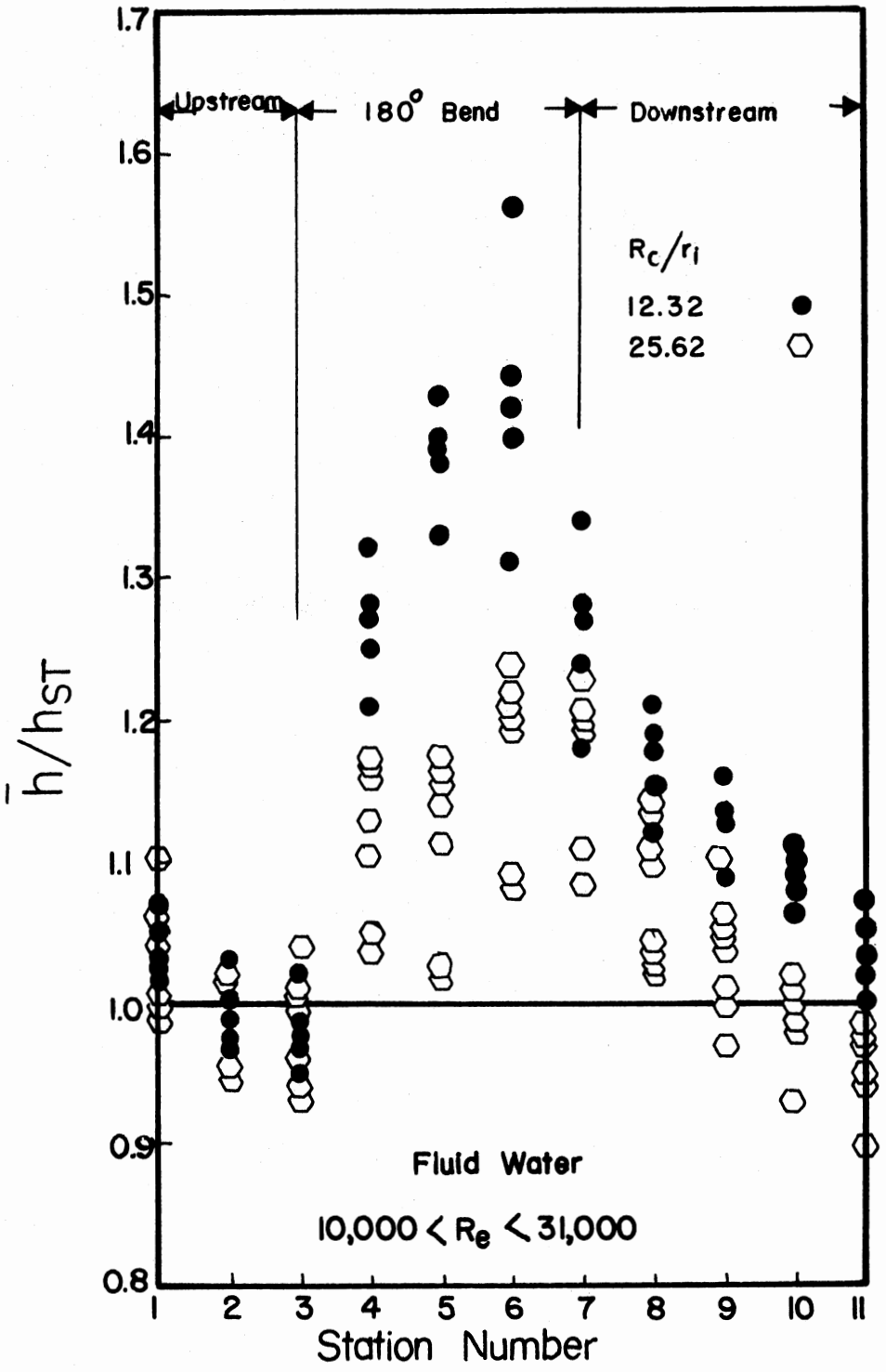

Figure 18. Comparison of Peripheral Average Heat Transfer with that Predicted by Sieder-Tate Equation

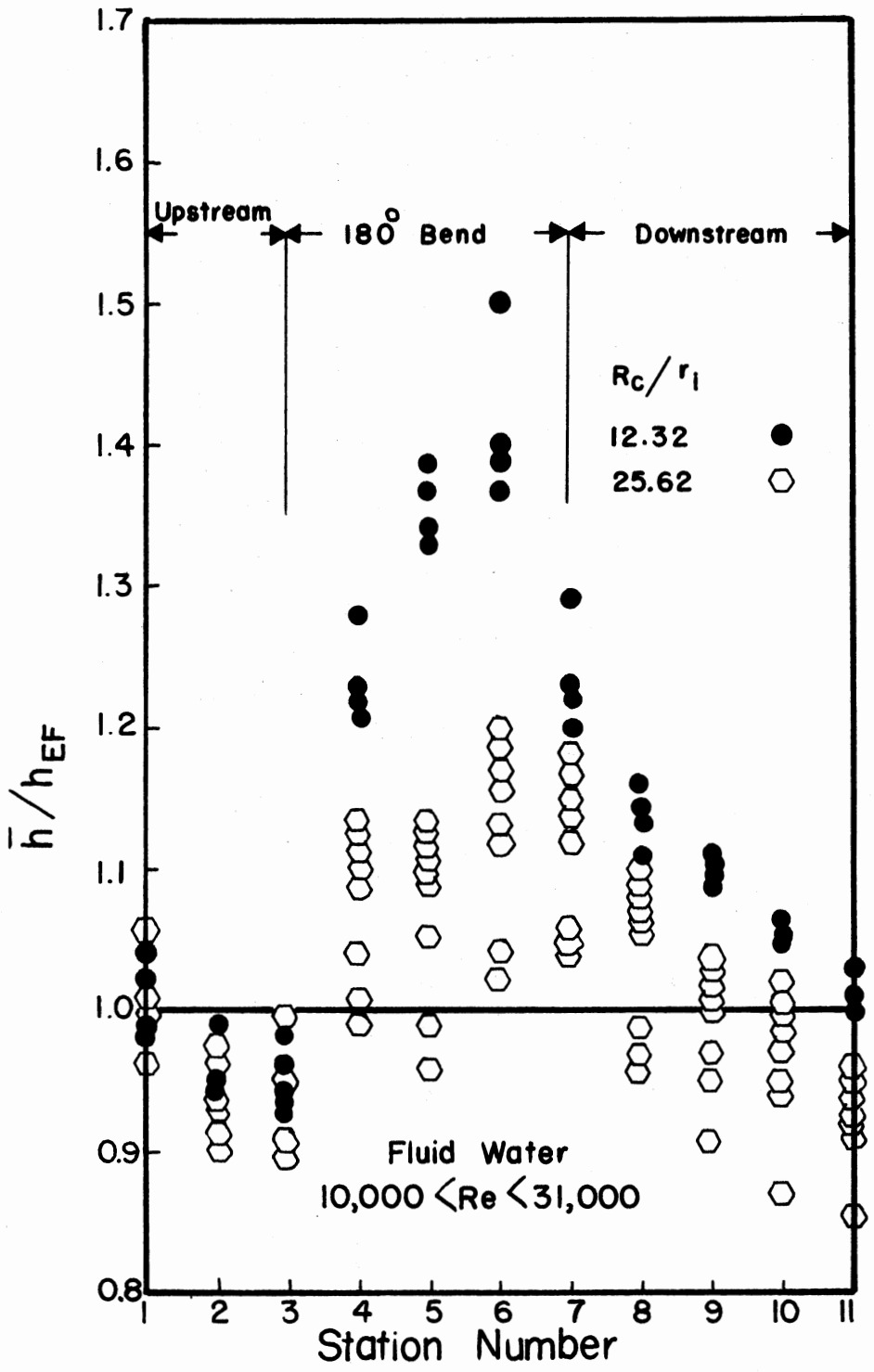

Figure 19. Comparison of Peripheral Average Heat Transfer with that Predicted by Eagle-Ferguson Equation

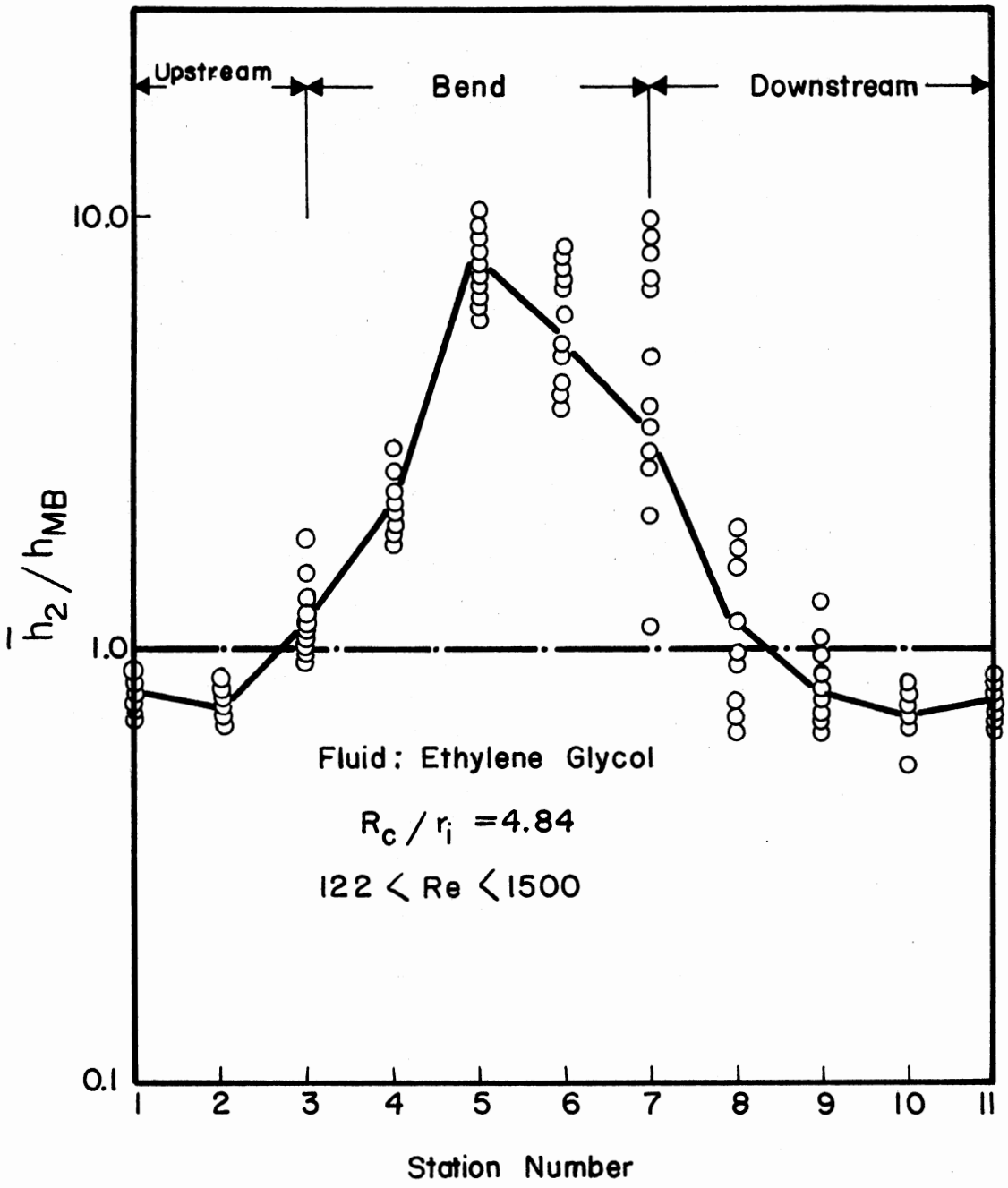

Figure 20. Comparison of Experimental Heat Transfer Coefficient with that Predicted by Morcos-Bergles Equation

transfer coefficient and the heat transfer coefficient predicted by the Morcos-Bergles correlation. The Morcos-Bergles correlation is chosen because it takes into account the effect of tertiary flow (natural convection) in laminar flow regime. The agreement between the experimental and the predicted heat transfer coefficient is not as good as obtained for turbulent flow. This can be explained by the fact that the mechanism of flow in the laminar regime is complicated due to the presence of both secondary and tertiary flows and their interaction. Even though the Morcos-Bergles correlation takes into account the tertiary flow effect, it is applicable only for fully developed flow, without the presence of the secondary flow. That is why the agreement at station 3 is excellent. Inspection of the comparison at station 3 also indicates that for Reynolds number greater than 1000, the Morcos-Bergles correlation underpredicts the heat transfer coefficient.

As shown on Figure 20, in the bend, the ratio of experimental heat transfer coefficient is about 2 to 10 times higher than the heat transfer coefficient predicted by straight tube correlation. The higher heat transfer coefficient in the bend is attributed to the secondary flow superimposed on the primary flow.

For a purely laminar flow where the transport processes are molecular in origin the effect of secondary flow is more pronounced. However, in turbulent flow regime where turbulent diffusivities are very much greater than for a purely molecular process the effect of secondary flow is less pronounced. That is why the ratio of heat transfer coefficients (shown on Figure 20) reaches 10 for laminar flow regime and only about 1.5 for turbulent flow regime. The secondary

flow removes the heated molecules from the vicinity of the wall, thus providing a better temperature gradient for the molecular transport (conduction) process.

Testing of Literature Correlations

Available literature correlations for the U-bend were tested against the experimental results to determine how well the two agreed. The average absolute percent deviation (AAPD) was used as a measure to determine the degree of fit of the literature correlations to the experimental data. Results of the tests are given in Table V for turbulent flow.

The AAPD is defined as follows:

$$AAPD = \frac{\sum_{i=1}^{n} \left[\left| \left\{ \frac{\left(\begin{matrix}\text{Calculated} \\ \text{Value}\end{matrix}\right) - \left(\begin{matrix}\text{Experimental} \\ \text{Value}\end{matrix}\right)}{(\text{Experimental Value})} \right\} \{100\} \right| \right]_i}{n} \qquad (6\text{-}16)$$

where n is the total number of data points evaluated and the summation is performed over all data runs evaluated.

Further discussion of the heat transfer results is subdivided into three sections depending upon the fluid flow regime. Reynolds number is used as the criterion to determine the flow regime. The three flow regimes and the Reynolds number range for each regime are:

1. Turbulent flow regime $Re \geqslant 10{,}000$;
2. Transition flow regime $2100 \leqslant Re \leqslant 10{,}000$;
3. Laminar flow regime $Re \leqslant 2100$.

TABLE V

TEST RESULTS OF LITERATURE CORRELATIONS FITTED TO EXPERIMENTAL DATA FOR THE TURBULENT FLOW REGIME

Investigator(s)	Reference	Stated Range of Applicability	AAPD%	Stations
Lis and Thellwell	(1)	$10^4 \leqslant Re \leqslant 9 \times 10^4$ $1 \leqslant X^*/d_i \leqslant 15,\ 2 \leqslant R_c/r_i \leqslant 4$	4.48	8,9,10,11
Tailby-Staddon	(4)	$10^4 \leqslant Re$ $7 \leqslant X/d \leqslant 30\ ,\ 4 \leqslant R_c/r_i \leqslant 14$	30.78	7,8,9,10,11
Present Work		$10^4 \leqslant Re \leqslant 3 \times 10^4$ $\frac{\pi}{2}(R_c/r_i) \leqslant (X/d_i) \leqslant 160,\ 4.84 \leqslant R_c/r_i \leqslant 25.62$	5.84 4.5	7,8,9,10,11 8,9,10,11
Present Work		$10^4 \leqslant Re \leqslant 3 \times 10^4$ $0 < (X/d_i) \leqslant \frac{\pi}{2}(R_c/r_i),\ 4.84 \leqslant R_c/r_i \leqslant 2.56$	8.71	4,5,6,7

Turbulent Flow Regime

Experimental data in the turbulent flow regime were gathered using water. In all, 207 points were obtained in the turbulent flow regime.

Literature correlations were tested against the experimental results to determine how well the two agreed. Test results are given in Table V for the four test sections. It may be noted from Table V that the Lis-Thelwell (1) correlation gave the best fit of the data.

Both of the available correlations were valid only for a small portion of straight section downstream of the bend; however, all of the experimental data at stations 7 through 11 are tested against the Tailby-Staddon (4) correlation. The Tailby-Staddon correlation was obtained for the case of cooling of the fluid whereas the data of this work were obtained for the case of heating of the fluid. That is probably why the AAPD is high for Tailby-Staddon correlation. In testing the Lis-Thellwell correlation, station 7 corresponded to $X^*/d_i = 0$ which was out of the recommended range ($1 \leq X^*/d_i \leq 15$) and predicted infinite heat transfer coefficient; therefore, the data at station 7 were not used for this test.

Development of Correlation

Turbulent Flow Regime

Since the literature correlations do not cover the bend portion of the test section, an attempt was made to find a correlation which would cover both the bend and the straight section downstream from the bend.

Due to the complex mechanism of secondary flow the attempt failed. Therefore, the test section was divided into two parts, the bend and the straight section downstream of the bend.

It follows from the previous discussions that in a correlation of J_X in terms of X/d_i and R_c/r_i, the effects of both of these ratios should be expressed as functions of the Reynolds number. In view of the complexity and doubtful utility in practical computations, no attempt has been made to obtain such correlations and a comparatively simple correlation was obtained instead. A correlation of the local values of the heat transfer parameter, J_X, was obtained in the following way. A correlation similar to the literature correlations was assumed as follows,

$$J_X = \frac{Nu}{Pr^{0.4}(\mu_b/\mu_w)^{0.14}} = aRe^b\,(X/d_i)^m(R_c/r_i)^n \qquad (6\text{-}17)$$

Then computer programs written by Chandler (20) were used to fit the experimental data to the above equation and estimate the parameters.

The data at stations 7 through 11 were used to find a correlation for the straight section downstream of the bend. For this section the following correlation was obtained.

$$J_X = 0.031\ Re^{0.825}\ (X/d_i)^{-0.116}(R_c/r_i)^{-0.048} \qquad (6\text{-}18)$$

where $10^4 \leqslant Re \leqslant 3 \times 10^4$, $\frac{\pi}{2}(R_c/r_i) \leqslant X/d_i \leqslant 160$, and $4.84 \leqslant (R_c/r_i) \leqslant 25.62$. In the above equation $X/d_i = 0$ represents station 3 which is at the entrance of the bend.

Similarly the data at stations 4 through 7 were used to fit the experimental data to Equation (6-17) to estimate the parameters for

the bend portion of the test section. The following correlation was obtained for this region.

$$J_X = 0.0285\ Re^{0.81}(X/d_i)^{0.046}(R_c/r_i)^{-0.133} \qquad (6\text{-}19)$$

where $10^4 \leq Re \leq 3 \times 10^4$, $0 < (X/d_i) \leq \frac{\pi}{2}(R_c/r_i)$, and $4.84 \leq (R_c/r_i) \leq 25.62$.

The AAPD's for Equations (6-18) and (6-19) are also given in Table V. In addition to Table V, Figures 21 and 22 give representation of how well the experimental data are fitted to Equations (6-18) and (6-19).

Transition Flow Regime

Of the experimental data gathered, 46 runs fell in the transition regime.

In most industrial processes, operation in the transition regime is avoided. However, should it be necessary, the heat transfer coefficient for transition regime fluid flow may be determined by extending the laminar and turbulent flow regime calculations into transition regime and interpolating between the values obtained from the turbulent and the laminar flow regime correlations at the Reynolds number in the transition regime.

Based on the foregoing discussion, no attempt was made to develop a correlation for prediction of the heat transfer coefficient in the transition regime. However, Equation (6-18), which was developed for turbulent flow along the straight section downstream of the bend, was used to predict the heat transfer parameter, J_X, in the transition regime along the straight section downstream of the bend. The AAPD between the predicted and the experimental heat transfer parameters for the 205 data points ($3000 < Re < 10{,}000$) tested was 13.28 percent.

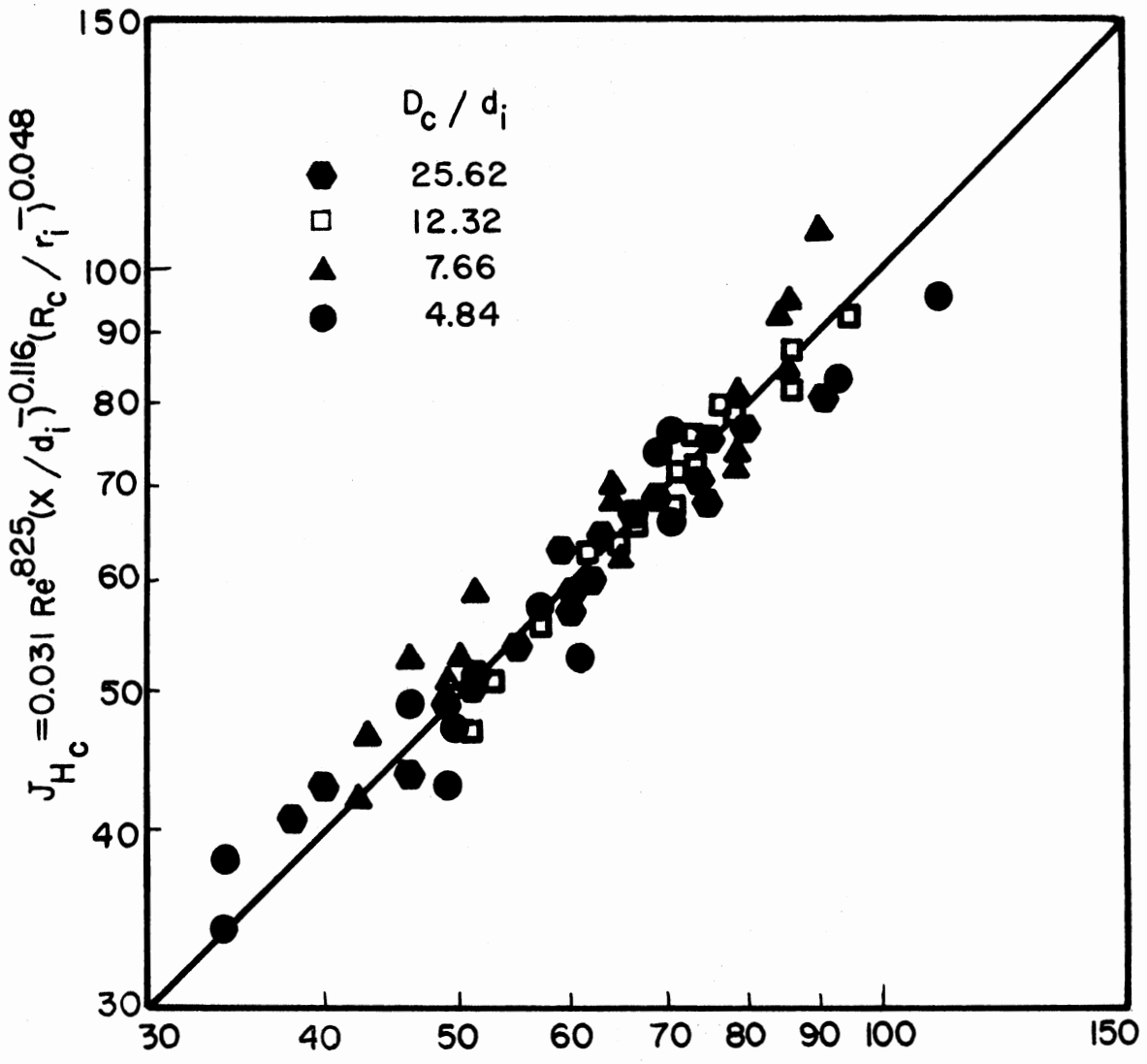

$$J_{H_E} = \frac{Nu}{Pr^{0.4}(\mu_b / \mu_w)^{0.14}}$$

Figure 21. Comparison Between Predicted and Experimental Heat Transfer Coefficients in a Straight Pipe Preceded by a 180^0 Bend

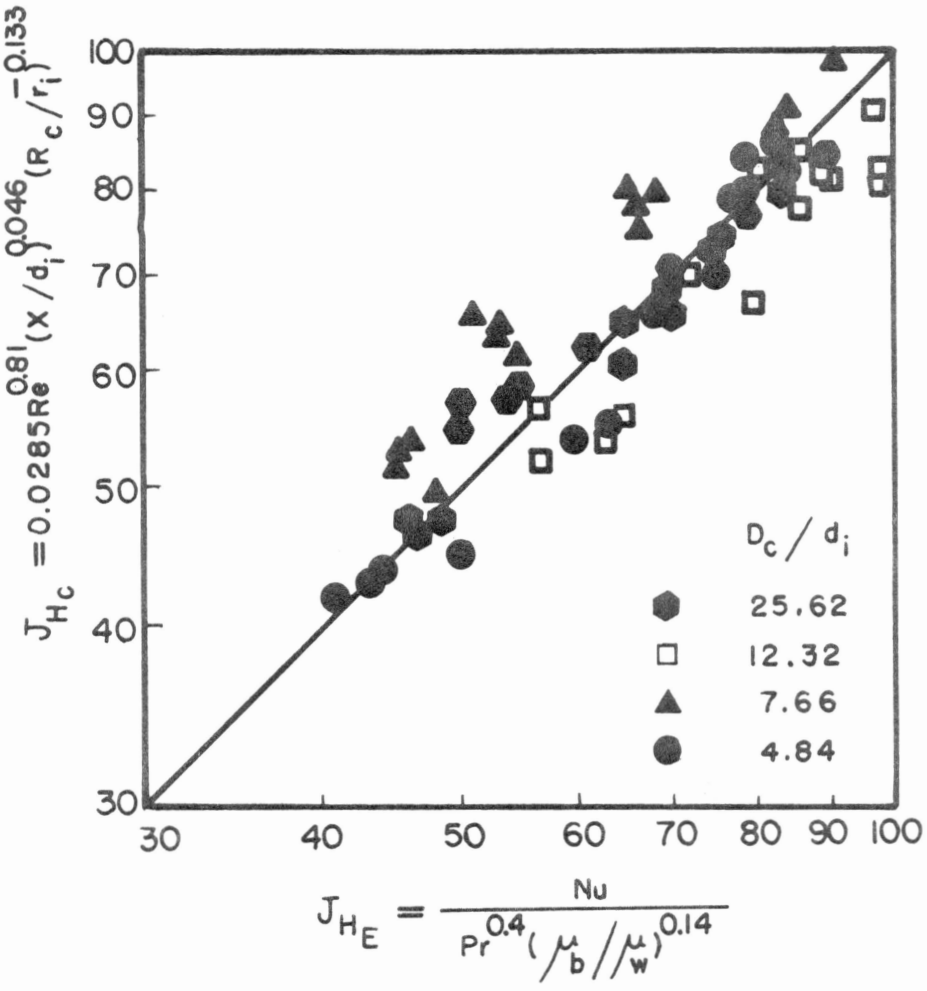

Figure 22. Comparison Between Predicted and Experimental Heat Transfer Coefficients in a 180° Bend

Laminar Flow Regime

Experimental data in the laminar flow regime were gathered using water, Dowtherm G and ethylene glycol. In all, 79 runs were obtained in the laminar flow regime.

There was no literature correlation to test against the experimental results for the bend portion and the straight section downstream of the bend.

As indicated earlier in this chapter, higher heat transfer coefficients were obtained for fluid flow in the bend. The heat transfer coefficients were about two to ten times the value for the straight tube under otherwise similar operating conditions. The higher heat transfer coefficients are attributed to the superimposed secondary flow due to centrifugal action.

Attempts were made to correlate the data in the bend portion of the test section but no satisfactory correlation could be developed that would fit the data satisfactorily.

For the straight section downstream of the bend, in addition to the secondary flow due to the bend, a tertiary flow due to natural convection was also detected. These two factors were acting in opposite directions. Figure 23 gives idealized flow patterns for the secondary and tertiary flows in a straight section preceded by 180^{o} bend. Depending on the heat flux and Reynolds number, the combination of these two effects could either increase or decrease the heat transfer coefficient compared to the undisturbed flow.

Due to presence of natural convection (tertiary flow), secondary flow and their interaction a simplified correlation such as Equation

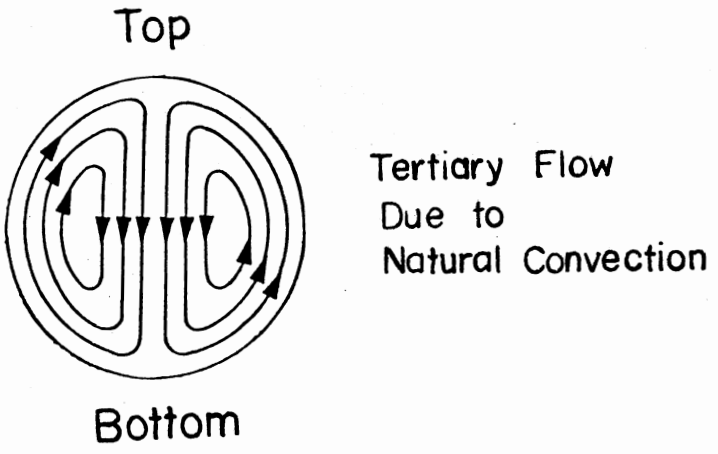

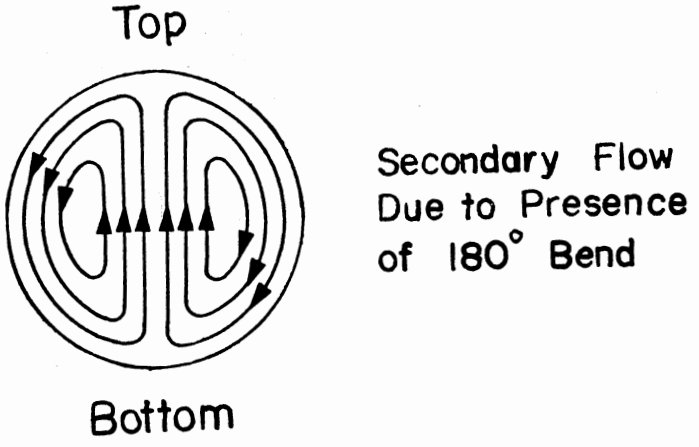

Figure 23. Idealized Secondary and Tertiary Flow Patterns Downstream from the U-Bend

(6-17) could not be obtained. The nondimensional group Gr/Re^2 was used to determine quantitatively the significance of natural convection with respect to forced convection. In addition, the nondimensional ratio, R_c/r_i, was used to represent quantitatively the significance of secondary flow. Finally, based on the above mentioned considerations, the following correlation was developed.

$$J_X = 0.00275 \left[Re\left\{0.733 + 14.33(R_c/r_i)^{-0.593}(X/d_i)^{-1.619}\right\}\right] \quad (6\text{-}20)$$
$$X \left[1.0 + 8.5\left(\frac{Gr}{Re^2}\right)^{0.429}\right]\left[1.0 + 4.79e\left\{-2.11(X/d_i)^{-0.237}\right\}\right]$$

where $Re \leqslant 2100$ and $\frac{\pi}{2}(R_c/r_i) \leqslant (X/d_i) \leqslant 160$ and X is the distance from the inlet of the bend (thermocouple station 3).

Figure 24 presents the comparison between predicted (using Equation 6-20) and experimental heat transfer parameters, J_X. The AAPD for 336 data points fitted to Equation (6.20) was 16.0%.

The limiting cases of Equation (6-20) are as follows:

1. For limiting case $(R_c/r_i) \longrightarrow \infty$, i.e., a straight tube, Equation (6-20) reduces to:

$$J_X = 0.00275\ Re^{0.733}\left[1.0 + 8.5\ (Gr/Re^2)^{0.429}\right] \quad (6\text{-}21)$$
$$X\left[1.0 + 4.79e\left\{-2.11(X/d_i)^{-0.237}\right\}\right]$$

2. For limiting cases $(R_c/r_i) \longrightarrow \infty$ and $(X/d_i) \longrightarrow \infty$, Equation (6-20) reduces to:

$$J = 0.0159\ Re^{0.733}\left[1.0 + 8.5(Gr/Re^2)^{0.429}\right] \quad (6\text{-}22)$$

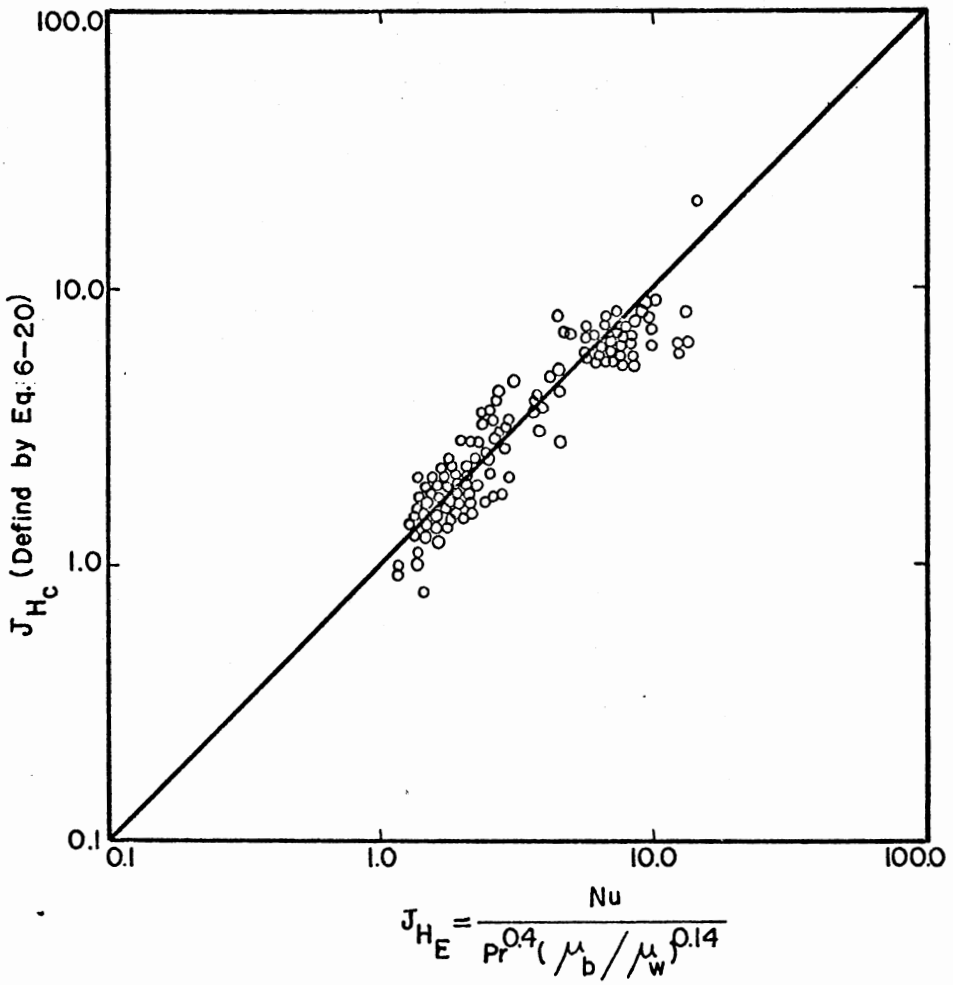

Figure 24. Comparison Between Predicted and Experimental Heat Transfer Coefficients in a Straight Section Preceded by 180° Bend

3. For limiting cases $(R_c/r_i) \to \infty$, $(X/d_i) \to \infty$, and no natural convection effect $(Gr/Re^2 = 0)$, Equation (6-20) reduces to:

$$J = 0.0159Re^{0.733} \tag{6-23}$$

Flow Regime Maps

To obtain a better and more quantitative insight into the effect of secondary and tertiary flows and their interactions, Reynolds number is plotted as a function of Gr/Re^2 on Figure 25 for thermocouple station 2, located far away from the entrance of the test section but before the bend. As shown on Figure 25, three separate regions, representing the relative importance of natural convection, have been obtained. The criterion for separating these regions was the ratio of heat transfer coefficients at the top to that at the bottom of the tube. If this ratio of heat transfer coefficients (top to bottom) was between 0.95 to 1.05, then forced convection of the primary flow is dominant. On the other hand if the ratio of heat transfer coefficient (top to bottom) is less than 0.95, then natural convection is dominant. The effect of natural convection is to increase heat transfer coefficient at the bottom and decrease heat transfer coefficient at the top of the tube.

Figures 26 through 29 present plots of Dean number $(Re\sqrt{d_i/D_c})$ as a function of Gr/Re^2 for stations 7 (located at the exit of the bend) through 10 for straight section downstream of the bend. Figure 26 indicates that at station 7, secondary flow is the dominating factor; secondary flow causes the heat transfer coefficients to become greater at the top than at the bottom of the tube. That is why for the

secondary flow the ratios of heat transfer coefficients (top to bottom) are greater than 1.05. As the fluid moves away from the bend and passes through station 8, 9, and 10 (see Figures 27, 28, and 29), the effect of secondary flow decreases and natural convection becomes more dominant.

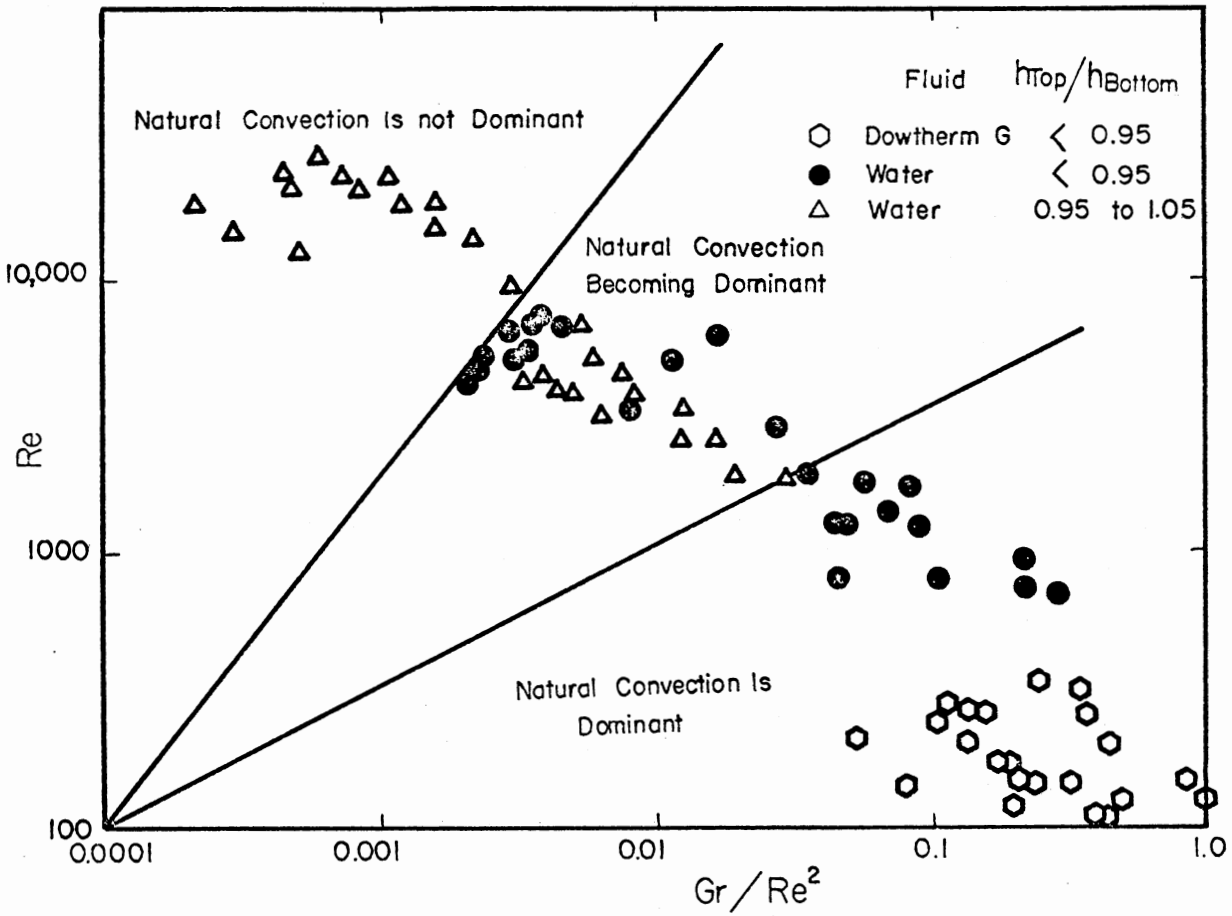

Figure 25. Flow Map for a Straight Pipe (Station 2)

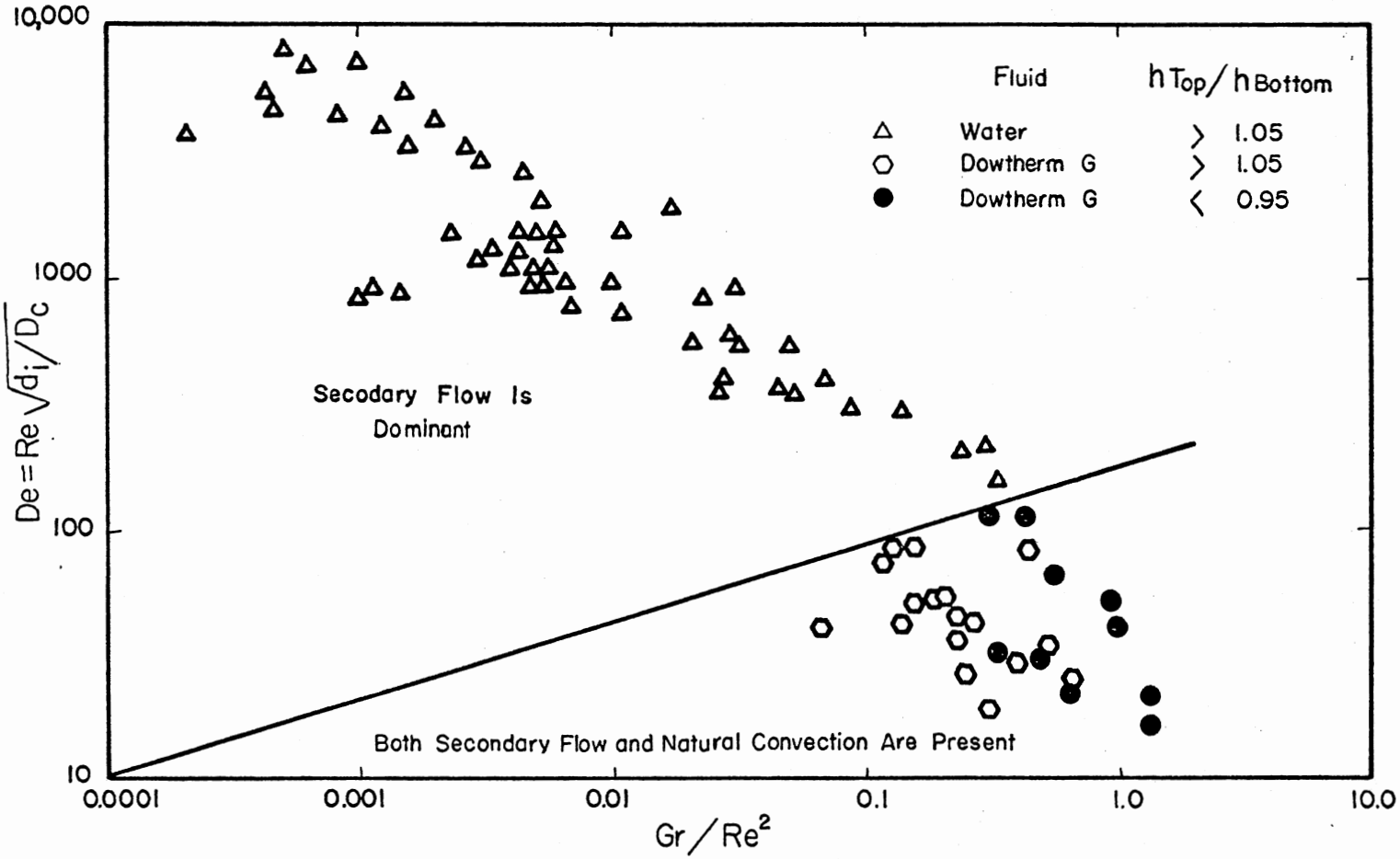

Figure 26. Flow Map for a Straight Pipe Preceded by 180° Bend (Station 7, $X/d_i = 0$)

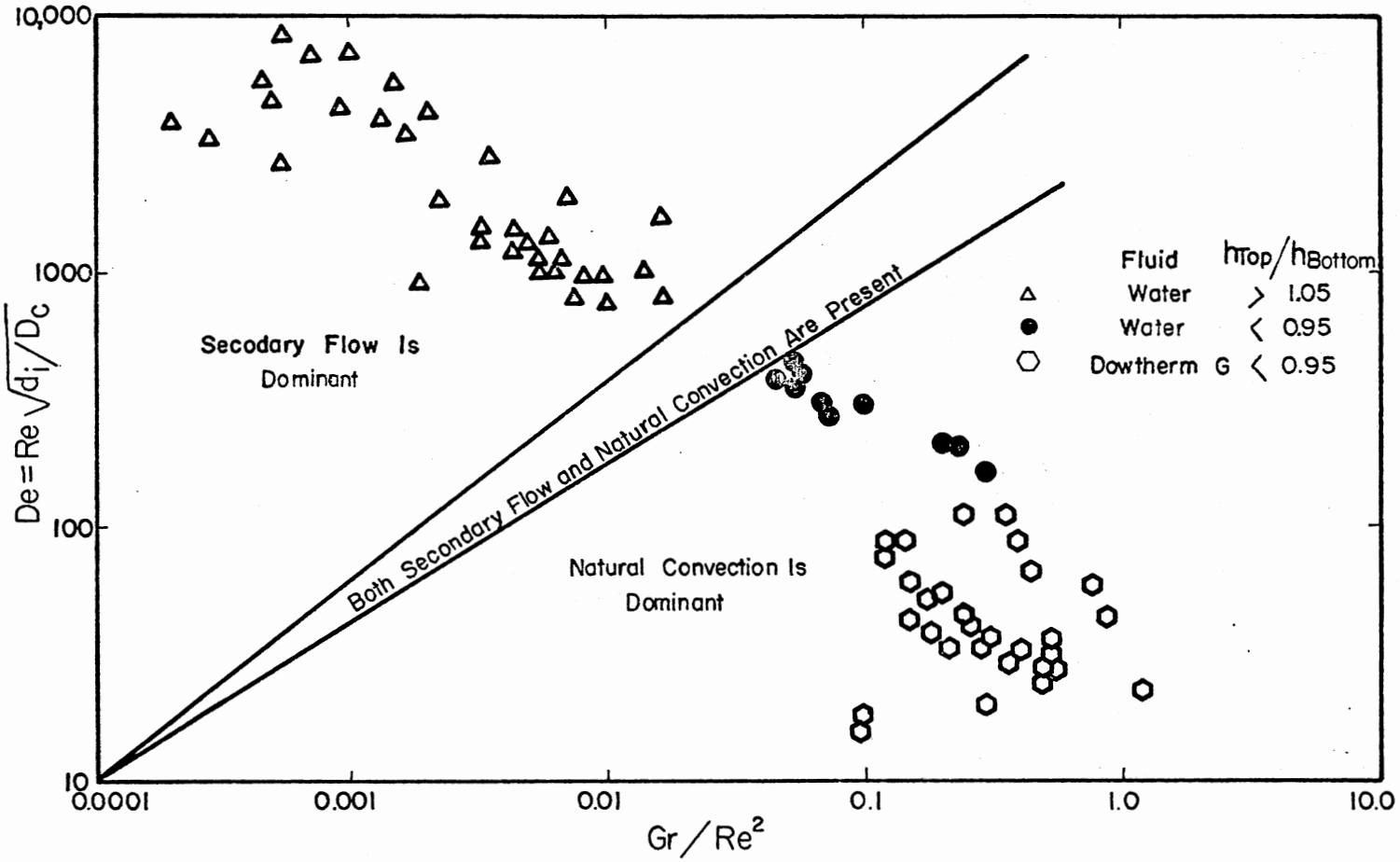

Figure 27. Flow Map for a Straight Pipe Preceded by 180° Bend (Station 8, X^*/d_i = 7.7)

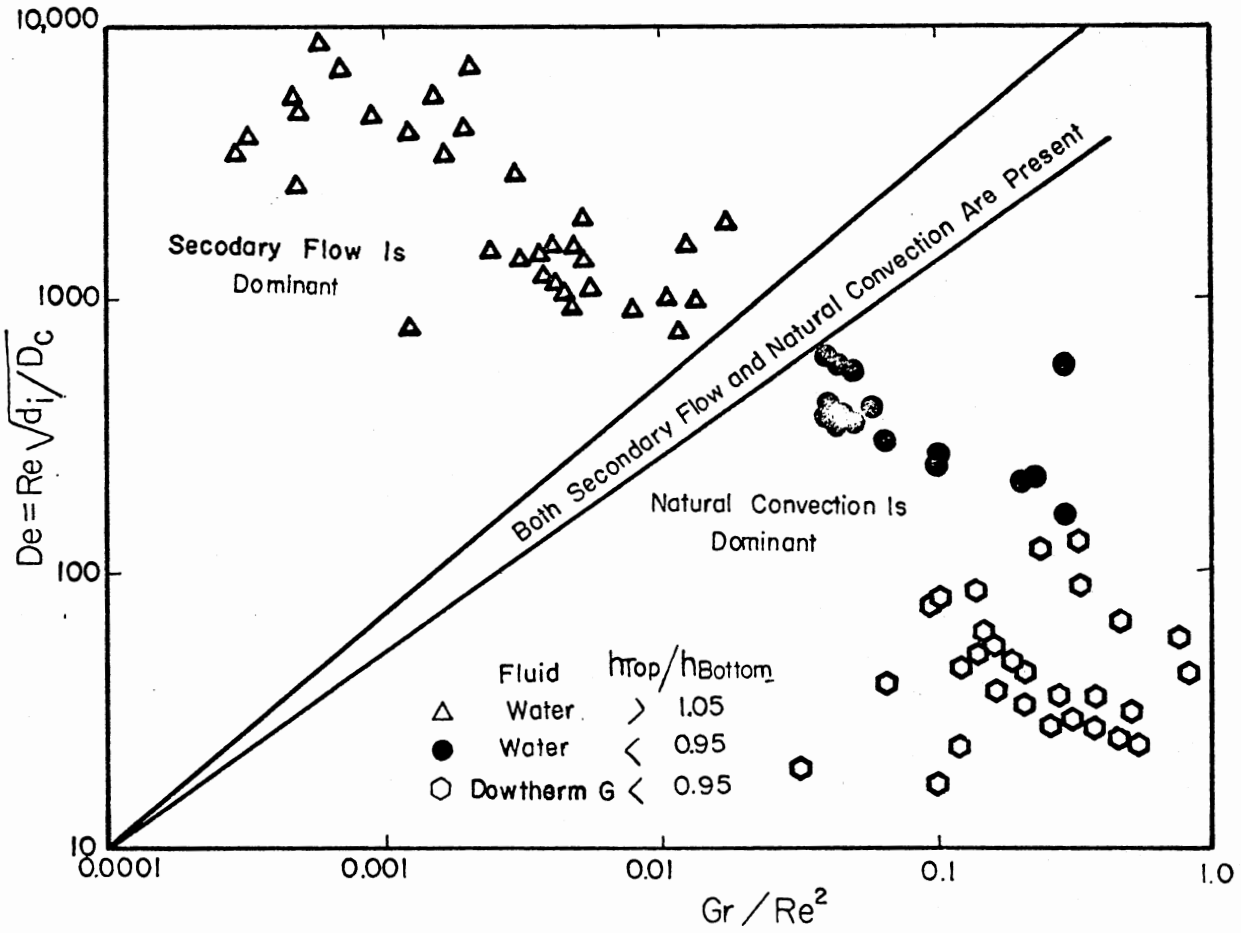

Figure 28. Flow Map for a Straight Pipe Preceded by 180° Bend (Station 9, X^*/d_i = 15.5)

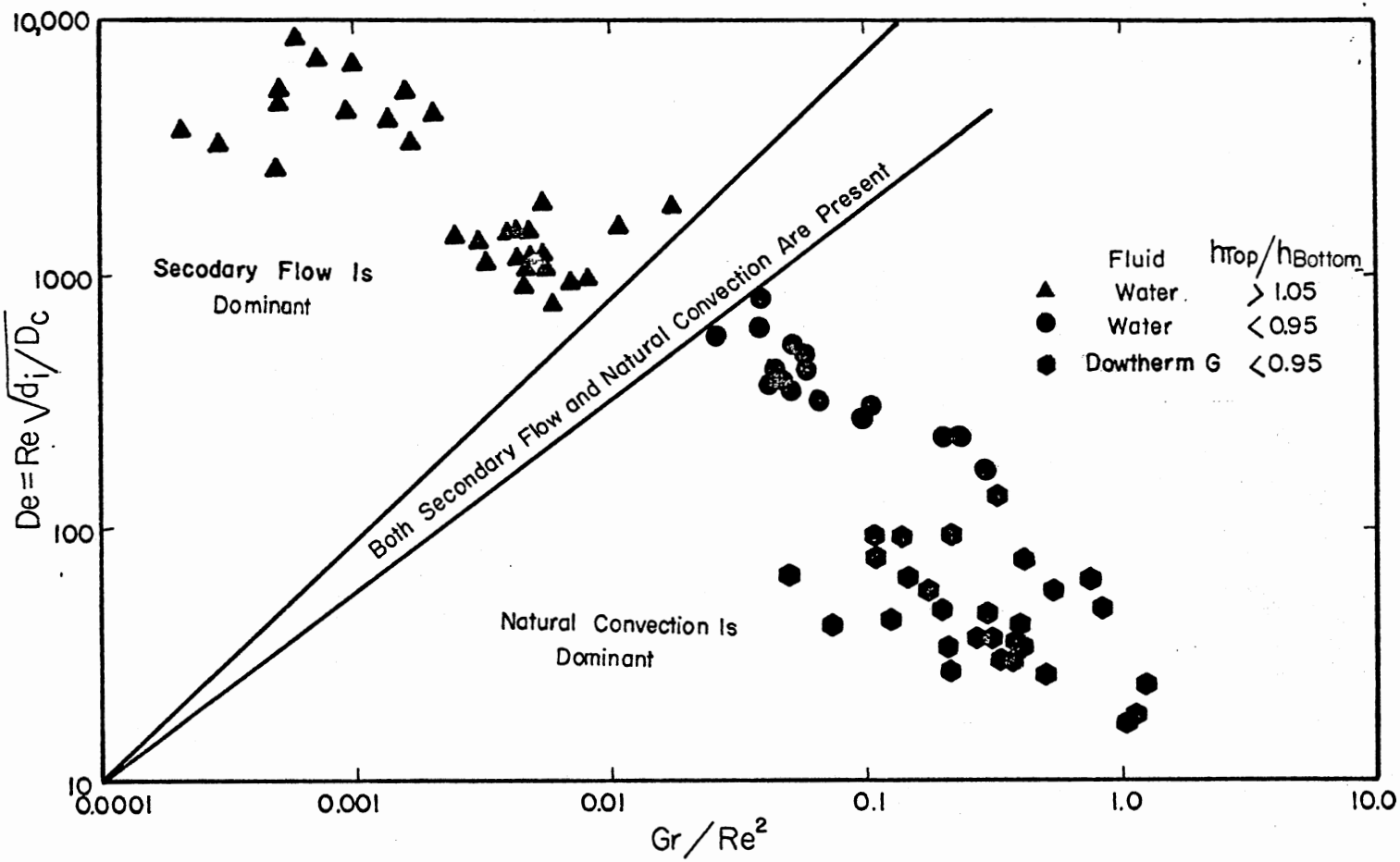

Figure 29. Flow Map for a Straight Pipe Preceded by 180° Bend (Station 10, X^*/d_i = 23.3)

CHAPTER VII

CONCLUSIONS AND RECOMMENDATIONS

An experimental study of the heat transfer processes when a single phase fluid flows through a 180^{o} bend pipe has been conducted. Experiments were made with water, Dowtherm G, and ethylene glycol flowing through an electrical-resistance-heated tube. Four test sections with curvature ratios ranging from 4.84 to 25.62 were studied. The entire fluid flow regime from laminar through transition to turbulent flow was investigated. In the course of the study, available literature correlations for both 180^{o} bends and straight tubes were tested to determine how well they could predict the experimental results.

The following conclusions were arrived at as a result of the total study:

1. At low Reynolds numbers (i.e., laminar flow regime), the effect of natural convection was detected in the straight section upstream of the bend through measuring higher heat transfer coefficients at the bottom of the tube than at the top. However, the intensity of natural convection was diminished as the Reynolds number increased.

2. The peripheral distribution of heat transfer coefficients is far from uniform in the bend. The local coefficients are much higher at the outside and lower at the inside of the bend, resulting in a

higher mean heat transfer coefficient as compared to a straight tube under similar flow conditions. The ratio of mean heat transfer coefficient in the bend to that for the straight tube was higher in the laminar flow regime (2 to 10) than in the turbulent flow regime (1 to 1.5). This is understandable in view of the fact that greater random mixing in the turbulent flow regime diminishes the augmentation of the heat transfer coefficient due to a superimposed secondary flow. The secondary flow results from the centrifugal action that a fluid is subjected to when flowing in a curved path.

3. As anticipated, at any cross section in the bend, the distribution of peripheral heat transfer coefficient is almost symmetrical about a plane containing the longitudinal axis of tube and the radius of the bend.

4. The secondary flow effect is carried to the straight section downstream of the bend, resulting in higher heat transfer coefficients at the top (outside of the bend) than that at the bottom (inside of the bend) of the tube. The net effect of the secondary flow is to increase the peripheral mean heat transfer coefficient in the straight section downstream of the bend as compared to a straight tube not preceded by a 180^{o} bend, under similar flow conditions. However, at lower Reynolds numbers (i.e. laminar flow regime) the secondary flow effect tends to be counteracted by the natural convection effect, resulting in lower peripheral mean heat transfer coefficient as compared to a straight tube not preceded by 180^{o} bend, under similar flow conditions.

5. Correlations have been developed to predict the local Nusselt number for fluids flowing in a U-bend and in the straight section

downstream of the bend for both turbulent and laminar flow regimes. The correlations are Equations (6-18), (6-19), and (6-20) in Chapter VI.

6. In addition to development of correlations, flow maps have been made which should be useful in understanding the mechanism of secondary and tertiary (natural convection) flows. These flow maps are presented on Figures 25 through 29 in Chapter VI.

Several gaps still exist in the complete understanding of the mechanism of heat transfer in U-bend tube. The following recommendations are made, based on the results of this study, for future research in the area:

1. Equations (6-18), (6-19) and (6-20) were developed for the case when a fluid is heated in a U-bend tube. It is felt that the same correlations should apply when a fluid is cooled in a U-bend tube. However, when the experimental data of this work were compared with those predicted by the Tailby-Staddon (4) correlation, developed for the case when a fluid was cooled in U-bend tube, a relatively large average absolute percentage deviation was obtained (see Table V in Chapter VI). Therefore, it is recommended that experimental studies be performed when a fluid is cooled in U-bend tube to make a better comparison.

2. In the laminar flow regime, the interaction between secondary flow and tertiary flow (natural convection) should be studied further to get a better and more quantitative insight into the mechanism of flow.

3. Flow visualization is also recommended to understand the mechanism of secondary flow in U-bend tubes.

BIBLIOGRAPHY

(1) Lis, J. and M. J. Thelwell, "Experimental Investigation of Turbulent Heat Transfer in a Pipe Preceded by a 180° Bend," Proc. Inst. of Mech. Engrs., V. 178, Pt. 3I, 1963-64, p. 17.

(2) Ede, A. J., "The Effect of a 180°Bend Heat Transfer to Water in a Tube," 3rd Intl. Heat Transfer Conf., Chicago, Ill., V. 1, 1966, p. 99.

(3) Ito, H., "Friction Factors for Turbulent Flow in Curved Pipes," Trans. Am. Soc. Mech. Engrs., J. Basic Engg., D81, 123(1959).

(4) Tailby, S. R. and P. W. Staddon, "The Influence of 90° and 180° Pipe Bends on Heat Transfer from an Internally Flowing Gas Stream," 4th Intl. Heat Transfer Conf., Paris-Vesailles, V.2 FC4.5(1970).

(5) Yang, J. W. and N. Liao, "Turbulent Heat Transfer in Rectangular Ducts with 180-Bend," 5th Intl. Heat Transfer Conf., Tohoku-Japan, V.2 FC4.10(1974).

(6) Moshfeghian, M., "The Effect of a 180° Bend on Turbulent Heat Transfer Coefficient in a Pipe," M.S. Thesis, Oklahoma State University, Stillwater, Oklahoma (1975).

(7) Singh, S. P., "Liquid Phase Heat Transfer in Helically Coiled Tubes," Ph.D. Thesis, Oklahoma State University, Stillwater, Oklahoma (1973).

(8) Schmidt, E. F., "Warmeubergang und Drukverlust in Rohrschlangen," Chemie Ingenier Thechnik 13, 781(1967).

(9) Farukhi, M. N., "An Experimental Investigation of Forced Convective Boiling at High Qualities Inside Tubes Preceded by 180 Degree Benes," Ph.D. Thesis, Oklahoma State University, Stillwater, Oklahoma (1974).

(10) Ross Type BCF Exchanger Bulletin 1.1KG, Copyrighted 1975 by American Radiator and Standard Sanitary Corp.

(11) Numatron Operations Manual, Manual No. 177626, Issue 2, Leeds and Northrup Co., Pa.

(12) Directions for 8687 Volt Potentiometer, Manual 177126, Issue 5, Leeds and Northrup Co., Pa.

(13) Curme, G. O., Jr. and F. Johnston, eds. Glycols. New York: Reinhold Publishing Corporation, 1952.

(14) Crain, Berry, Jr., "Forced Convection Heat Transfer to a Two-Phase Mixture of Water and Steam in a Helical Coil," Ph.D. Thesis, Oklahoma State University, Stillwater, Oklahoma (1973).

(15) Morcos, S. M. and A. E. Bergles, "Experimental Investigation of Combined Forced and Free Laminar Convection in Horizontal Tubes," Transactions of ASME, Journal of Heat Transfer, (1975) p. 212.

(16) Kays, W. M., "Convective Heat and Mass Transfer," New York, New York: McGraw-Hill Book Company, (1966) p. 111.

(17) Sieder, E. N. and C. E. Tate, "Heat Transfer and Pressure Drop of Liquids in Tubes," Ind. Eng. Chem., V. 28, (1936), p. 1429.

(18) Dittus, F. W. and L. M. K. Boelter, Univ. of Calif. (Berkeley) Eng. Pub., V. 2, (1930), p. 443.

(19) Eagle, A. and R. M. Ferguson, Pro. Roy. Soc., A127, 540-566(1930).

(20) Chandler, J. P., "MARQ 2.3 A.N.S.I. Standard Fortran," Dept. of Computing and Information Sciences, Oklahoma State University, Stillwater, Oklahoma (1975).

(21) Weast, R. C., ed., CRC Handbook of Chemistry and Physics, 52nd edition, The Chemical Ruber Company, Cleveland, Ohio (1972).

(22) Owhadi, A., K. J. Bell and B. Crain, Jr., "Forced Convection Boiling Inside Helically Coiled Tubes," Intl. J. of Heat and Mass Transfer, V. 11, 1968, p. 1779.

(23) Carver, J. R., C. R. Kakavala, and J. S. Slotnik, "Heat Transfer in Coiled Tubes with Two Phase Flow," U.S.A.E.C. Report, TID-20988, 1964.

(24) Chen, S. J., and A. R. Macdonald, "Motionless Mixers for Viscous Polymers," Chemical Engineering, 1973, p. 105.

APPENDIX A

EXPERIMENTAL DATA

Run Number	Test Fluid	Test Section
200-249	Water	D
300-349	Water	C
400-449	Water	B
500-549	Water	A
250-299	Ethylene Glycol	D
350-399	Ethylene Glycol	C
450-499	Dowtherm G	B
550-599	Dowtherm G	A

Only those experimental data which were referred to are presented here. The rest of the experimental data are available at:

School of Chemical Engineering
Oklahoma State University
Stillwater, Oklahoma 74074 USA

RUN NUMBER 203

FLUID FLOW RATE	=	266.00	LBM/HOUR
CURRENT TO TUBE	=	139.00	AMPS
VOLTAGE DROP IN TUBE	=	6.20	VOLTS
ROOM TEMPERATURE	=	87.90	DEGREES F
UNCORRECTED INLET TEMPERATURE	=	85.70	DEGREES F
UNCORRECTED OUTLET TEMPERATURE	=	97.10	DEGREES F

OUTSIDE SURFACE TEMPERATURES - DEGREES F

	1	2	3	4	5	6	7	8	9	10	11
1	94.2	96.7	94.7	94.1	93.4	93.5	93.6	98.6	99.6	100.7	110.4
2	94.3	96.7	95.1	94.4	93.7	93.8	94.0	98.6	99.5	100.9	105.2
3	94.4	96.7	96.3	95.6	94.6	94.6	94.7	98.7	99.4	100.7	101.3
4	94.5	96.7	97.9	97.4	96.8	97.1	97.3	98.6	99.5	100.7	100.1
5	94.5	96.6	98.9	99.2	99.4	99.4	99.8	98.6	99.4	100.5	99.9
6	94.5	96.7	97.7	97.5	97.2	97.2	97.3	98.6	99.4	100.7	100.2
7	94.4	96.8	95.8	95.3	94.8	95.1	95.3	98.6	99.4	100.8	102.0
8	94.4	96.7	95.0	94.4	93.8	94.0	94.1	98.6	99.6	100.3	107.6

RUN NUMBER 205

FLUID FLOW RATE	=	407.00	LBM/HOUR
CURRENT TO TUBE	=	165.00	AMPS
VOLTAGE DROP IN TUBE	=	7.30	VOLTS
ROOM TEMPERATURE	=	85.30	DEGREES F
UNCORRECTED INLET TEMPERATURE	=	87.60	DEGREES F
UNCORRECTED OUTLET TEMPERATURE	=	97.90	DEGREES F

OUTSIDE SURFACE TEMPERATURES - DEGREES F

	1	2	3	4	5	6	7	8	9	10	11
1	95.3	97.6	95.8	95.4	95.0	95.2	95.3	99.4	99.7	101.2	102.8
2	95.4	97.6	96.3	95.4	95.4	95.5	95.7	99.4	99.8	101.4	102.9
3	95.5	97.5	97.4	96.9	96.3	96.3	96.4	99.5	100.0	101.5	102.8
4	95.5	97.5	99.0	98.8	98.6	98.6	98.7	99.6	100.3	101.6	102.9
5	95.5	97.3	100.1	100.5	100.8	101.0	101.2	99.6	100.3	101.6	102.8
6	95.4	97.5	98.8	98.8	98.8	98.8	98.9	99.6	100.3	101.6	102.8
7	95.4	97.6	97.0	96.7	96.5	96.9	97.2	99.4	100.0	101.4	102.7
8	95.4	97.5	96.2	95.8	95.4	95.6	95.9	99.4	99.7	101.3	102.7

RUN NUMBER 213

FLUID FLOW RATE	=	1557.00	LBM/HOUR
CURRENT TO TUBE	=	378.00	AMPS
VOLTAGE DROP IN TUBE	=	16.80	VOLTS
ROOM TEMPERATURE	=	88.80	DEGREES F
UNCORRECTED INLET TEMPERATURE	=	98.10	DEGREES F
UNCORRECTED OUTLET TEMPERATURE	=	113.00	DEGREES F

OUTSIDE SURFACE TEMPERATURES - DEGREES F

	1	2	3	4	5	6	7	8	9	10	11
1	111.6	114.9	111.4	110.7	109.9	110.2	110.4	116.4	117.2	118.8	120.7
2	111.7	114.7	112.1	111.5	110.8	110.9	111.0	116.5	117.2	118.8	120.9
3	111.8	114.5	114.1	113.7	113.2	113.0	112.8	116.2	117.0	118.8	120.8
4	111.7	114.5	117.6	117.6	117.6	117.2	116.7	116.4	117.0	118.8	121.1
5	111.7	114.7	120.4	120.9	121.4	120.9	120.3	116.4	117.3	118.8	121.0
6	111.7	114.6	117.5	117.9	118.2	117.2	116.1	116.4	117.3	118.8	121.0
7	111.6	114.4	113.7	113.6	113.5	113.6	113.6	116.3	117.3	118.8	120.7
8	111.7	114.5	112.3	111.7	111.0	111.2	111.0	116.2	117.3	118.8	120.7

RUN NUMBER 215

FLUID FLOW RATE	=	84.60	LBM/HOUR
CURRENT TO TUBE	=	142.00	AMPS
VOLTAGE DROP IN TUBE	=	6.40	VOLTS
ROOM TEMPERATURE	=	87.30	DEGREES F
UNCORRECTED INLET TEMPERATURE	=	85.80	DEGREES F
UNCORRECTED OUTLET TEMPERATURE	=	122.80	DEGREES F

OUTSIDE SURFACE TEMPERATURES - DEGREES F

	1	2	3	4	5	6	7	8	9	10	11
1	99.6	106.2	103.8	103.4	102.9	105.8	108.7	123.4	127.0	132.3	137.6
2	100.9	107.0	104.1	103.9	103.7	106.4	109.0	120.8	123.8	128.9	134.0
3	104.2	111.6	107.2	106.2	105.2	107.4	109.6	116.8	119.7	123.7	128.5
4	109.1	117.5	113.7	111.5	109.3	110.9	112.5	113.2	115.9	120.3	125.2
5	112.5	120.2	118.8	116.3	113.7	114.3	114.9	112.2	115.0	119.5	124.1
6	110.7	117.9	113.6	111.9	110.1	111.2	112.4	113.4	115.9	120.7	125.5
7	103.9	112.9	106.6	106.2	105.7	107.9	110.1	117.0	118.9	124.3	130.1
8	101.1	108.1	104.3	104.1	103.8	106.2	108.6	121.5	123.7	130.6	135.9

RUN NUMBER 252

FLUID FLOW RATE	=	1310.00	LBM/HOUR
CURRENT TO TUBE	=	188.00	AMPS
VOLTAGE DROP IN TUBE	=	8.30	VOLTS
ROOM TEMPERATURE	=	88.20	DEGREES F
UNCORRECTED INLET TEMPERATURE	=	95.40	DEGREES F
UNCORRECTED OUTLET TEMPERATURE	=	102.20	DEGREES F

OUTSIDE SURFACE TEMPERATURES - DEGREES F

	1	2	3	4	5	6	7	8	9	10	11
1	132.5	137.7	112.6	106.4	100.1	100.1	100.1	118.8	130.0	145.6	150.2
2	133.3	138.4	115.0	108.0	100.9	100.9	100.9	119.9	130.3	143.9	146.1
3	134.9	141.3	121.4	112.7	104.0	103.5	103.0	121.7	131.3	141.5	141.3
4	137.2	145.5	132.9	122.6	112.3	111.0	109.6	124.4	132.6	139.9	138.7
5	139.0	147.9	140.6	132.8	125.0	120.2	115.4	125.3	133.3	139.7	138.0
6	138.2	145.7	132.6	123.3	114.0	111.8	109.5	124.4	133.0	140.6	139.4
7	134.9	142.1	120.0	112.3	104.6	104.6	104.6	121.8	131.8	142.5	143.0
8	133.3	139.0	114.5	107.9	101.3	101.3	101.4	119.5	130.4	145.4	148.0

RUN NUMBER 253

FLUID FLOW RATE	=	979.00	LBM/HOUR
CURRENT TO TUBE	=	146.00	AMPS
VOLTAGE DROP IN TUBE	=	6.50	VOLTS
ROOM TEMPERATURE	=	89.20	DEGREES F
UNCORRECTED INLET TEMPERATURE	=	97.90	DEGREES F
UNCORRECTED OUTLET TEMPERATURE	=	103.90	DEGREES F

OUTSIDE SURFACE TEMPERATURES - DEGREES F

	1	2	3	4	5	6	7	8	9	10	11
1	124.3	127.7	113.1	107.4	101.6	101.6	101.6	116.6	125.0	133.9	136.8
2	124.8	128.2	114.8	108.5	102.2	102.2	102.2	117.0	124.7	132.1	134.1
3	126.0	130.3	113.6	111.5	104.4	104.0	103.7	117.6	124.4	130.0	130.5
4	127.4	133.4	125.7	117.9	110.2	109.2	108.1	118.7	124.5	128.8	128.6
5	128.5	135.0	130.3	124.4	118.4	115.1	111.8	119.1	124.9	128.8	128.3
6	128.0	133.4	125.4	118.4	111.3	109.7	108.0	118.6	124.9	129.4	129.6
7	125.9	130.8	117.6	111.3	104.9	104.8	104.7	117.5	124.8	130.8	132.1
8	124.9	128.7	114.5	108.5	102.5	102.5	102.4	116.7	124.9	133.4	135.6

RUN NUMBER 262

FLUID FLOW RATE	=	203.00	LBM/HOUR
CURRENT TO TUBE	=	120.00	AMPS
VOLTAGE DROP IN TUBE	=	5.40	VOLTS
ROOM TEMPERATURE	=	89.80	DEGREES F
UNCORRECTED INLET TEMPERATURE	=	87.20	DEGREES F
UNCORRECTED OUTLET TEMPERATURE	=	106.40	DEGREES F

OUTSIDE SURFACE TEMPERATURES - DEGREES F

	1	2	3	4	5	6	7	8	9	10	11
1	109.6	111.4	108.1	101.6	95.0	100.5	106.0	123.5	124.3	126.6	128.7
2	110.6	112.1	108.9	102.4	95.8	100.9	106.0	121.4	121.6	124.0	126.2
3	112.4	115.1	111.2	104.6	97.9	102.0	106.1	118.7	118.4	120.4	122.4
4	115.0	118.9	116.0	109.3	102.5	105.2	107.8	117.4	116.5	118.3	120.3
5	117.0	120.7	119.4	113.1	106.8	107.9	109.0	118.5	116.9	117.7	119.5
6	115.8	119.2	115.7	109.5	103.2	105.5	107.7	119.4	118.1	118.7	120.3
7	112.2	115.8	110.4	104.4	98.4	102.4	106.4	120.2	120.5	120.9	123.2
8	110.6	112.7	108.9	102.4	95.9	100.8	105.6	122.7	123.0	125.2	127.2

RUN NUMBER 402

FLUID FLOW RATE	=	70.60	LBM/HOUR
CURRENT TO TUBE	=	80.00	AMPS
VOLTAGE DROP IN TUBE	=	3.00	VOLTS
ROOM TEMPERATURE	=	79.80	DEGREES F
UNCORRECTED INLET TEMPERATURE	=	85.20	DEGREES F
UNCORRECTED OUTLET TEMPERATURE	=	94.80	DEGREES F

OUTSIDE SURFACE TEMPERATURES - DEGREES F

	1	2	3	4	5	6	7	8	9	10	11
1	91.0	92.4	92.7	90.8	93.1	97.0	98.4	101.2	102.3	103.1	106.9
2	91.3	93.1	93.3	91.2	93.3	96.9	99.5	99.4	99.9	101.4	104.9
3	91.8	95.1	95.3	92.3	94.3	97.5	99.8	96.9	98.2	98.2	101.3
4	92.6	98.9	99.1	95.8	95.8	98.8	99.0	96.0	96.9	96.7	99.6
5	92.9	100.8	101.4	99.2	97.4	99.2	98.4	95.8	96.8	96.4	99.2
6	92.2	98.6	99.6	96.3	96.0	98.6	98.7	96.1	97.2	97.0	99.5
7	91.2	94.9	95.5	92.1	94.1	97.6	99.9	97.3	98.2	98.4	101.8
8	91.0	93.0	93.2	91.0	93.3	97.0	99.1	99.4	100.4	101.2	105.1

RUN NUMBER 419

FLUID FLOW RATE	=	2124.90	LBM/HOUR
CURRENT TO TUBE	=	436.00	AMPS
VOLTAGE DROP IN TUBE	=	17.40	VOLTS
ROOM TEMPERATURE	=	85.50	DEGREES F
UNCORRECTED INLET TEMPERATURE	=	90.50	DEGREES F
UNCORRECTED OUTLET TEMPERATURE	=	103.10	DEGREES F

OUTSIDE SURFACE TEMPERATURES - DEGREES F

	1	2	3	4	5	6	7	8	9	10	11
1	112.5	115.0	114.5	108.5	107.3	107.4	109.5	111.4	112.3	113.7	118.4
2	112.1	115.7	115.5	110.4	108.4	109.0	109.9	111.6	112.4	113.8	118.8
3	110.7	115.7	115.8	112.6	111.9	112.1	112.1	113.7	114.4	115.1	119.7
4	109.8	115.1	116.5	117.4	116.6	120.2	116.4	117.0	118.0	118.3	122.0
5	109.2	114.7	116.2	123.8	122.7	127.1	122.9	121.8	122.0	122.2	123.0
6	108.4	113.5	115.3	116.3	115.2	116.8	117.0	118.7	119.2	119.5	121.8
7	108.5	113.5	114.2	110.9	110.4	111.0	113.3	114.6	115.9	116.7	119.9
8	110.9	114.0	115.5	108.9	107.8	108.1	110.5	111.6	113.3	114.8	118.5

RUN NUMBER 420

FLUID FLOW RATE	= 2428.40	LBM/HOUR
CURRENT TO TUBE	= 470.00	AMPS
VOLTAGE DROP IN TUBE	= 18.70	VOLTS
ROOM TEMPERATURE	= 83.60	DEGREES F
UNCORRECTED INLET TEMPERATURE	= 94.40	DEGREES F
UNCORRECTED OUTLET TEMPERATURE	= 107.20	DEGREES F

OUTSIDE SURFACE TEMPERATURES - DEGREES F

	1	2	3	4	5	6	7	8	9	10	11
1	116.7	119.7	119.1	112.7	112.1	111.2	113.2	115.7	117.0	118.4	123.5
2	116.5	119.9	120.3	115.2	113.4	113.0	113.8	115.9	117.0	118.6	124.0
3	114.9	120.4	120.9	118.2	117.2	116.3	116.4	118.0	119.4	120.0	124.9
4	113.9	119.9	121.4	122.8	122.0	124.5	120.8	121.7	123.0	123.7	127.6
5	113.2	119.1	121.1	129.3	128.3	132.2	127.6	126.9	127.3	127.7	128.6
6	112.1	118.2	120.2	121.8	120.2	121.1	121.8	123.7	124.3	125.1	127.1
7	112.6	118.0	119.1	116.2	115.5	115.1	117.7	119.6	120.8	121.7	125.0
8	115.2	118.7	120.1	114.0	112.7	111.9	114.6	115.9	118.2	119.6	123.3

RUN NUMBER 428

FLUID FLOW RATE	=	559.00	LBM/HOUR
CURRENT TO TUBE	=	209.00	AMPS
VOLTAGE DROP IN TUBE	=	8.25	VOLTS
ROOM TEMPERATURE	=	84.20	DEGREES F
UNCORRECTED INLET TEMPERATURE	=	73.80	DEGREES F
UNCORRECTED OUTLET TEMPERATURE	=	84.50	DEGREES F

OUTSIDE SURFACE TEMPERATURES - DEGREES F

	1	2	3	4	5	6	7	8	9	10	11
1	87.0	91.7	88.9	84.2	85.4	85.3	85.3	87.9	88.8	88.9	94.6
2	87.3	90.1	92.5	84.9	85.7	86.2	85.4	87.4	89.0	88.5	94.0
3	87.4	90.9	92.3	86.6	88.1	88.0	86.4	87.1	89.9	90.1	93.8
4	87.3	89.5	91.5	92.7	92.9	93.4	91.5	91.0	92.8	93.2	96.3
5	87.1	88.5	92.2	95.5	96.1	96.6	97.4	93.8	94.5	94.0	96.7
6	86.1	90.9	90.9	91.8	91.7	91.2	92.5	92.4	93.3	93.6	94.6
7	86.4	91.4	92.7	86.0	87.5	87.2	87.4	88.7	90.0	91.4	93.3
8	87.1	91.1	92.5	84.7	85.7	86.2	85.9	87.4	89.4	89.2	94.2

RUN NUMBER 514

FLUID FLOW RATE	= 2426.70	LBM/HOUR
CURRENT TO TUBE	= 459.00	AMPS
VOLTAGE DROP IN TUBE	= 18.00	VOLTS
ROOM TEMPERATURE	= 79.50	DEGREES F
UNCORRECTED INLET TEMPERATURE	= 76.70	DEGREES F
UNCORRECTED OUTLET TEMPERATURE	= 88.70	DEGREES F

OUTSIDE SURFACE TEMPERATURES - DEGREES F

	1	2	3	4	5	6	7	8	9	10	11
1	98.5	100.3	99.8	96.8	96.6	96.3	97.9	99.7	101.3	102.8	106.6
2	99.0	100.7	100.8	97.5	97.1	97.2	99.5	101.6	103.2	104.3	108.1
3	98.6	101.3	101.9	99.4	100.5	100.6	102.7	105.0	106.0	106.9	109.6
4	98.6	101.9	103.2	103.7	106.6	107.7	107.5	109.0	109.6	110.4	111.7
5	97.9	102.1	103.9	109.2	113.7	115.7	114.4	111.3	112.0	112.1	112.4
6	96.6	102.0	103.3	103.8	106.3	107.6	105.9	105.9	107.4	107.7	109.1
7	95.6	100.6	101.4	100.0	101.2	101.3	100.2	102.2	103.3	103.6	106.1
8	96.8	100.4	100.5	98.0	97.9	97.9	98.2	100.0	101.4	102.4	105.8

RUN NUMBER 515

FLUID FLOW RATE	=	2724.00	LBM/HOUR
CURRENT TO TUBE	=	520.00	AMPS
VOLTAGE DROP IN TUBE	=	20.50	VOLTS
ROOM TEMPERATURE	=	83.40	DEGREES F
UNCORRECTED INLET TEMPERATURE	=	77.10	DEGREES F
UNCORRECTED OUTLET TEMPERATURE	=	91.00	DEGREES F

OUTSIDE SURFACE TEMPERATURES - DEGREES F

	1	2	3	4	5	6	7	8	9	10	11
1	103.7	105.7	104.8	100.9	100.6	100.1	101.6	103.4	105.4	107.5	111.9
2	104.5	106.0	105.7	101.6	101.1	100.7	103.6	105.6	107.8	109.4	113.7
3	103.7	106.5	107.0	104.0	104.9	104.8	107.2	109.6	111.1	112.4	115.5
4	103.8	107.2	108.8	107.8	111.9	113.0	112.7	114.6	115.8	116.9	118.6
5	102.8	107.6	109.5	115.4	120.6	123.2	120.8	117.6	119.0	119.4	119.9
6	101.2	107.3	108.7	108.6	111.8	113.3	110.8	111.0	113.2	113.8	115.4
7	99.8	105.5	106.4	104.5	105.9	106.0	103.9	106.5	108.0	108.3	111.0
8	101.4	105.6	105.2	102.3	102.0	101.6	101.6	103.8	105.6	106.9	110.8

RUN NUMBER 522

FLUID FLOW RATE	=	641.40	LBM/HOUR
CURRENT TO TUBE	=	234.00	AMPS
VOLTAGE DROP IN TUBE	=	9.00	VOLTS
ROOM TEMPERATURE	=	79.10	DEGREES F
UNCORRECTED INLET TEMPERATURE	=	63.00	DEGREES F
UNCORRECTED OUTLET TEMPERATURE	=	74.70	DEGREES F

OUTSIDE SURFACE TEMPERATURES - DEGREES F

	1	2	3	4	5	6	7	8	9	10	11
1	78.3	81.4	80.4	77.6	78.1	78.5	80.1	88.8	84.8	85.7	89.8
2	78.0	80.0	80.2	78.4	79.5	78.5	80.7	90.0	85.5	86.8	90.5
3	80.C	80.4	79.6	80.4	83.4	81.8	82.4	89.8	86.6	88.0	91.3
4	82.0	80.3	79.4	88.9	89.6	89.9	88.9	90.7	87.7	88.8	91.0
5	82.4	78.8	78.9	87.0	99.2	102.3	104.4	92.2	89.2	89.2	90.0
6	83.0	79.7	79.1	82.6	88.8	90.8	96.9	91.0	87.9	87.9	89.0
7	81.3	79.9	80.2	79.4	81.0	81.8	83.7	88.1	85.9	86.6	88.2
8	79.4	81.3	81.4	77.8	78.3	78.9	80.8	88.0	84.9	85.9	88.7

RUN NUMBER 528

FLUID FLOW RATE	=	84.00	LBM/HOUR
CURRENT TO TUBE	=	135.00	AMPS
VOLTAGE DROP IN TUBE	=	5.30	VOLTS
ROOM TEMPERATURE	=	82.20	DEGREES F
UNCORRECTED INLET TEMPERATURE	=	62.00	DEGREES F
UNCORRECTED OUTLET TEMPERATURE	=	91.00	DEGREES F

OUTSIDE SURFACE TEMPERATURES - DEGREES F

	1	2	3	4	5	6	7	8	9	10	11
1	73.7	77.6	76.3	77.1	87.3	97.8	103.0	106.8	106.7	106.9	110.8
2	73.8	80.5	80.1	78.6	86.9	97.9	102.2	102.1	106.9	107.7	105.4
3	77.2	90.4	89.1	81.6	87.8	94.7	96.1	95.2	98.0	99.7	100.8
4	83.5	101.3	102.2	95.3	90.9	92.7	92.2	90.8	93.1	93.7	95.6
5	91.8	104.0	105.8	95.0	93.0	92.3	90.1	89.5	90.2	91.1	94.4
6	84.8	90.7	99.4	85.7	89.3	91.6	90.5	89.4	90.0	90.8	98.0
7	78.8	82.4	86.7	79.9	86.4	92.9	92.8	91.3	93.0	93.2	102.3
8	75.8	78.3	79.4	77.7	86.4	97.0	96.5	98.4	101.9	100.6	105.1

APPENDIX B

CALIBRATION DATA

TABLE VI

CALIBRATION DATA FOR ROTAMETER 1 FOR DISTILLED WATER

Rotameter Setting % Maximum Flow	Mass Flow Rate, lbm/hr
10	71.8
20	136.0
30	205.6
40	262.6
50	323.9
60	368.2
70	453.8
80	520.8
90	589.2
100	645.6

TABLE VII

CALIBRATION DATA FOR ROTAMETER 2 FOR DISTILLED WATER

Rotameter Setting % Maximum Flow	Mass Flow Rate, lbm/hr
10	355.0
20	655.2
30	931.8
40	1228.0
50	1517.8
60	1764.7
70	2089.0
80	2415.6
90	2733.4
95	2927.5

For Dowtherm G and ethylene glycol, the flow rate was measured for each individual data run; the rotameter was used merely as an indication of flow rate.

TABLE VIII

CALIBRATION DATA FOR CALIBRATION OF OUTSIDE SURFACE THERMOCOUPLES (TEST SECTION B)

Station Number	Δ = (Steam Temperature) - (Thermocouple Reading), °F Peripheral Position							
	1	2	3	4	5	6	7	8
1	+0.10	+0.10	+0.10	-0.03	-0.33	-0.33	-0.33	-0.37
2	-0.17	+0.07	+0.07	+0.07	+0.07	0.0	-0.07	-0.20
3	-0.20	-0.20	-0.10	-0.13	-0.07	-0.13	-0.17	-0.17
4	-0.30	-0.33	-0.33	-0.27	-0.20	-0.20	-0.20	-0.20
5	-0.43	-0.43	-0.43	-0.43	-0.40	-0.37	-0.37	-0.23
6	-0.23	-0.40	-0.40	-0.43	-0.53	-0.53	-0.47	-0.47
7	-0.37	-0.27	-0.27	-0.23	-0.37	-0.37	-0.37	-0.50
8	-0.30	-0.30	-0.30	-0.30	-0.17	-0.37	-0.43	-0.43
9	+0.43	+0.43	+0.43	+0.37	-0.53	-0.53	-0.53	-0.53
10	-0.43	-0.46	-0.47	-0.47	-0.47	-0.47	-0.37	-0.37
11	-0.37	-0.37	-0.40	0.40	-0.07	-0.07	0.0	0.0

Note:

1. The temperature corrections are the computed arithmetic average of the corrections after 6, 12 and 18 hours of continuous operation.
2. Temperatures were measured with a precision of 0.1°F. The precision of the temperature corrections given above results from the calculation of the corrections and should not be construed to indicate the precision of the temperature measurement.
3. As is shown on Table VIII, the difference between the thermocouple reading and the true temperature of the surface was small; therefore, no correction for surface temperatures was made through the further calculations.
4. Calibration of the other three test sections indicates also that the corrections of the surface thermocouples were small; therefore, no correction for surface temperatures was made for any of the test sections.

TABLE IX

CALIBRATION DATA FOR INLET AND OUTLET THERMOCOUPLES DURING IN-SITU CALIBRATION OF SURFACE THERMOCOUPLES ON THE TEST SECTION B

Thermocouple Location	Saturated Steam Temperature, ^{o}F	Thermocouple Correction, ^{o}F	Average Room Temperature
Inlet	210.7	-0.7	72.0
Outlet	210.7	-0.9	

Therefore the correlations for the inlet and the outlet bulk fluid temperatures are

$$(T_{in})_{corrected} = T_{in} - (0.7)\frac{(T_{in} - T_{room})}{(210.7 - 72.0)}$$

and

$$(T_{out})_{corrected} = T_{out} - (0.9)\frac{(T_{out} - T_{room})}{(210.7 - 72.0)}$$

TABLE X

CALIBRATION DATA FOR HEAT LOSS FROM TEST SECTION B

Average temperature of steam in test section	=	211.4°F
Room temperature during calibration	=	78.1°F
Amount of mass of steam condensed	=	0.42 lbm/hr
Heat of vaporization of water vapor at 211.4°F	=	970.7 Btu/lbm

$$\left\{\begin{matrix}\text{Heat loss from} \\ \text{Heat transfer loop}\end{matrix}\right\} = Q = m\lambda$$

$$= (0.42)(970.7)$$

$$= 408 \text{ Btu/hr}$$

So heat loss during experimental run, Q_{loss}; Btu/hr

$$Q_{loss} = \frac{408\ (T_{avg} - T_{room})}{(211.4 - 78.1)}$$

or, heat loss from the test section, q_{loss}; Btu/hr

$$q_{loss} = \left(\frac{l}{L_{total}}\right) Q_{loss}$$

where

l = length of test section

and

L = total length of heat transfer loop.

$T_{avg} = (1/2)(T_{in} + T_{out})$, °F

Similarly, the heat loss for the other test sections was calculated in the same manner.

APPENDIX C

PHYSICAL PROPERTIES

A. Water

The following correlations which were developed by Singh (7) based on the CRC Handbook of Chemistry and Physics (21) were used to compute the physical properties of water.

1. Density in kg/m^3

$$\rho = 999.986 + 0.01890\ (T) - 0.005886\ (T^2) + (0.1548 \times 10^{-7})\ (T^3)$$

where T = temperature, ^oC

Range: 0^oC to 100^oC ; 1 kg/m^3 = 0.62428×10^{-1} lbm/ft^3

2. Viscosity in Ns/m^2

$$\log_{10}\ (\mu_T/\mu_{20}) = \frac{1.3272(20-T) - 0.001053(20-T)^2}{T + 105}$$

where T = temperature, ^oC

and μ_{20} = viscosity of water at 20^oC = 1.0×10^{-3} Ns/m^2

Range: 20^oC to 100^oC ; 1 Ns/m^2 = 2.42×10^3 $lb_m/hr\text{-}ft$

3. Specific heat in $Btu/lbm\text{-}^oF$

$$C_p = 1.01881 - 0.4802 \times 10^{3}\ (T) + 0.3274 \times 10^{-4}\ (T^2) - 0.604 \times 10^{-8}\ (T^3)$$

where T = temperature, ^oF

Range: 32^oF to 212^oF ; 1 $J/kg\text{-}K$ = 0.238846×10^{-3} $Btu/lbm\text{-}^oF$

4. Thermal conductivity in $Btu/hr\text{-}ft\text{-}^oF$

$$k = 0.30289 + 0.7029 \times 10^{-3}\ (T) - 0.1178 \times 10^{-5}\ (T^2) - 0.550 \times 10^{-9}\ (T^3)$$

where T = temperature, ^oF

Range: 44^oF to 206^oF ; 1 $W/m\text{-}K$ = 0.57779 $Btu/hr\text{-}ft\text{-}^oF$

5. Coefficient of thermal expansion in $1/^oC$

$$\rho = -\frac{1}{\rho}\ \frac{d\rho}{dT}$$

$$\rho = \frac{1}{\rho} [0.0189 - 0.011772\ (T) + 0.4644 \times 10^{-3}\ (T^2)]$$

where ρ = density in kg/m^3 and T = temperature, ^oC

Range: 0^oC to 100^oC ; $1^oC = 1.8^oF$

B. Ethylene Glycol

The following correlations were used to compute the physical properties of ethylene glycol (13).

1. Density in kg/m^3

$$\rho = 1000.0/[0.924848 + 6.2796 \times 10^{-4}\ (T-65) + 9.2444 \times 10^{-7}\ (T-65)^2 + 3.0570 \times 10^{9}\ (T-65)^3]$$

where T = temperature in ^oC

Range: 4.5^oC to 100^oC ; 1 kg/m^3 = 0.62428×10^{-1} lbm/ft^3

2. Viscosity in Ns/m^2

$$\mu = 0.16746 - 5.4455 \times 10^{-3}\ (T) + 8.3752 \times 10^{-5}\ (T)^2 - 7.3076 \times 10^{-7}\ (T)^3 + 3.7748 \times 10^{-9}\ (T)^4 - 1.1386 \times 10^{-11}\ (T)^5 + 1.8487 \times 10^{-14}\ (T)^6 - 1.2463 \times 10^{-7}\ (T)^7$$

where T = temperature, ^oF

Range: 20^oF to 350^oF ; 1 Ns/m^2 = 2.42×10^3 lbm/hr-ft

3. Specific heat in Btu/lbm-^oF

$$C_p = 5.18956 \times 10^{-1} + 6.2290 \times 10^{-4}\ (T)$$

where T = temperature, ^oF

Range: 6^oF to 350^oF ; 1 J/kg-K = 6.238846 Btu/lbm-^oF

4. Thermal conductivity in Btu/hr-ft-^oF

$$k = 0.18329 - 0.24191 \times 10^{-3}\ (T)$$

where T = temperature, ^oF

Range: 50^oF to 350^oF ; 1 W/m-K = 0.57779 Btu/hr-ft-^oF

5. Coefficient of thermal expansion in $1/^{o}C$

$\beta = \rho[6.2796 \times 10^{-1} + 18.4888 \times 10^{-4} (T-65) + 9.171 \times 10^{-6} (T-65)^2]$

where ρ = density, kg/m^3 and T = temperature, ^{o}C

Range: $4.5^{o}C$ to $170^{o}C$; $1^{o}C = 1.8^{o}F$

C. Dowtherm G

The following correlations were used to compute the physical properties of Dowtherm G (7).

1. Density in lbm/ft^3

$= 70.70705 - 0.25338 \times 10^{-1} (T) - 0.3095 \times 10^{-4} (T^2) + 0.8890 \times 10^{-7} (T^3)$

where T = temperature, ^{o}F

Range: $0^{o}F$ to $300^{o}F$; 1 $kg/m^3 = 0.62428 \times 10^{-1}$ lbm/ft^3

2. Viscosity in Ns/m^2

$\mu = 1.05786 \times 10^{-1} - 1.6867 \times 10^{-3} (T) + 0.15058 \times 10^{-4} (T^2) - 0.29936 \times 10^{-7} (T^3) + 0.31818 \times 10^{-10} (T^4)$

where T = temperature, ^{o}F

Range: $90^{o}F$ to $200^{o}F$; 1 $Ns/m^2 = 2.42 \times 10^{3}$ lbm/hr-ft

3. Specific heat in Btu/lbm - ^{o}F

$C_p = 0.369356 + 0.20216 \times 10^{-3} (T) + 0.8285 \times 10^{-6} (T)^2 - 0.19987 \times 10^{-8} (T^3)$

where T = temperature, ^{o}F

Range: $0^{o}F$ to $300^{o}F$, 1 J/kg-K = 0.23886×10^{-3} Btu/lbm-^{o}F

4. Thermal conductivity in Btu/hr-ft-^{o}F

$k = 0.076189 - 0.22498 \times 10^{-4} (T)$

where T = temperature, ^{o}C

Range: $0^{o}C$ to $300^{o}C$; 1 W/m-K = 0.57779 Btu/hr-ft^{o}F

5. Coefficient of thermal expansion in $1/^{o}F$

$\beta = (1/\rho)\ [0.25338 \times 10^{-1} + 0.619 \times 10^{-4}\ (T) = 2.667 \times 10^{-7}\ (T)^{2}]$

where ρ = density, lbm/ft^{3}, T = temperature, ^{o}F

Range: $0^{o}F$ to $300^{o}F$; $1^{o}C = 1.8^{o}F$

D. Inconel 600

The following physical correlations which were developed by Farukhi (9) were used to compute the physical properties of Inconel 600.

1. Electrical resistivity in $Ohms\text{-}in^{2}/in$

$\rho = (10^{-6})\ [40.4029 + 2.51538\ (T)]$

T = temperature, ^{o}F

2. Thermal conductivity in $Btu/hr\text{-}ft\text{-}^{o}F$

$k = 0.8313769 + 3.846154 \times 10^{-3}\ (T)$

where T = temperature ; 1 W/m-K = 0.57779 $Btu/hr\text{-}ft\text{-}^{o}F$

E. Stainless Steel

The following correlations which were developed by Singh (7) were used to compute the physical properties of stainless steel.

1. Electrical resistivity in $Ohms\text{-}in^{2}/in$

$\rho = 2.601 \times 10^{-5} + 1.37904 \times 10^{-8}\ (T) + 8.5158 \times 10^{-12}\ (T^{2}) - 10.11924 \times 10^{-17}\ (T^{3})$

where T = temperature, ^{o}F

2. Thermal conductivity in $Btu/hr\text{-}ft\text{-}^{o}F$

$k = 7.8034 + 0.51691 \times 10^{-2}\ (T) - 0.88501 \times 10^{-6}\ (T^{2})$

where T = temperature, ^{o}F ; 1 W/m-K = 0.57779 $Btu/hr\text{-}ft\text{-}^{o}F$

APPENDIX D

NUMERICAL SOLUTION OF WALL TEMPERATURE GRADIENT WITH INTERNAL HEAT GENERATION

The following numerical solution of the conduction equation with internal heat generation and variable thermal conductivity and electrical resistivity was originally developed by Farukhi (9). The solution also takes into account the variation of wall thickness in the bend.

Heat Balance on an Incremental Element

Assumption and Conditions

The following assumptions and conditions are used in deriving the numerical solution.

1. Electrical resistivity of tube wall is a function of temperature.
2. Thermal conductivity of tube wall is a function of temperature.
3. Peripheral and radial wall conduction exist.
4. Axial conduction is negligible.
5. Steady state conditions exist.
6. Heat losses to the atmosphere are present.

The tube wall thickness was divided into ten equal slices (see Figure 30) and the inside surface temperature was obtained directly (since the outside wall temperature was known) by performing heat balances on each node in the radial direction. The tube cross-section was divided into octants about the axis.

Interior Nodes

Consider the cross-section of a typical interior element as shown in Figure 31.

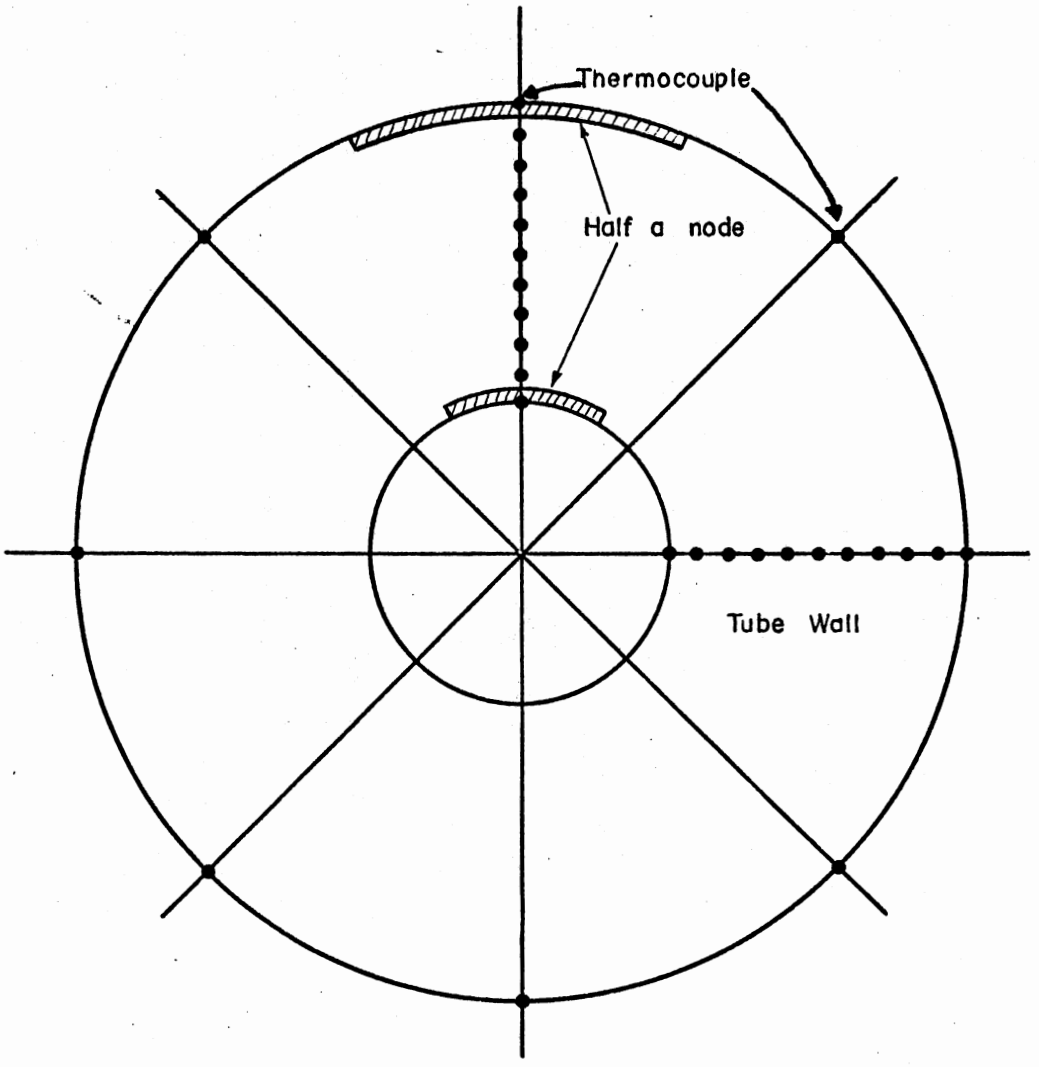

Figure 30. Division of Tube Wall Thickness

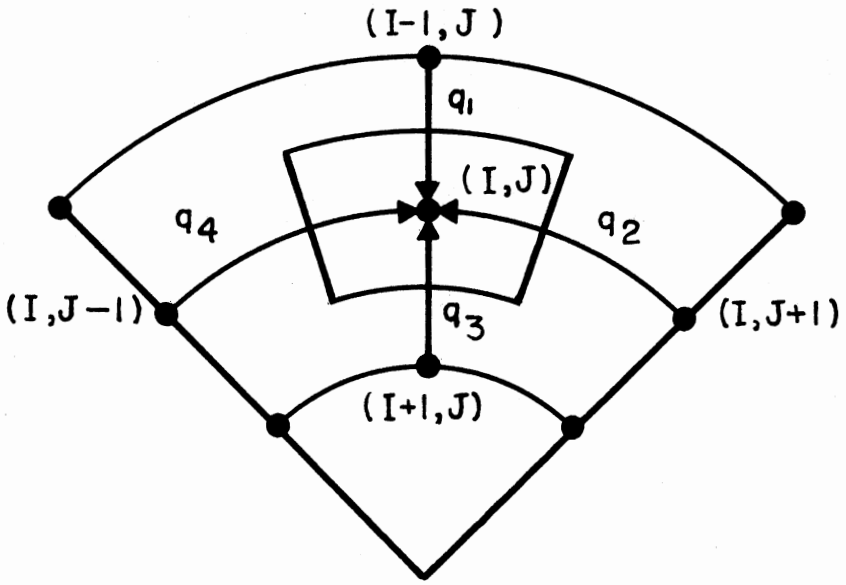

Figure 31. Interior Element

An energy balance on the element gives,

$$q_1 + q_2 + q_3 + q_4 + q_g = 0 \qquad \text{(D-1)}$$

From Fourier's law we know that

$$q = - kA \frac{dT}{dX} \qquad \text{(D-2)}$$

Now using subscripts I and J for the radial and peripheral direction respectively (as shown in Figure 31), and writing Fourier's equation for side 1, we obtain

$$q_1 = - \bar{k} (rd\theta)_{I-1/2}(dZ)[T_{I-1,J} - T_{I,J}]/(r_{I-1} - r_I) \qquad \text{(D-3)}$$

where

$$d\theta = \pi/4 \text{ (eight thermocouple locations)}$$

$$r_{I-1} - r_I = \Delta r \text{ (taking equal thickness)}$$

$$k = (k_{I-1} + k_I)/2.0$$

$$r_{I-1/2} = (r_{I-1} - \frac{\Delta r}{2}) \text{ and } r_{I+1/2} = (r_{I+1} + \frac{\Delta r}{2}).$$

Assuming that heat transfer into the element is positive since Δr is a negative term, the minus sign can be deleted from Equation D-3.

Substituting the definitions into Equation (D-3) gives

$$q_1 = (1/2)(k_{I-1,J} + k_{I,J})(\pi/4)(r_{I-1} - \frac{\Delta r}{2})(dZ) \cdot (T_{I-1,J} - T_{I,J})/\Delta r \qquad \text{(D-4)}$$

Similarly for side 3,

$$q_3 = (1/2)(k_{I+1,J} + k_{I,J})(\pi/4)(r_{I+1} + \frac{\Delta r}{2})(dZ)\cdot (T_{I+1,J} - T_{I,J})/\Delta r \ . \tag{D-5}$$

Writing Fourier's equation for side 2 gives

$$q_2 = \bar{k}(drdZ)(T_{I,J+1} - T_{I,J})/(rd\theta)_I . \tag{D-6}$$

Substituting the definitions for some of the variables gives

$$q_2 = (1/2)(k_{I,J+1} + k_{I,J})(\Delta r)(dZ)(T_{I,J+1} - T_{I,J})(4.0)/(\pi r_I). \tag{D-7}$$

Similarly for side 4,

$$q_4 = (1/2)(k_{I,J-1} + k_{I,J})(\Delta r)(dZ)(T_{I,J-1} - T_{I,J})(4.0)/(\pi r_I). \tag{D-8}$$

The heat generation term is calculated from the equation for Joulean heating.

$$q_g = I^2R \tag{D-9}$$

where

$$R = \frac{\rho dZ}{A_{cs}} \quad (3.41213)$$

ρ = electrical resistivity (function of temperature at node (I,J)), Ohms-in^2/in

and

$$A_{cs} = \pi(r_I\Delta r)/4.0 \ . \tag{D-10}$$

Substituting the above definitions into Equation (D-9) gives,

$$q_g = I^2 \left[\frac{\rho dZ(3.412)}{\pi(r_I \Delta r)/4.0} \right] \qquad \text{(D-11)}$$

Combining Equations (D-4), (D-5), (D-7), (D-8), and (D-11) and rearranging the terms give

$$\begin{aligned} T_{I+1,J} = T_{I,J} - \Bigg[& \frac{3.412}{(XAREA)} (\rho I^2) \\ & + \left(\frac{DPHI}{2\ DELR}\right) (k_{I-1,J} + k_{I,J}) \left(r_{I-1} - \frac{DELR}{2}\right)(T_{I-1,J} - T_{I,J}) \\ & + \left(\frac{DELR}{2\ DPHI}\right) (k_{I,J-1} + k_{I,J})(T_{I,J-1} - T_{I,J})/r_I \\ & + \left(\frac{DELR}{2\ DPHI}\right) (k_{I,J+1} + k_{I,J})(T_{I,J+1} - T_{I,J})/r_I \Bigg] \Bigg/ \\ & \left[\left(\frac{DPHI}{2\ DELR}\right) (k_{I+1,J} + k_{I,J}) \left(r_{I+1} + \frac{DELR}{2}\right)\right] \end{aligned} \qquad \text{(D-12)}$$

where

$$DPHI = \pi/4$$

$$XAREA = r_I(\pi/4)(\Delta r)$$

$$DELR = \Delta r$$

Equation (D-12) is used for all the interior elements. For the outside wall element, which is really a "half-size" element, Equations (D-5), (D-7), (D-8), and (D-9) are solved simultaneously in conjunction with the following equation, which accounts for the heat loss.

$$\dot{q}_L = \left(\frac{\dot{q}_T}{8.0}\right)\left(\frac{T_{room} - T_{I,J}}{T_o - T_{or}}\right)\left(\frac{dZ}{L_T}\right) \qquad \text{(D-13)}$$

where

$\dot{q}_T$ = total heat loss from test section (from calibration run)

L_T = total heated length

T_o = surface temperature during calibration run

T_{or} = room temperature during calibration run

For the outside wall node the temperatures for nodes (I-1,J), (I,J+1), and (I,J-1), are known since the first node condition is given by Equation (D-13) and the other three nodal temperatures are thermocouple readings. Consequently, the temperature at node (I+1,J) can be calculated. After all the (I+1,J) temperature values are calculated, successive use of Equation (D-12) gives the temperature at the inside surface.

Heat Flux at Inside Wall

The procedure for performing heat balances outlined above gives the radial heat flux at the inside wall when the heat balance is made on the inside surface ("half-size") node. This heat flux value was used in calculating the heat transfer coefficients.

Wall Thickness Calculations in the Bend

The variation in wall thickness in the bend was incorporated in the computer program by using a procedure similar to the one outlined by Carver et al. (23).

Assumptions

The following assumptions were made for the tube geometry:

1. Negligible ovality.

2. Conservation of tube material volume during bending.

For a straight tube the cross-section would be similar to the one shown in Figure 32 and for a bent tube it would be similar to the one shown in Figure 33.

The mean length for the three different elements can be written as

$$L_o = (R_c + r_i + \frac{t_o}{2})\, d\theta \tag{D-14}$$

$$L_i = (R_c - r_i - \frac{t_i}{2})\, d\theta \tag{D-15}$$

$$L_c = R_c d\theta\ . \tag{D-16}$$

Using the conservation of tube material volume assumption gives

$$[r_i d\alpha + (r_i + t_o)\, d\alpha](\frac{t_o}{2})[(R_c + r_i + \frac{t_o}{2})d\theta] =$$

$$[r_i d\alpha + (r_i + t_c)d\alpha](\frac{t_c}{2})[R_c d\theta] \tag{D-17}$$

The terms $d\alpha$ and $d\theta$ drop out of the equation and the following equation is then obtained

$$(2r_i + t_o)(t_o)(R_c + r_i + \frac{t_o}{2}) = (2r_i + t_c)(t_c)(R_c). \tag{D-18}$$

Similarly

$$(2r_i + t_i)(t_i)(R_c - r_i - \frac{t_i}{2}) = (2r_i + t_c)(t_c)(R_c) \tag{D-19}$$

In Equations (D-18) and (D-19) all the variables except t_o and t_i are known. Solving these equations by trial and error gives the values for the maximum and minimum thickness. For the thickness at

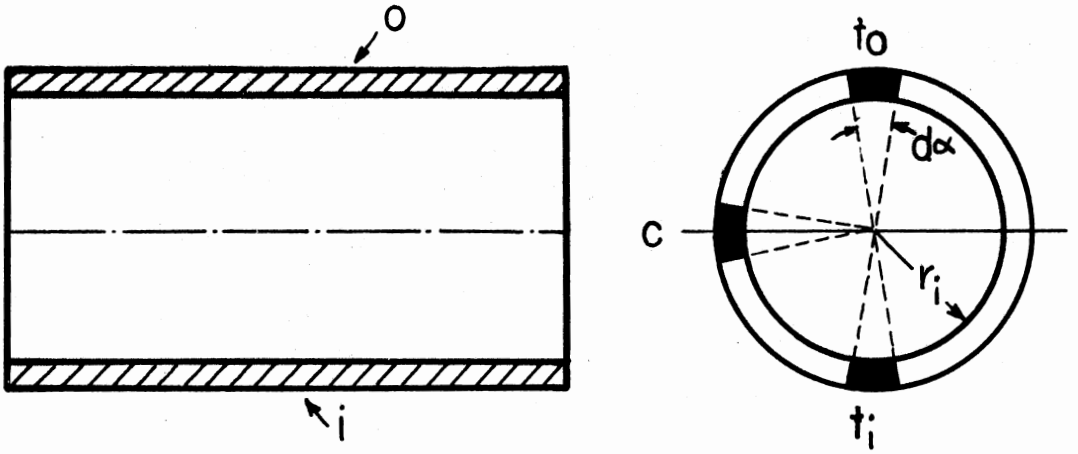

Figure 32. Cross-Section for Straight Tube

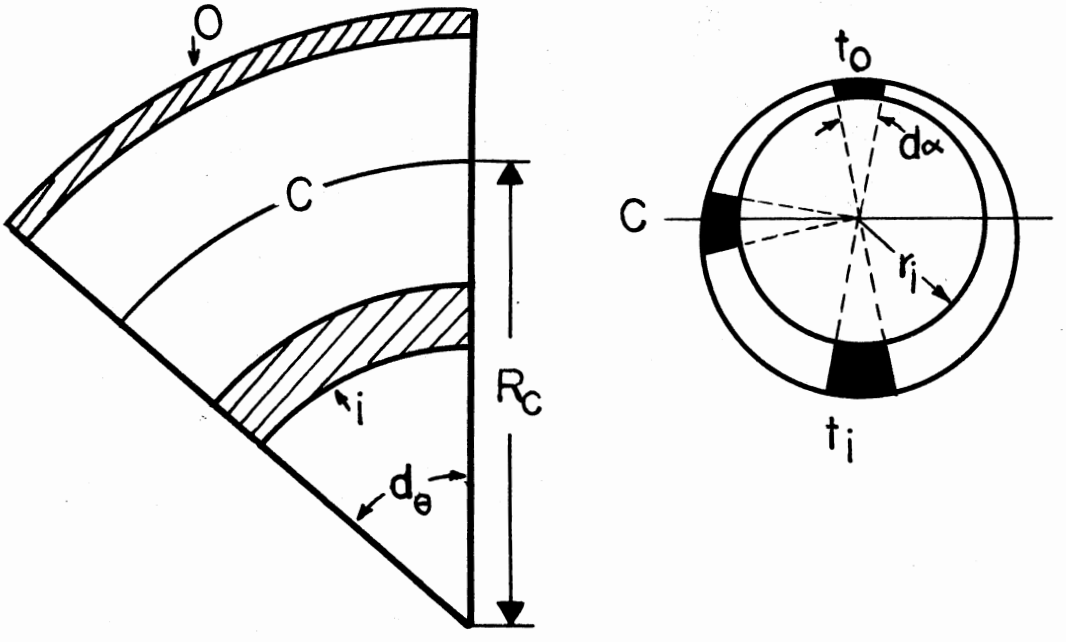

Figure 33. Cross-Section for Curved Tube

the other peripheral and axial locations, an average value of the adjacent thickness were used.

Table XI presents the calculated t_o and t_i for the four test section.

TABLE XI

CALCULATED WALL THICKNESS IN THE BEND

Tube	R_c, mm	r_i, mm	t_c, mm	t_i, mm	t_o, mm
A	251	9.79	1.32	1.37	1.27
B	121	9.79	1.32	1.44	1.22
C	60	7.87	1.65	1.78	1.54
D	38	7.87	1.65	1.87	1.48

APPENDIX E

SAMPLE CALCULATIONS

Calculations for experimental data run 420 are presented as a sample calculation. The experimental data values for run 420 are presented on page 101 in Appendix A. The sample calculations given here are based on the following assumptions and conditions:

1. Electrical resistivity and thermal conductivity of tube walls are functions of temperature.
2. Peripheral and radial wall conduction exist.
3. Axial conduction is negligible.
4. Steady state conditions exist.
5. Heat losses to the atmosphere are present, but small.

Computer programs written originally by Farukhi (9) were modified and developed further to perform the calculations for all the data runs on IBM 370 computer.

The sample calculations given below follow the steps outlines on page 32 in Chapter V.

Calculation of the Heat Balance

Heat input rate, Btu/hr = q_{input}

$$q_{input} = \left\{\begin{matrix}\text{current}\\ \text{in tube}\end{matrix}\right\} \left\{\begin{matrix}\text{voltage drop}\\ \text{across tube}\end{matrix}\right\} (3.41213)$$

$$= (470.0)(18.7)(3.41213)$$

$$= 29{,}989.2 \text{ Btu/hr}$$

Heat loss rate, Btu/hr = Q_{loss}

Calibration data for heat losses to the atmosphere given in Table X, Appendix B.

$$q_{loss} = \frac{596.0}{(211.5 - 78.2)} \left[\frac{1}{2}(T_{b_{in}} + T_{b_{out}}) - T_{room}\right]$$

$$= \frac{596.0}{(211.5 - 78.2)} \left[\frac{1}{2} (94.4 + 107.2) - 83.6\right]$$

$$= 76.9 \text{ Btu/hr}$$

Heat output rate, Btu/hr = q_{output}

$$q_{output} = (W)(C_p) \left[T_{b_{out}} - T_{b_{in}}\right]$$

The inlet and outlet bulk fluid temperatures measured by the thermocouples were corrected, based on their calibration correction. Calibration data for these thermocouples are given in Table IX in Appendix B.

$$\left\{\begin{matrix}\text{corrected inlet} \\ \text{fluid temperature}\end{matrix}\right\} = T_{b_{in}} - (0.7)\left[\frac{T_{b_{in}} - T_{room}}{210.7 - 72.0}\right]$$

$$= 94.4 - (0.7)\left[\frac{94.4 - 83.6}{210.7 - 72.0}\right]$$

$$= 94.35^{o}F$$

$$\left\{\begin{matrix}\text{corrected outlet} \\ \text{fluid temperature}\end{matrix}\right\} = T_{b_{out}} - (0.9)\left[\frac{T_{b_{out}} - T_{room}}{210.7 - 72.0}\right]$$

$$= 107.2 - (0.9)\left[\frac{107.2 - 83.6}{210.7 - 72.0}\right]$$

$$= 107.05^{o}F$$

$$\left\{\begin{matrix}\text{average bulk} \\ \text{fluid temperature}\end{matrix}\right\} = \frac{1}{2} (T_{b_{in}} + T_{b_{out}})$$

$$= \frac{1}{2} (94.35 + 107.05)$$

$$= 100.7^{o}F$$

For water, from Appendix C,

$$C_p = 1.01881 - (0.4802)(10^{-3})(T) + (0.3274)(10^{-5})(T^2) - (0.604)(10^{-8})(T^3)$$

at $\overline{T} = 100.7^{o}F$

$$C_p = 1.01881 - 0.4802 \times 10^{-3} (100.7) + 0.3274 \times 10^{-5} (100.7^2) - 0.604 \times 10^{-8} (100.7^3)$$

$$= 0.9975 \text{ Btu/lbm-}^{o}F$$

$$q_{output} = (2428.4)(0.9975)(107.05 - 94.35)$$

$$= 30,763.6 \text{ Btu/hr}$$

$$\text{percent error in heat balance} = \frac{\dot{q}_{input} - \dot{q}_{loss} - q_{output}}{\dot{q}_{input}} \times 100.0$$

$$= \frac{29,982.2 - 76.9 - 30,763.6}{29,982.2} \times 100.0$$

$$= - 2.86\%$$

Calculation of the Local Inside Wall Temperature and the Inside Wall Radial Heat Flux

As indicated in Chapter V, a numerical solution developed and applied by Owhadi (22), Crain (14), Singh (7), and Farukhi (9), was used to compute the inside wall temperatures and the inside wall radial heat flux at each thermocouple location. The trial-and-error solution is complex and hence a sample calculation will not be given here; however, the derivation of equations which were given in Appendix B of Farukhi's (9) thesis are presented in Appendix D.

Tables XII to XIV give the outside surface temperatures, the computed inside wall temperatures and the inside wall radial heat fluxes for every thermocouple located on the test section.

Calculation of the local heat transfer coefficient for thermocouple station 11-1 (station 11, peripheral position 1):

$$\left\{\begin{matrix}\text{local heat transfer} \\ \text{coefficient}\end{matrix}\right\} = \frac{(q/A)}{(T_{w_{11}} - T_{b_{11}})}$$

$$T_{b_{11}} = T_{b_{in}} + (T_{b_{out}} - T_{b_{in}}) \left(\frac{L_{11}}{L_{total}}\right)$$

$$= 94.35 + (106.7 - 94.35)\left(\frac{127.4}{131.4}\right)$$

$$= 106.3^{o}F$$

$$\left\{\begin{matrix}\text{local heat transfer} \\ \text{coefficient}\end{matrix}\right\} = \frac{13,581.4}{120.2 - 106.3}$$

$$= 977.1 \text{ Btu/(hr-ft}^2\text{-}^{o}\text{F)}$$

Similarly the local heat transfer coefficients at the other thermocouple locations at station 11 can be calculated and the results are presented in Table XV.

The peripheral average heat transfer coefficient at station 11 is calculated as follows:

$$\bar{h} = (1/8) \sum_{i=1}^{8} h_i$$

TABLE XII

RUN 420 - OUTSIDE SURFACE TEMPERATURES, ^{o}F

Thermocouple* Peripheral Location	Thermocouple Station Number										
	1	2	3	4	5	6	7	8	9	10	11
1	116.7	119.7	119.1	112.7	112.1	111.2	113.2	115.7	117.0	118.4	123.5
2	116.5	119.9	120.3	115.2	113.4	113.0	113.8	115.9	117.0	118.6	124.0
3	114.9	120.4	120.9	118.2	117.2	116.3	116.4	118.0	119.4	120.0	124.9
4	113.9	119.9	121.4	122.8	122.0	124.5	120.8	121.7	123.0	123.7	127.6
5	113.2	119.1	121.1	129.3	128.3	132.2	127.6	126.9	127.3	127.7	128.6
6	112.1	118.2	120.2	121.8	120.2	121.1	121.8	123.7	124.3	125.1	127.1
7	112.6	118.0	119.1	116.2	115.5	115.1	117.7	119.6	120.8	121.7	125.0
8	115.2	118.7	120.1	114.2	112.7	111.9	114.6	115.9	118.2	119.6	123.3

*See the position of each thermocouple on Figure 4.

TABLE XIII

RUN 420 - CALCULATED INSIDE SURFACE TEMPERATURES, ^{o}F

Thermocouple Peripheral Location	Thermocouple Station Number										
	1	2	3	4	5	6	7	8	9	10	11
1	113.4	116.4	115.8	109.0	108.7	107.4	109.9	112.4	113.7	115.1	120.2
2	113.2	116.6	117.0	111.7	110.0	109.5	110.5	112.6	113.7	115.3	120.7
3	111.6	117.1	117.6	115.0	114.0	113.0	113.1	114.7	116.1	116.7	121.6
4	110.6	116.6	118.1	119.6	118.7	121.4	117.5	118.4	119.7	120.4	124.4
5	109.9	115.8	117.8	126.5	125.2	129.6	124.5	123.7	124.1	124.5	125.4
6	108.8	114.9	116.9	118.6	116.9	118.0	118.5	120.4	121.0	121.8	123.8
7	109.3	114.7	115.8	112.9	112.3	111.8	114.4	116.3	117.5	118.4	121.7
8	111.9	115.4	116.9	110.5	109.3	108.4	111.3	112.6	114.9	116.3	120.0

TABLE XIV

RUN 420 - RADIAL HEAT FLUX FOR INSIDE SURFACE, BTU/(HR-FT^2)

Thermocouple Peripheral Location	Thermocouple Station Number										
	1	2	3	4	5	6	7	8	9	10	11
1	13,458.6	13,513.3	13,686.0	15,799.4	15,099.1	16,024.5	13,675.2	13,585.3	13,630.9	13,643.6	13,581.4
2	13,475.7	13,575.9	13,525.8	14,528.6	14,399.9	14,701.9	13,675.0	13,670.7	13,699.7	13,631.0	13,587.0
3	13,590.5	13,502.1	13,554.8	13,488.6	13,364.4	13,719.1	13,661.9	13,651.0	13,629.0	13,693.0	13,666.8
4	13,574.0	13,541.9	13,513.8	12,842.5	13,169.7	12,528.1	13,695.0	13,644.8	13,600.1	13,577.9	13,464.6
5	13,534.1	13,553.4	13,525.8	11,165.0	11,708.5	10,599.9	12,833.8	13,076.8	13,140.3	13,180.9	13,419.1
6	13,648.4	13,600.4	13,548.2	12,843.8	13,283.3	12,852.5	13,654.8	13,507.4	13,530.0	13,513.7	13,527.8
7	13,676.9	13,611.3	13,680.4	13,591.3	13,415.0	13.600.5	13,615.4	13,582.0	13,611.6	13,635.1	13,585.8
8	13,493.7	13,577.2	13,446.8	14,550.8	14,383.9	14,758.8	13,658.2	13,761.5	13,642.1	13,614.1	13,673.2

TABLE XV

PERIPHERAL HEAT TRANSFER COEFFICIENT
AT STATION 11

	Peripheral Location							
	1	2	3	4	5	6	7	8
h, Btu/(hr-ft^2-^{o}F)	977.1	943.4	894.1	746.5	704.5	772.1	882.0	979.4
	(Top)				(Bottom)			

$$= (1/8)(977.1 + 943.4 + 894.1 + 746.5 + 704.5 + 772.1 + 882.0 + 999.4)$$

$$= 864.9 \text{ Btu/(hr-ft}^2\text{-}^{o}\text{F)}$$

In the above calculation h_i's were taken from Table XV.

Calculation of Relevant Dimensionless Number at Station 11

Physical Properties:

Using correlations given in Appendix C, calculate viscosity, specific heat, thermal conductivity, density, and thermal expansion coefficient of water.

1. Viscosity

$$\log (\mu_T/\mu_{20}) = \frac{1.3272(20-T) - 0.001053(20-T)^2}{T + 105}$$

where T measured in ^{o}C and $\mu_{20} = 1.0 \times 10^{-3}$ Ns/m^2

at $T_{b_{11}} = 106.3^{o}\text{F} = 41.28^{o}\text{C}$

$$\log_{10} (\mu/1.0 \times 10^{-3}) = \frac{1.3272(20-41.28) - 0.001053(20-41.28)^2}{41.28 + 105}$$

$$\mu = 0.6376 \times 10^{-3} \text{ Ns/m}^2$$

$$= 10.6376 \times 10^{-3})(2.42 \times 10^{3})$$

$$= 1.543 \text{ lbm/(hr-ft)}$$

Similarly, for average inside surface temperature, $\bar{T}_w$:

$$\bar{T}_w = (1/8) \sum_{i=1}^{8} (T_{w_i})$$

$$= (1/8)(120.2 + 120.7 + 121.6 + 124.4 + 125.4 + 123.8 + 121.7 + 120.0)$$

$$= 122.2^{o}F$$

$$= 50.11^{o}C$$

So at $\bar{T}_w = 50.11^{o}C$

$$\mu_w = 0.5458 \times 10^{-3}\ Ns/m^2$$

$$= 1.321\ lbm/(hr\text{-}ft)$$

2. Specific Heat:

$$C_p = 1.01881 - (0.4802)(10^{-3})(T) + (0.3274)(10^{-5})(T^2) - (0.604)(10^{-8})(T^3)$$

at $T_{b_{11}} = 106.3^{o}F$

$$C_p = 1.01881 - (0.4802)(10^{-3})(106.3) + 10.3274)(10^{-5})(106.3)^2 - (0.604)(10^{-8})(106.3)^3$$

$$= 0.9975\ Btu/(lbm\text{-}^{o}F)$$

3. Thermal Conductivity:

$$k = 0.30289 + (0.7029)(10^{-3})(T) - (0.1178)(10^{-5})(T^2) - (0.550)(10^{-9})(T^3)$$

at $T_{b_{11}} = 106.3^{o}F$

$$k = 0.30289 + (0.7029)(10^{-3})(106.3) = (0.1178)(10^{-5})(106.3)^2 - (0.550)(10^{-9})(106.3)^3$$

$$= 0.364\ Btu/(hr\text{-}ft\text{-}^{o}F)$$

4. Density, ρ

$$\rho = [0.999986 + (0.1890)(10^{-4})(T) = (0.5886)(10^{-5})(T^2) + (0.1548)(10^{-7})(T^3)] \times 10^3$$

at $T_{b_{11}} = 106.3^{o}F = 41.28^{o}C$

$$\rho = [0.999986 + (0.1890)(10^{-4})(41.28) = (0.5886)(10^{-5})(41.28)^2 + (0.1548)(10^{-7})(41.28)^3] \times 10^3$$

$$= 991.8 \text{ kb/m}^3$$

$$= (991.8)(0.62428 \times 10^{-1})$$

$$= 61.86 \text{ lbm/ft}^3$$

5. Thermal Expansion Coefficient

$$\beta = -\frac{1}{\rho}\frac{d\rho}{dT}$$

$$\frac{d\rho}{dT} = (0.189)(10^{-4}) - (2)(0.5886)(10^{-5})(T) + (3)(0.1548)(10^{-7})(T^2)$$

at $T_{b_{11}} = 41.28^oC$

$$\frac{d\rho}{dT} = (0.189)(10^{-1}) - (2)(0.5886)(10^{-2})(41.28) + (3)(0.1548)(10^{-4})(41.28)^2$$

$$= -3.88 \times 10^{-1} \text{ kg/m}^3\text{-}^oC$$

$$= 2.155 \times 10^{-1} \text{ kg/m}^3\text{-}^oF$$

$$\beta = (-1/991.8)(-2.155 \times 10^{-1})$$

$$\beta = 2.17 \times 10^{-4} \ (1/^oF)$$

1. Reynolds Number: Re

$$Re = (d_i)(G)/\mu$$

where $G = W/(\pi d_i^2/4)$

$$= 2428.4/(\pi(0.771/12)^2/4)$$

$$= 7.49 \times 10^5 \text{ lbm/(hr-ft}^2)$$

$$Re = (0.771/12)(7.49 \times 10^5)/(1.543)$$

$$= 3.12 \times 10^4$$

2. Prandtl Number: Pr

$$Pr = (C_p)(\mu)/k$$

$$= (0.9975)(1.543)/(0.364)$$

$$= 4.23$$

3. Peripheral Average Nusselt Number

$$Nu = (\bar{h})(d_i)/k$$

$$= (864.9)(0.771/12)/(0.364)$$

$$= 152.7$$

4. Grashof Number: Gr

$$Gr = (d_i^3)\ (\rho^2)(g)(\beta)(\bar{T}_w - T_b)/(\mu^2)$$

where $g = 32.174\ ft/sec^2 = 4.17 \times 10^8\ ft/hr^2$

$$Gr = (0.771/12)^3(61.86)^2(4.17 \times 10^8)(2.17 \times 10^{-4})$$

$$(122.2 - 106.3)/(1.543^2)$$

$$= 6.13 \times 10^5$$

5. Rayleigh Number: Ra

$$Ra = (Gr)(Pr)$$

$$= (6.13 \times 10^5)(4.23)$$

$$= 2.59 \times 10^6$$

6. Gr/Re^2

$$Gr/Re^2 = (6.13 \times 10^5)/(3.12 \times 10^4)^2$$

$$= 6.3 \times 10^{-4}$$

Comparison of Experimental Data with Literature

1. Sieder-Tate equation

$$\bar{h}_{ST} = 0.023\ (k/d_i)(Re^{0.8})(Pr^{0.333})(\mu/\mu_w)^{0.14}$$

$$= 0.023(0.364/(0.771/12))(3.12 \times 10^4)^{0.8}(4.23)^{0.333}$$
$$(1.543/1.321)^{0.14}$$
$$= 848.2 \text{ Btu/(hr-ft}^2\text{-}^o\text{F)}$$

At station 11 the peripheral average heat transfer coefficient was calculated to be 864.9 Btu/(hr-ft^2-^{o}F).

$$\text{ratio of heat transfer coefficients (experimental to Sieder-Tate)} = \frac{864.9}{848.2}$$
$$= 1.02$$

2. Dittus - Boelter equation

$$\bar{h}_{DB} = 0.023\ (k/d_i)(Re^{0.8})(Pr^{0.4})$$
$$= 0.023(0.364/(0.771/12))(3.12 \times 10^4)^{0.8}(4.23)^{0.4}$$
$$= 913.7 \text{ Btu/(hr-ft}^2\text{-}^o\text{F)}$$

$$\text{ratio of heat transfer coefficient (experimental to Dittus-Boelter)} = \frac{864.9}{913.7}$$
$$= 0.95$$

3. Eagle-Ferguson equation

$$\bar{h}_{EF} = C(1.75\ T_b + 160)(V^{0.80})$$

where $C = 0.9109 - 0.4292 \log (d_i)$

$d_i = 0.771$ in.

$C = 0.9109 - 0.4292 \log (0.62) = 0.9595$

$T_{b_{11}} = 106.3^o\text{F}$

$$V = \frac{W}{\rho A_c} = \frac{W}{\rho(\frac{\pi}{4} d_i^2)}$$

$$V = \frac{(2428.4)}{(61.86)(\frac{\pi}{4})(\frac{0.771}{12})^2(3600)} = 3.363 \text{ ft/sec}$$

$$h_{EF} = (0.9594)(1.75 \times 106.3 + 160)(3.363)^{0.80}$$

$$h_{EF} = 876.0 \text{ Btu/hr-ft}^2\text{-}^o\text{F}$$

$$\text{ratio of heat transfer coefficient (experimental to Eagle-Ferguson)} = \frac{864.9}{876.0}$$

$$= 0.99$$

APPENDIX F

CALCULATED RESULTS

LIT(1) = Ratio of the experimental heat transfer coefficient (H_1) to that predicted by Sieder-Tate correlation (for Re $>$ 2100).

LIT(1) = Ratio of the experimental heat transfer coefficient (H_1) to that predicted by Morcos-Bergles correlation (for Re $>$ 2100)

LIT(2) = Ratio of the experimental heat transfer coefficient (H_1) to that predicted by Dittus-Boelter (for Re $>$ 2100).

LIT(2) = Ratio of the experimental heat transfer coefficient (H_2) to that predicted by Morcos-Bergles correlation (for Re $>$ 2100).

LIT(3) = Ratio of the experimental heat transfer coefficient (H_1) to that predicted by Eagle-Ferguson correlation (for Re $>$ 2100).

The calculated results for those experimental runs which were presented in Appendix A are presented here. The rest of the calculated results are available at:

School of Chemical Engineering
Oklahoma State University
Stillwater, Oklahoma 74074 USA

RUN NUMBER 203

INSIDE SURFACE TEMPERATURES - DEGREES F

	1	2	3	4	5	6	7	8	9	10	11
1	93.9	96.4	94.4	93.9	93.2	93.3	93.3	98.3	99.3	100.4	110.3
2	94.0	96.4	94.8	94.2	93.5	93.6	93.7	98.3	99.2	100.6	104.9
3	94.1	96.4	96.0	95.3	94.3	94.3	94.3	98.4	99.1	100.4	100.9
4	94.2	96.4	97.6	97.0	96.4	96.7	97.0	98.3	99.2	100.4	99.8
5	94.2	96.3	98.7	98.8	99.0	99.0	99.6	98.3	99.1	100.2	99.6
6	94.2	96.4	97.4	97.1	96.8	96.8	97.0	98.3	99.1	100.4	99.9
7	94.1	96.5	95.5	95.0	94.5	94.8	95.0	98.3	99.1	100.5	101.6
8	94.1	96.4	94.7	94.2	93.6	93.8	93.8	98.3	99.3	100.0	107.4

INSIDE SURFACES HEAT FLUXES BTU/HR/FT2

	1	2	3	4	5	6	7	8	9	10	11
1	985.7	955.6	1026.4	617.8	580.9	637.1	1046.7	956.8	947.8	937.6	143.3
2	954.5	955.9	1037.1	793.9	728.6	752.7	984.3	967.6	957.3	917.2	1096.8
3	954.9	955.9	996.7	961.2	1013.5	1073.4	1148.0	937.0	978.3	979.1	1232.6
4	945.4	946.3	896.2	1189.5	1250.6	1168.2	947.9	967.6	937.4	937.6	1059.5
5	954.9	976.8	734.2	1248.3	1157.2	1139.6	447.2	956.8	968.0	999.0	1009.3
6	945.3	955.9	886.4	1136.4	1185.7	1200.4	1009.8	957.0	957.2	948.4	1109.4
7	965.6	935.9	1067.3	1033.2	1024.0	1001.9	1035.8	957.0	978.3	897.2	1347.8
8	934.5	966.4	1006.2	763.3	728.4	763.9	1025.7	957.0	937.5	1050.6	677.5

RUN NUMBER 203

AVERAGE REYNOLDS NUMBER	= 0.361E+04	
AVERAGE PRANDTL NUMBER	= 0.508E+01	
MASS FLUX	= 0.127E+06	LBM/(SQ.FT-HR)
AVERAGE HEAT FLUX	= 0.981E+03	BTU/(SQ.FT-HR)
Q=AMP*VOLT	= 0.294E+04	BTU/HR
Q=M*C*(T2-T1)	= 0.301E+04	BTU/HR
HEAT LOST	= 0.116E+02	BTU/HR
HEAT BALANCE ERROR %	=-0.265E+01	

PERIPHERAL HEAT TRANSFER COEFFICIENT BTU/(SQ.FT-HR-DEG.F)

	1	2	3	4	5	6	7	8	9	10	11
1	170.6	158.3	314.3	225.1	289.6	315.2	544.0	154.3	146.9	154.8	9.9
2	162.1	158.3	283.1	265.8	323.5	330.1	420.2	156.1	150.7	146.4	121.7
3	159.5	158.3	204.4	232.9	332.0	360.6	383.3	148.6	156.6	162.0	243.1
4	155.2	156.7	137.8	203.6	242.7	215.1	167.6	156.1	147.5	154.8	270.2
5	156.9	164.7	97.2	164.1	149.4	147.6	53.9	154.3	154.9	171.1	270.2
6	155.2	158.3	140.5	190.7	212.8	217.4	179.2	154.3	153.1	156.7	276.9
7	161.4	152.3	245.1	271.4	315.0	286.5	285.5	154.3	156.6	145.4	234.9
8	155.9	160.2	281.7	254.8	309.6	308.4	422.0	154.3	145.2	186.8	58.7

AVERAGE HEAT TRANSFER COEFFICIENT-BTU/(SQ.FT.HR-DEG.F)

	1	2	3	4	5	6	7	8	9	10	11
(H1)	159.6	158.4	213.0	226.1	271.8	272.6	307.0	154.0	151.4	159.7	185.7
(H2)	159.5	158.4	190.8	214.7	244.3	242.3	232.3	154.0	151.4	159.4	133.5

RATIO OF CALCULATED HEAT TRANSFER COEFFICIENT TO THOSE PREDICTED BY LITERATURE

	1	2	3	4	5	6	7	8	9	10	11
LIT(1)	0.84	0.82	1.11	1.17	1.41	1.42	1.59	0.79	0.78	0.81	0.93
LIT(2)	0.76	0.75	1.00	1.06	1.27	1.28	1.44	0.72	0.70	0.74	0.85
LIT(3)	0.80	0.78	1.05	1.11	1.34	1.34	1.51	0.75	0.74	0.77	0.89

RUN NUMBER 205

INSIDE SURFACE TEMPERATURES - DEGREES F

	1	2	3	4	5	6	7	8	9	10	11
1	94.9	97.2	95.3	95.2	94.8	94.9	94.8	99.0	99.3	100.8	102.4
2	95.0	97.2	95.9	95.1	95.1	95.2	95.3	99.0	99.4	101.0	102.5
3	95.1	97.1	97.0	96.5	95.9	95.9	95.9	99.1	99.6	101.1	102.4
4	95.1	97.1	98.6	98.3	98.0	98.1	98.3	99.2	99.9	101.2	102.5
5	95.1	96.9	99.7	99.9	100.1	100.4	100.9	99.2	99.9	101.2	102.4
6	95.0	97.1	98.4	98.3	98.2	98.2	98.5	99.2	99.9	101.2	102.4
7	95.0	97.2	96.5	96.3	96.1	96.5	96.8	99.0	99.6	101.0	102.3
8	95.0	97.1	95.8	95.5	95.1	95.3	95.5	99.0	99.3	100.9	102.3

INSIDE SURFACES HEAT FLUXES BTU/HR/FT2

	1	2	3	4	5	6	7	8	9	10	11
1	1365.8	1337.0	1438.6	827.4	801.8	857.3	1448.9	1348.6	1359.3	1381.2	1351.1
2	1345.6	1337.1	1407.7	1142.4	993.1	1042.1	1376.0	1359.1	1359.4	1339.4	1330.3
3	1335.6	1357.8	1398.0	1309.8	1385.8	1422.0	1509.7	1348.7	1359.1	1350.3	1371.7
4	1345.7	1326.2	1297.1	1654.0	1687.9	1685.4	1369.5	1338.0	1318.2	1339.6	1330.3
5	1335.6	1388.2	1103.5	1924.3	1924.1	1793.5	857.0	1348.8	1349.4	1350.4	1361.2
6	1356.1	1337.2	1297.4	1632.1	1666.0	1707.1	1411.8	1327.9	1318.5	1329.3	1340.5
7	1345.6	1326.8	1449.5	1392.2	1365.4	1329.6	1386.7	1368.9	1349.1	1360.0	1361.0
8	1335.5	1367.6	1386.8	1042.8	1012.9	1082.2	1418.3	1348.3	1379.6	1349.8	1360.8

RUN NUMBER 205

AVERAGE REYNOLDS NUMBER	= 0.561E+04	
AVERAGE PRANDTL NUMBER	= 0.499E+01	
MASS FLUX	= 0.194E+06	LBM/(SQ.FT-HR)
AVERAGE HEAT FLUX	= 0.137E+04	BTU/(SQ.FT-HR)
Q=AMP*VOLT	= 0.411E+04	BTU/HR
C=M*C*(T2-T1)	= 0.415E+04	BTU/HR
HEAT LOST	= 0.248E+02	BTU/HR
HEAT BALANCE ERROR %	=-0.168E+01	

PERIPHERAL HEAT TRANSFER COEFFICIENT BTU/(SQ.FT-HR-DEG.F)

	1	2	3	4	5	6	7	8	9	10	11
1	268.1	249.9	507.1	319.9	372.3	377.5	683.8	242.3	262.5	260.3	243.6
2	258.8	249.9	420.7	459.5	399.9	415.6	541.7	244.3	257.5	242.7	235.3
3	251.9	258.9	314.2	333.9	426.8	446.9	471.6	238.0	248.1	240.5	247.6
4	253.9	252.4	213.4	290.3	311.7	313.2	247.0	231.9	227.6	234.3	235.3
5	251.9	275.6	152.5	264.1	256.9	232.4	104.6	233.9	233.4	236.3	245.5
6	261.0	254.7	220.7	286.1	296.3	306.2	246.3	230.1	227.7	232.4	241.5
7	258.8	247.8	359.3	376.4	395.4	349.0	343.4	246.2	246.1	246.8	250.0
8	256.7	260.9	426.4	357.8	408.7	416.9	519.9	242.2	266.7	249.3	250.0

AVERAGE HEAT TRANSFER COEFFICIENT-BTU/(SQ.FT.HR-DEG.F)

	1	2	3	4	5	6	7	8	9	10	11
(H1)	257.6	256.3	326.8	336.0	358.5	357.2	394.8	238.6	246.2	242.8	243.6
(H2)	257.6	256.1	290.4	318.6	335.1	330.5	316.1	238.5	245.5	242.6	243.5

RATIO OF CALCULATED HEAT TRANSFER COEFFICIENT TO THOSE PREDICTED BY LITERATURE

	1	2	3	4	5	6	7	8	9	10	11
LIT(1)	0.96	0.94	1.20	1.23	1.31	1.31	1.45	0.87	0.89	0.87	0.87
LIT(2)	0.87	0.85	1.08	1.11	1.19	1.18	1.31	0.79	0.81	0.79	0.79
LIT(3)	0.91	0.89	1.14	1.17	1.24	1.24	1.37	0.83	0.85	0.83	0.83

RUN NUMBER 213

INSIDE SURFACE TEMPERATURES - DEGREES F

	1	2	3	4	5	6	7	8	9	10	11
1	109.4	112.7	109.1	109.4	108.8	108.9	108.1	114.2	115.0	116.6	118.5
2	109.5	112.5	109.8	109.9	109.3	109.3	108.7	114.3	115.0	116.6	118.7
3	109.6	112.3	111.8	111.5	111.1	110.8	110.5	114.0	114.8	116.6	118.6
4	109.5	112.3	115.4	114.8	114.6	114.4	114.5	114.2	114.8	116.6	118.9
5	109.5	112.5	118.4	117.1	117.2	117.2	118.3	114.2	115.1	116.6	118.8
6	109.5	112.4	115.3	115.1	115.3	114.4	113.8	114.2	115.1	116.6	118.8
7	109.4	112.2	111.4	111.4	111.4	111.5	111.4	114.1	115.1	116.6	118.5
8	109.5	112.3	110.1	110.1	109.5	109.6	108.7	114.0	115.1	116.6	118.5

INSIDE SURFACES HEAT FLUXES BTU/HR/FT2

	1	2	3	4	5	6	7	8	9	10	11
1	7142.6	7069.7	7310.5	4364.8	4050.1	4353.9	7264.9	7129.6	7154.0	7149.4	7178.8
2	7121.6	7132.8	7275.4	5408.8	5163.2	5408.1	7262.8	7097.9	7122.6	7149.4	7126.1
3	7100.8	7153.8	7290.4	6903.9	6798.4	6943.9	7349.3	7192.3	7164.5	7149.4	7199.3
4	7132.2	7153.9	7055.8	8788.2	8912.1	8798.0	7094.9	7118.7	7174.7	7149.4	7115.1
5	7121.6	7101.2	6528.6	11428.7	11903.0	11301.1	6303.6	7140.0	7111.9	7149.4	7167.8
6	7111.2	7122.2	7034.7	8712.3	8810.8	8862.5	7304.2	7129.6	7143.1	7149.4	7125.8
7	7142.6	7164.3	7385.2	6977.3	6818.9	6849.6	7119.3	7140.0	7143.1	7149.4	7189.2
8	7100.8	7164.0	7192.2	5358.1	5152.7	5407.6	7346.0	7171.5	7132.7	7149.4	7157.4

RUN NUMBER 213

AVERAGE REYNOLDS NUMBER	= 0.245E+05	
AVERAGE PRANDTL NUMBER	= 0.430E+01	
MASS FLUX	= 0.743E+06	LBM/(SQ.FT-HR)
AVERAGE HEAT FLUX	= 0.724E+04	BTU/(SQ.FT-HR)
Q=AMP*VOLT	= 0.217E+05	BTU/HR
Q=M*C*(T2-T1)	= 0.230E+05	BTU/HR
HEAT LOST	= 0.557E+02	BTU/HR
HEAT BALANCE ERROR %	=-0.628E+01	

PERIPHERAL HEAT TRANSFER COEFFICIENT BTU/(SQ.FT-HR-DEG.F)

	1	2	3	4	5	6	7	8	9	10	11
1	861.6	805.4	1717.3	977.3	1080.9	1139.7	2444.7	883.0	903.0	936.5	940.1
2	848.2	833.3	1464.4	1100.0	1213.0	1297.5	2032.6	867.3	898.0	936.5	907.6
3	835.1	856.4	1046.4	1044.2	1120.0	1207.5	1373.4	915.6	928.2	936.5	931.3
4	849.7	856.4	669.4	893.3	925.0	947.5	760.3	881.3	929.8	936.5	883.3
5	848.2	828.7	483.7	938.0	974.0	935.9	478.8	884.6	885.2	936.5	902.7
6	846.6	841.6	673.4	857.5	858.2	956.4	842.4	883.0	890.0	936.5	896.1
7	861.6	868.4	1129.4	1075.0	1071.4	1073.8	1144.8	895.8	890.0	936.5	941.8
8	845.1	857.9	1385.1	1044.1	1155.4	1210.1	2069.7	912.2	888.4	936.5	936.5

AVERAGE HEAT TRANSFER COEFFICIENT-BTU/(SQ.FT.HR-DEG.F)

	1	2	3	4	5	6	7	8	9	10	11
(H1)	849.5	843.5	1071.1	991.2	1049.7	1096.0	1393.3	890.4	901.6	936.5	917.4
(H2)	849.5	843.2	914.5	968.9	1010.4	1049.1	1079.8	890.2	901.3	936.5	917.0

RATIO OF CALCULATED HEAT TRANSFER COEFFICIENT TO THOSE PREDICTED BY LITERATURE

	1	2	3	4	5	6	7	8	9	10	11
LIT(1)	1.01	0.98	1.24	1.15	1.22	1.27	1.62	1.03	1.03	1.06	1.03
LIT(2)	0.92	0.90	1.14	1.05	1.12	1.16	1.48	0.94	0.95	0.98	0.95
LIT(3)	0.96	0.94	1.19	1.10	1.17	1.22	1.55	0.98	0.99	1.02	0.99

RUN NUMBER 215

INSIDE SURFACE TEMPERATURES - DEGREES F

	1	2	3	4	5	6	7	8	9	10	11
1	99.2	105.8	103.5	103.2	102.7	105.6	108.4	123.2	126.9	132.1	137.4
2	100.5	106.6	103.7	103.6	103.5	106.2	108.7	120.5	123.5	128.6	133.7
3	103.8	111.2	106.8	105.8	104.8	107.0	109.2	116.5	119.4	123.3	128.1
4	108.8	117.3	113.4	111.1	108.9	110.5	112.2	112.8	115.5	119.9	124.8
5	112.3	120.0	118.8	116.0	113.4	114.0	114.7	111.8	114.6	119.1	123.7
6	110.5	117.7	113.3	111.5	109.7	110.8	112.1	113.0	115.5	120.3	125.1
7	103.5	112.6	106.1	105.8	105.3	107.6	109.8	116.7	118.5	123.9	129.8
8	100.7	107.7	103.9	103.8	103.6	105.9	108.2	121.3	123.4	130.4	135.7

INSIDE SURFACES HEAT FLUXES BTU/HR/FT2

	1	2	3	4	5	6	7	8	9	10	11
1	1264.5	1276.0	1082.7	702.4	697.4	683.7	1022.5	543.6	335.8	483.9	463.3
2	1202.8	1390.6	1286.4	915.7	768.6	776.5	1032.4	864.3	918.8	825.3	816.2
3	1164.2	1138.2	1349.6	1250.5	1189.0	1200.1	1238.0	1046.6	1036.6	1195.7	1240.4
4	849.9	677.5	864.8	1198.4	1301.2	1238.0	953.9	1272.2	1304.4	1275.9	1236.7
5	471.8	492.4	-55.0	702.7	866.4	997.5	499.9	1228.7	1189.2	1213.5	1267.3
6	489.9	729.2	822.9	1112.8	1181.3	1228.1	1026.8	1251.0	1221.7	1254.0	1340.4
7	1412.9	1025.2	1483.3	1313.3	1179.9	1107.6	1082.7	1098.8	1191.8	1290.9	1137.8
8	1128.9	1299.9	1183.3	875.3	798.0	867.1	1166.3	740.1	856.0	534.6	588.4

RUN NUMBER 215

AVERAGE REYNOLDS NUMBER	= 0.132E+04	
AVERAGE PRANDTL NUMBER	= 0.435E+01	
MASS FLUX	= 0.404E+05	LBM/(SQ.FT-HR)
AVERAGE HEAT FLUX	= 0.102E+04	BTU/(SQ.FT-HR)
Q=AMP*VOLT	= 0.310E+04	BTU/HR
C=M*C*(T2-T1)	= 0.310E+04	BTU/HR
HEAT LOST	= 0.566E+02	BTU/HR
HEAT BALANCE ERROR %	=-0.190E+01	

PERIPHERAL HEAT TRANSFER COEFFICIENT BTU/(SQ.FT-HR-DEG.F)

	1	2	3	4	5	6	7	8	9	10	11
1	231.5	266.0	********	-1523.9	-611.4	438.4	246.4	32.9	18.9	26.7	25.0
2	175.0	249.9	5318.2	********	-2055.7	365.3	232.2	62.4	63.9	56.5	55.1
3	114.3	111.2	405.9	578.4	1204.2	401.1	248.2	106.9	101.2	128.6	135.1
4	56.0	41.6	86.8	160.6	259.0	191.5	119.7	207.6	204.9	217.3	210.3
5	25.2	25.9	-3.6	56.7	90.9	100.6	47.6	239.1	216.3	238.4	265.6
6	29.0	43.8	83.3	141.1	201.5	181.5	130.8	197.5	191.2	199.7	217.9
7	144.0	88.6	552.2	612.6	791.7	314.8	195.7	110.1	126.8	130.8	105.2
8	159.1	194.3	2507.7	4822.0	-2828.1	456.5	291.0	50.8	59.9	32.6	35.1

AVERAGE HEAT TRANSFER COEFFICIENT-BTU/(SQ.FT.HR-DEG.F)

	1	2	3	4	5	6	7	8	9	10	11
(H1)	116.8	127.7	********	-3215.6	-368.5	306.2	188.9	125.9	122.9	128.8	131.2
(H2)	88.7	88.4	191.3	254.3	378.4	229.8	162.2	97.7	95.5	94.4	93.1

RATIO OF CALCULATED HEAT TRANSFER COEFFICIENT TO THOSE PREDICTED BY LITERATURE

	1	2	3	4	5	6	7	8	9	10	11
LIT(1)	1.25	1.29	1409.66	-44.59	-5.76	4.10	2.27	1.26	1.20	1.22	1.20
LIT(2)	0.95	0.89	2.44	3.53	5.91	3.08	1.95	0.98	0.94	0.89	0.85

RUN NUMBER 252

INSIDE SURFACE TEMPERATURES - DEGREES F

	1	2	3	4	5	6	7	8	9	10	11
1	131.9	137.1	111.9	106.0	99.8	99.7	99.5	118.2	129.4	145.1	149.8
2	132.7	137.8	114.3	107.5	100.5	100.5	100.3	119.3	129.7	143.4	145.6
3	134.3	140.7	120.7	112.0	103.3	102.8	102.3	121.1	130.7	140.9	140.7
4	136.7	145.0	132.5	121.9	111.4	110.2	109.1	123.9	132.1	139.3	138.1
5	138.5	147.5	140.5	132.5	124.8	119.8	115.2	124.8	132.8	139.1	137.4
6	137.7	145.2	132.2	122.6	113.2	111.1	108.9	123.9	132.5	140.0	138.8
7	134.3	141.5	119.2	111.6	103.9	104.0	104.0	121.2	131.3	141.9	142.4
8	132.7	138.4	113.8	107.4	100.9	100.8	100.8	118.9	129.8	144.9	147.5

INSIDE SURFACES HEAT FLUXES BTU/HR/FT2

	1	2	3	4	5	6	7	8	9	10	11
1	1950.3	1997.7	2216.1	1337.2	1136.9	1224.7	1971.5	1956.6	1852.2	1592.6	1130.2
2	1866.2	2019.1	2183.4	1610.8	1457.6	1473.7	1886.7	1842.3	1852.4	1717.1	1720.0
3	1856.9	1926.1	2303.5	2200.7	2153.2	2156.9	2216.2	1864.9	1811.4	1873.3	2020.7
4	1731.8	1603.2	1386.5	2242.3	2722.0	2376.3	1679.5	1584.6	1717.6	1936.3	1988.5
5	1513.3	1307.3	137.1	827.2	377.3	1056.0	551.6	1536.1	1676.2	1905.2	2010.2
6	1522.6	1645.4	1303.4	2049.1	2413.9	2323.7	1865.4	1595.6	1686.6	1894.2	2019.7
7	1961.9	1842.2	2511.0	2346.4	2247.9	2054.6	1927.7	1802.4	1759.1	1896.0	1938.1
8	1865.1	1978.1	2140.6	1590.1	1437.3	1504.3	1949.9	1936.3	1884.2	1506.9	1499.4

RUN NUMBER 252

AVERAGE REYNOLDS NUMBER	= 0.124E+04		
AVERAGE PRANDTL NUMBER	= 0.948E+02		
MASS FLUX	= 0.625E+06	LBM/(SQ.FT-HR)	
AVERAGE HEAT FLUX	= 0.177E+04	BTU/(SQ.FT-HR)	
Q=AMP*VOLT	= 0.532E+04	BTU/HR	
Q=M*C*(T2-T1)	= 0.513E+04	BTU/HR	
HEAT LOST	= 0.353E+02	BTU/HR	
HEAT BALANCE ERROR %	= 0.302E+01		

PERIPHERAL HEAT TRANSFER COEFFICIENT BTU/(SQ.FT-HR-DEG.F)

	1	2	3	4	5	6	7	8	9	10	11
1	55.7	51.5	168.5	185.7	1211.2	1427.1	3464.9	104.0	62.6	35.9	23.5
2	52.1	51.1	140.3	184.9	896.1	937.1	1353.8	92.4	62.0	40.3	39.2
3	49.6	45.4	105.0	166.5	479.2	545.4	652.0	85.8	58.7	46.7	51.9
4	43.5	34.3	41.1	97.1	216.5	209.1	165.3	64.6	53.3	50.3	54.7
5	36.3	26.6	3.3	24.6	14.5	50.5	33.9	62.4	50.9	49.7	56.4
6	37.3	35.1	39.0	86.0	168.0	190.8	186.4	65.1	51.7	48.3	54.5
7	52.4	42.6	122.7	183.6	443.7	404.0	379.2	82.5	56.0	46.1	47.7
8	52.0	49.3	142.0	184.6	707.2	765.8	1039.5	99.2	62.9	34.1	32.7

AVERAGE HEAT TRANSFER COEFFICIENT-BTU/(SQ.FT.HR-DEG.F)

	1	2	3	4	5	6	7	8	9	10	11
(H1)	47.4	42.0	95.2	139.1	517.1	566.2	909.4	82.0	57.3	43.9	45.1
(H2)	46.9	41.3	72.7	108.3	208.0	244.7	288.0	80.4	57.1	43.6	43.9

RATIO OF CALCULATED HEAT TRANSFER COEFFICIENT TC THOSE PREDICTED BY LITERATURE

	1	2	3	4	5	6	7	8	9	10	11
LIT(1)	0.84	0.71	1.96	3.27	15.09	17.29	29.26	1.74	1.08	0.75	0.77
LIT(2)	0.84	0.70	1.50	2.55	6.07	7.47	9.27	1.71	1.08	0.74	0.75

RUN NUMBER 253

INSIDE SURFACE TEMPERATURES - DEGREES F

	1	2	3	4	5	6	7	8	9	10	11
1	123.9	127.3	112.7	107.2	101.4	101.4	101.2	116.3	124.7	133.6	136.6
2	124.4	127.8	114.6	108.2	101.9	101.9	101.8	116.7	124.4	131.8	133.8
3	125.7	129.9	112.9	111.1	104.0	103.6	103.3	117.3	124.1	129.6	130.1
4	127.1	133.1	125.6	117.5	109.7	108.8	107.8	118.4	124.2	128.4	128.2
5	128.2	134.8	130.3	124.2	118.3	114.9	111.7	118.8	124.6	128.5	127.9
6	127.7	133.1	125.2	118.0	110.8	109.3	107.7	118.3	124.6	129.0	129.2
7	125.5	130.5	117.1	110.9	104.5	104.4	104.3	117.2	124.5	130.4	131.7
8	124.6	128.3	114.1	108.2	102.2	102.2	102.0	116.3	124.6	133.1	135.3
	125.09	130.6	119.06	113.16	106.6	105.81	104.98	117.41	124.46	130.55	131.6

INSIDE SURFACES HEAT FLUXES BTU/HR/FT2

	1	2	3	4	5	6	7	8	9	10	11
1	1182.3	1225.9	1388.5	835.4	711.0	765.9	1201.3	1116.1	1027.6	834.5	668.4
2	1141.4	1236.3	756.5	970.8	897.3	898.2	1148.3	1085.2	1068.7	1041.6	980.5
3	1089.3	1176.0	2442.8	1350.3	1343.5	1344.3	1354.9	1116.7	1110.2	1164.6	1248.2
4	1039.2	918.1	291.7	1341.6	1612.2	1398.3	991.4	993.9	1099.8	1195.6	1236.5
5	905.2	740.7	90.4	439.0	120.4	569.1	290.5	973.9	1027.5	1133.5	1237.3
6	903.8	970.0	770.8	1213.7	1426.3	1377.5	1115.3	1003.5	1058.6	1153.6	1195.2
7	1184.4	1123.5	1551.7	1443.8	1386.4	1263.2	1158.6	1095.8	1089.1	1197.3	1177.3
8	1109.5	1184.7	1235.3	950.5	887.6	918.3	1210.7	1136.5	1068.6	854.5	835.1

RUN NUMBER 253

AVERAGE REYNOLDS NUMBER	= 0.958E+03	
AVERAGE PRANDTL NUMBER	= 0.922E+02	
MASS FLUX	= 0.467E+06	LBM/(SQ.FT-HR)
AVERAGE HEAT FLUX	= 0.107E+04	BTU/(SQ.FT-HR)
Q=AMP*VOLT	= 0.324E+04	BTU/HR
Q=M*C*(T2-T1)	= 0.339E+04	BTU/HR
HEAT LOST	= 0.389E+02	BTU/HR
HEAT BALANCE ERROR %	=-0.590E+01	

PERIPHERAL HEAT TRANSFER COEFFICIENT BTU/(SQ.FT-HR-DEG.F)

	1	2	3	4	5	6	7	8	9	10	11
1	47.6	45.2	115.0	128.1	967.1	1129.1	2400.4	73.7	44.3	26.6	19.9
2	45.0	44.8	54.2	128.2	706.9	729.2	1029.1	69.8	46.7	35.3	31.9
3	41.0	39.6	199.2	129.2	404.6	465.1	530.0	69.2	49.2	42.5	46.1
4	37.1	27.9	11.7	79.7	179.0	173.5	140.3	57.5	48.5	45.7	49.1
5	31.1	21.4	3.0	18.6	6.8	40.1	26.5	55.1	44.5	43.3	49.7
6	31.6	29.5	31.4	69.9	140.3	160.9	161.0	58.4	45.9	43.1	45.6
7	44.8	37.2	93.9	141.2	364.0	340.1	320.6	68.3	47.4	42.5	41.0
8	43.5	42.1	91.4	125.4	564.6	601.7	932.8	74.6	46.3	27.7	25.8

AVERAGE HEAT TRANSFER COEFFICIENT-BTU/(SQ.FT.HR-DEG.F)

	1	2	3	4	5	6	7	8	9	10	11
(H1)	40.2	36.0	75.0	102.5	416.7	455.0	692.6	65.8	46.6	38.3	38.6
(H2)	39.9	35.3	57.8	85.3	176.4	208.9	248.8	65.4	46.6	37.9	37.5

RATIO OF CALCULATED HEAT TRANSFER COEFFICIENT TO THOSE PREDICTED BY LITERATURE

	1	2	3	4	5	6	7	8	9	10	11
LIT(1)	0.80	0.68	1.68	2.62	13.43	15.34	24.63	1.54	0.97	0.74	0.74
LIT(2)	0.79	0.67	1.30	2.18	5.69	7.05	8.85	1.53	0.97	0.73	0.72

RUN NUMBER 262

INSIDE SURFACE TEMPERATURES - DEGREES F

	1	2	3	4	5	6	7	8	9	10	11
1	109.3	111.1	107.8	101.4	94.8	100.4	105.8	123.4	124.2	126.5	128.6
2	110.4	111.8	108.6	102.2	95.6	100.7	105.8	121.2	121.4	123.8	126.0
3	112.2	114.9	110.9	104.3	97.6	101.7	105.8	118.4	118.1	120.1	122.1
4	114.8	118.7	115.8	109.0	102.2	104.9	107.6	117.1	116.2	118.0	120.0
5	116.9	120.6	119.4	112.9	106.6	107.7	108.9	118.3	116.7	117.4	119.2
6	115.6	119.0	115.5	109.3	102.9	105.2	107.5	119.2	117.8	118.4	120.0
7	111.9	115.6	110.4	104.1	98.1	102.1	106.2	119.9	120.3	120.6	122.9
8	110.4	112.4	108.7	102.2	95.7	100.6	105.3	122.5	122.8	125.1	127.1

INSIDE SURFACES HEAT FLUXES BTU/HR/FT2

	1	2	3	4	5	6	7	8	9	10	11
1	922.6	921.7	881.1	573.6	540.9	486.2	674.9	424.2	309.8	312.0	312.1
2	798.3	953.3	869.1	664.6	624.7	595.4	725.8	660.6	672.0	620.6	590.0
3	800.4	801.9	974.4	930.4	913.4	888.0	879.6	863.6	853.3	875.8	898.2
4	658.7	516.2	579.8	799.7	873.9	838.7	665.8	967.0	955.7	873.4	853.6
5	392.5	382.5	-8.8	415.5	369.6	664.3	461.2	699.4	800.7	884.3	884.9
6	473.5	526.7	557.6	736.4	776.8	817.9	718.5	709.5	843.9	841.9	936.7
7	925.2	750.9	1108.1	992.3	893.7	826.4	766.2	897.3	731.2	939.4	836.2
8	776.9	902.7	786.5	644.2	653.5	654.7	838.7	546.5	601.0	423.8	466.5

RUN NUMBER 262

AVERAGE REYNOLDS NUMBER	= 0.184E+03	
AVERAGE PRANDTL NUMBER	= 0.983E+02	
MASS FLUX	= 0.968E+05	LBM/(SQ.FT-HR)
AVERAGE HEAT FLUX	= 0.733E+03	BTU/(SQ.FT-HR)
Q=AMP*VOLT	= 0.221E+04	BTU/HR
Q=M*C*(T2-T1)	= 0.224E+04	BTU/HR
HEAT LOST	= 0.233E+02	BTU/HR
HEAT BALANCE ERROR %	=-0.254E+01	

PERIPHERAL HEAT TRANSFER COEFFICIENT BTU/(SQ.FT-HR-DEG.F)

	1	2	3	4	5	6	7	8	9	10	11
1	51.1	57.4	76.6	114.5	-323.8	130.1	74.4	16.7	12.4	12.6	12.8
2	41.8	56.9	70.6	115.0	-690.9	145.2	80.1	28.5	30.3	28.2	27.2
3	38.3	40.5	66.8	117.9	831.2	173.9	96.5	42.2	45.2	47.7	50.4
4	28.0	21.8	29.7	63.4	153.6	100.9	61.2	50.6	56.3	53.7	54.3
5	15.3	15.0	-0.4	25.1	36.5	60.1	38.0	34.5	46.0	56.5	59.3
6	19.4	22.0	29.0	57.4	121.0	94.9	66.8	33.5	45.4	50.5	59.6
7	44.8	36.6	80.6	129.3	556.8	149.6	81.1	40.9	34.8	49.9	44.9
8	40.7	52.0	63.8	111.4	-804.6	164.3	97.3	22.3	25.5	18.2	20.5

AVERAGE HEAT TRANSFER COEFFICIENT-BTU/(SQ.FT.HR-DEG.F)

	1	2	3	4	5	6	7	8	9	10	11
(H1)	34.9	37.8	52.1	91.7	-15.0	127.4	74.4	33.6	37.0	39.7	41.1
(H2)	33.6	35.2	45.5	77.7	262.0	114.4	72.5	32.7	35.3	37.0	38.1

RATIO OF CALCULATED HEAT TRANSFER COEFFICIENT TO THOSE PREDICTED BY LITERATURE

	1	2	3	4	5	6	7	8	9	10	11
LIT(1)	0.77	0.84	1.25	2.62	-0.61	4.09	2.08	0.72	0.81	0.87	0.90
LIT(2)	0.74	0.78	1.09	2.22	10.69	3.67	2.02	0.70	0.77	0.81	0.84

RUN NUMBER 402

INSIDE SURFACE TEMPERATURES - DEGREES F

	1	2	3	4	5	6	7	8	9	10	11
1	90.9	92.3	92.6	90.7	93.0	96.9	98.3	101.2	102.3	103.1	106.2
2	91.2	93.0	93.2	91.1	93.2	96.8	99.4	99.3	99.8	101.3	104.8
3	91.7	95.0	95.2	92.2	94.2	97.4	99.7	96.8	98.1	98.1	101.2
4	92.5	98.8	99.0	95.7	95.7	98.7	98.9	95.9	96.8	96.6	99.5
5	92.8	100.8	101.4	99.2	97.3	99.1	98.3	95.7	96.7	96.3	99.1
6	92.1	98.5	99.5	96.2	95.9	98.5	98.6	96.0	97.1	96.9	99.4
7	91.1	94.8	95.4	92.0	94.0	97.5	99.8	97.2	98.1	98.3	101.7
8	90.9	92.9	93.1	90.9	93.2	96.9	99.0	99.3	100.3	101.1	105.0

INSIDE SURFACES HEAT FLUXES BTU/HR/FT2

	1	2	3	4	5	6	7	8	9	10	11
1	408.8	464.5	453.2	482.9	455.0	453.7	492.6	189.9	150.4	189.5	177.7
2	403.0	464.3	469.6	457.4	455.7	461.2	346.8	353.0	432.4	307.7	302.0
3	408.5	492.8	492.9	520.3	412.5	427.4	329.6	481.2	414.3	486.7	498.4
4	364.9	285.8	308.7	364.0	384.8	312.7	403.1	430.8	459.0	458.6	463.8
5	337.6	162.2	162.3	-20.5	182.2	280.9	442.0	420.3	419.9	441.9	430.4
6	375.5	308.6	263.1	295.3	349.3	340.5	442.2	441.9	424.6	436.8	503.8
7	437.4	492.8	492.9	559.0	445.3	410.7	279.4	441.9	459.0	471.0	447.6
8	402.9	464.6	492.3	468.2	443.9	455.6	397.3	375.5	375.4	341.6	307.3

RUN NUMBER 402

AVERAGE REYNOLDS NUMBER	= 0.766E+03	
AVERAGE PRANDTL NUMBER	= 0.511E+01	
MASS FLUX	= 0.218E+05	LBM/(SQ.FT-HR)
AVERAGE HEAT FLUX	= 0.356E+03	BTU/(SQ.FT-HR)
Q=AMP*VOLT	= 0.819E+03	BTU/HR
Q=M*C*(T2-T1)	= 0.671E+03	BTU/HR
HEAT LOST	= 0.352E+02	BTU/HR
HEAT BALANCE ERROR %	= 0.143E+02	

PERIPHERAL HEAT TRANSFER COEFFICIENT BTU/(SQ.FT-HR-DEG.F)

	1	2	3	4	5	6	7	8	9	10	11
1	75.9	172.3	182.1	1800.8	201.2	77.7	71.3	20.5	15.2	18.7	16.3
2	70.8	136.7	152.2	680.5	185.4	80.4	43.1	47.5	58.4	36.5	34.1
3	66.1	91.4	97.0	296.1	119.0	67.4	39.5	98.1	72.5	93.9	95.5
4	52.1	30.9	34.6	68.8	77.5	40.8	53.5	107.3	104.3	124.3	131.4
5	46.2	14.5	14.4	-2.3	27.6	34.8	63.8	110.1	97.4	130.2	137.2
6	56.9	34.5	27.9	50.9	67.5	45.6	61.2	107.4	90.2	109.3	147.3
7	78.4	95.0	93.4	361.0	136.6	63.7	33.0	83.2	80.5	87.4	78.1
8	74.8	141.0	165.2	997.1	180.4	78.0	52.0	50.5	47.4	41.6	33.9

AVERAGE HEAT TRANSFER COEFFICIENT-BTU/(SQ.FT.HR-DEG.F)

	1	2	3	4	5	6	7	8	9	10	11
(H1)	65.1	89.6	95.9	531.6	124.4	61.0	52.2	78.1	70.8	80.2	84.2
(H2)	63.9	63.6	64.6	127.1	102.0	58.8	51.3	67.7	62.7	64.7	62.8

RATIO OF CALCULATED HEAT TRANSFER COEFFICIENT TO THOSE PREDICTED BY LITERATURE

	1	2	3	4	5	6	7	8	9	10	11
LIT(1)	0.94	1.25	1.34	9.17	2.00	0.82	0.67	1.09	0.96	1.10	1.11
LIT(2)	0.92	0.89	0.90	2.19	1.64	0.79	0.66	0.95	0.85	0.88	0.83

RUN NUMBER 419

INSIDE SURFACE TEMPERATURES - DEGREES F

	1	2	3	4	5	6	7	8	9	10	11
1	109.7	112.2	111.6	105.3	104.4	104.1	106.7	108.6	109.5	110.9	115.6
2	109.3	112.9	112.7	107.4	105.5	106.0	107.0	108.7	109.5	111.0	116.0
3	107.9	112.9	113.0	109.8	109.2	109.2	109.2	110.9	111.6	112.3	116.9
4	107.0	112.3	113.7	114.7	113.7	117.6	113.6	114.2	115.2	115.5	119.2
5	106.4	111.9	113.4	121.4	120.1	124.9	120.3	119.1	119.3	119.5	120.2
6	105.6	110.7	112.5	113.6	112.3	114.1	114.2	115.9	116.4	116.7	119.0
7	105.6	110.7	111.3	108.1	107.6	108.2	110.5	111.8	113.1	113.9	117.1
8	108.1	111.2	112.7	105.9	104.9	105.0	107.6	108.7	110.5	112.0	115.7

INSIDE SURFACES HEAT FLUXES BTU/HR/FT2

	1	2	3	4	5	6	7	8	9	10	11
1	11551.2	11650.6	11782.8	13539.9	12989.5	13796.6	11749.3	11692.8	11732.8	11739.2	11700.6
2	11608.0	11627.8	11628.4	12493.4	12403.3	12661.8	11771.0	11778.0	11777.9	11738.7	11701.0
3	11693.9	11633.7	11690.3	11675.1	11518.0	11849.8	11786.7	11736.2	11759.5	11778.2	11751.1
4	11682.7	11679.4	11611.0	11049.7	11339.6	10738.6	11792.9	11753.1	11691.6	11708.9	11596.8
5	11654.7	11622.6	11634.1	9500.	10003.3	9066.1	10957.7	11215.6	11279.3	11291.4	11544.8
6	11717.8	11736.5	11657.1	11078.7	11417.5	11066.4	11792.5	11610.4	11639.8	11663.0	11631.3
7	11796.7	11696.8	11805.4	11720.	11574.2	11730.5	11718.1	11730.5	11708.1	11719.8	11700.2
8	11620.1	11696.2	11537.6	12565.0	12387.1	12702.6	11770.9	11828.6	11761.0	11715.8	11745.8

RUN NUMBER 419

AVERAGE REYNOLDS NUMBER	= 0.246E+05	
AVERAGE PRANDTL NUMBER	= 0.475E+01	
MASS FLUX	= 0.655E+06	LBM/(SQ.FT-HR)
AVERAGE HEAT FLUX	= 0.117E+05	BTU/(SQ.FT-HR)
Q=AMP*VOLT	= 0.259E+05	BTU/HR
Q=M*C*(T2-T1)	= 0.265E+05	BTU/HR
HEAT LOST	= 0.390E+02	BTU/HR
HEAT BALANCE ERROR %	=-0.260E+01	

PERIPHERAL HEAT TRANSFER COEFFICIENT BTU/(SQ.FT-HR-DEG.F)

	1	2	3	4	5	6	7	8	9	10	11
1	612.7	690.9	747.0	1485.9	1663.9	1917.6	1252.0	1088.6	1059.5	985.2	881.2
2	629.5	661.8	691.8	1115.3	1388.9	1401.0	1203.6	1078.4	1055.0	976.9	855.5
3	687.1	662.2	683.8	860.0	914.8	961.3	983.9	900.4	892.9	885.0	806.7
4	724.7	688.8	651.7	598.9	660.5	519.8	724.2	719.5	696.3	708.4	686.0
5	750.7	701.5	664.4	377.3	425.8	324.5	476.8	527.4	539.9	550.0	644.3
6	796.6	765.0	702.1	638.9	725.0	644.2	698.4	642.5	646.5	657.4	696.6
7	797.5	762.0	763.2	988.0	1045.0	1042.5	888.0	841.7	797.3	785.3	791.6
8	674.2	737.9	685.5	1297.5	1486.5	1563.0	1133.9	1084.2	974.5	899.7	878.7

AVERAGE HEAT TRANSFER COEFFICIENT-BTU/(SQ.FT.HR-DEG.F)

	1	2	3	4	5	6	7	8	9	10	11
(H1)	709.1	708.8	698.7	920.2	1038.8	1046.7	920.1	860.4	832.7	806.0	780.1
(H2)	703.3	706.8	697.1	804.3	890.5	823.2	841.9	810.2	792.1	778.1	770.4

RATIO OF CALCULATED HEAT TRANSFER COEFFICIENT TO THOSE PREDICTED BY LITERATURE

	1	2	3	4	5	6	7	8	9	10	11
LIT(1)	1.02	0.99	0.97	1.28	1.45	1.45	1.28	1.19	1.15	1.10	1.05
LIT(2)	0.94	0.91	0.90	1.18	1.33	1.34	1.17	1.09	1.06	1.02	0.97
LIT(3)	0.98	0.95	0.94	1.23	1.39	1.40	1.23	1.14	1.10	1.06	1.01

RUN NUMBER 420

INSIDE SURFACE TEMPERATURES - DEGREES F

	1	2	3	4	5	6	7	8	9	10	11
1	113.4	116.4	115.8	109.0	108.7	107.4	109.9	112.4	113.7	115.1	120.2
2	113.2	116.6	117.0	111.7	110.0	109.5	110.5	112.6	113.7	115.3	120.7
3	111.6	117.1	117.6	115.0	114.0	113.0	113.1	114.7	116.1	116.7	121.6
4	110.6	116.6	118.1	119.6	118.7	121.4	117.5	118.4	119.7	120.4	124.4
5	109.9	115.8	117.8	126.5	125.2	129.6	124.5	123.7	124.1	124.5	125.4
6	108.8	114.9	116.9	118.6	116.9	118.0	118.5	120.4	121.0	121.8	123.8
7	109.3	114.7	115.8	112.9	112.3	111.8	114.4	116.3	117.5	118.4	121.7
8	111.9	115.4	116.9	110.5	109.3	108.4	111.3	112.6	114.9	116.3	120.0

INSIDE SURFACES HEAT FLUXES BTU/HR/FT2

	1	2	3	4	5	6	7	8	9	10	11
1	13458.6	13513.3	13686.0	15799.4	15099.1	16024.5	13676.2	13585.3	13630.9	13643.6	13581.4
2	13475.7	13575.9	13525.8	14528.6	14399.9	14701.9	13675.0	13670.7	13699.7	13631.0	13587.0
3	13590.5	13502.1	13554.8	13468.6	13364.4	13719.1	13661.9	13651.0	13629.0	13693.0	13666.8
4	13574.0	13541.9	13513.8	12842.5	13169.7	12528.1	13695.0	13644.8	13600.1	13577.9	13464.6
5	13534.1	13553.4	13525.8	11165.0	11708.5	10599.9	12833.8	13076.8	13140.3	13180.9	13419.1
6	13648.4	13600.4	13548.2	12843.8	13283.3	12852.5	13654.8	13507.4	13530.0	13513.7	13527.8
7	13676.9	13611.3	13680.4	13591.3	13415.0	13600.5	13615.4	13582.0	13611.6	13635.1	13585.8
8	13493.7	13577.2	13446.8	14550.8	14383.9	14758.8	13658.2	13761.5	13642.1	13614.1	13673.2

RUN NUMBER 420

AVERAGE REYNOLDS NUMBER	= 0.294E+05	
AVERAGE PRANDTL NUMBER	= 0.453E+01	
MASS FLUX	= 0.749E+06	LBM/(SQ.FT-HR)
AVERAGE HEAT FLUX	= 0.136E+05	BTU/(SQ.FT-HR)
Q=AMP*VOLT	= 0.300E+05	BTU/HR
Q=M*C*(T2-T1)	= 0.308E+05	BTU/HR
HEAT LOST	= 0.594E+02	BTU/HR
HEAT BALANCE ERROR %	=-0.280E+01	

PERIPHERAL HEAT TRANSFER COEFFICIENT BTU/(SQ.FT-HR-DEG.F)

	1	2	3	4	5	6	7	8	9	10	11
1	718.8	786.4	856.6	1786.3	1844.0	2460.0	1578.9	1279.2	1201.4	1120.3	976.9
2	727.7	781.6	785.7	1254.8	1512.7	1710.1	1476.3	1265.7	1209.2	1100.9	943.4
3	804.7	754.8	761.1	911.3	989.4	1131.4	1151.0	1057.5	991.2	994.4	894.1
4	854.2	779.3	737.6	659.7	725.1	608.9	841.8	821.2	783.3	775.8	746.5
5	890.4	817.8	750.7	424.2	473.9	369.2	551.3	595.6	603.5	610.3	704.5
6	969.9	868.4	791.8	695.6	813.2	751.9	790.2	724.2	724.3	714.3	772.1
7	939.0	880.5	856.2	1063.9	1137.5	1242.0	1032.8	934.9	898.1	880.5	882.0
8	784.0	839.8	789.4	1403.0	1630.5	1972.4	1356.6	1276.6	1087.5	1017.0	999.4

AVERAGE HEAT TRANSFER COEFFICIENT-BTU/(SQ.FT.HR-DEG.F)

	1	2	3	4	5	6	7	8	9	10	11
(H1)	836.1	813.6	791.1	1024.9	1140.8	1280.7	1097.3	994.4	937.3	901.7	864.9
(H2)	827.4	811.5	789.2	887.4	980.1	970.9	987.2	928.3	889.6	866.4	852.5

RATIO OF CALCULATED HEAT TRANSFER COEFFICIENT TO THOSE PREDICTED BY LITERATURE

	1	2	3	4	5	6	7	8	9	10	11
LIT(1)	1.05	1.00	0.97	1.25	1.39	1.56	1.34	1.21	1.13	1.09	1.02
LIT(2)	0.97	0.92	0.89	1.16	1.29	1.44	1.23	1.11	1.05	1.00	0.95
LIT(3)	1.02	0.96	0.93	1.21	1.34	1.50	1.29	1.16	1.09	1.05	0.99

RUN NUMBER 428

INSIDE SURFACE TEMPERATURES - DEGREES F

	1	2	3	4	5	6	7	8	9	10	11
1	86.3	91.1	88.1	83.5	84.7	84.5	84.6	87.3	88.1	88.2	94.0
2	86.6	89.4	91.9	84.2	85.0	85.5	84.7	86.7	88.3	87.8	93.3
3	86.7	90.3	91.7	85.9	87.4	87.3	85.7	86.4	89.2	89.4	93.1
4	86.6	88.8	90.8	92.1	92.3	92.8	90.8	90.4	92.2	92.6	95.7
5	86.5	87.8	91.6	95.0	95.6	96.1	96.9	93.2	93.9	93.4	96.1
6	85.4	90.3	90.2	91.2	91.0	90.6	91.8	91.8	92.7	93.0	93.9
7	85.7	90.8	92.1	85.3	86.8	86.5	86.7	88.0	89.3	90.7	92.6
8	86.5	90.4	91.9	84.0	85.0	85.5	85.2	86.7	88.7	88.5	93.6

INSIDE SURFACES HEAT FLUXES BTU/HR/FT2

	1	2	3	4	5	6	7	8	9	10	11
1	2701.4	2555.7	3084.2	3144.1	2992.9	3236.3	2718.1	2623.3	2724.6	2673.4	2624.7
2	2667.7	2814.3	2465.9	2917.9	2930.4	2936.5	2729.1	2690.4	2718.0	2791.0	2702.6
3	2667.8	2556.7	2646.5	2891.6	2762.1	2857.2	2907.6	2914.4	2791.2	2763.8	2831.8
4	2673.3	2702.1	2764.0	2328.0	2493.3	2359.3	2726.1	2618.5	2612.6	2551.0	2562.9
5	2634.1	2869.5	2567.2	1994.0	2029.7	1821.7	2074.3	2444.8	2518.4	2613.7	2540.7
6	2751.8	2573.2	2853.9	2397.2	2598.6	2562.2	2669.9	2551.4	2562.1	2579.7	2725.8
7	2701.0	2635.0	2568.6	2896.7	2761.3	2822.9	2879.8	2813.7	2830.9	2680.1	2803.8
8	2634.1	2731.0	2488.6	2907.4	2898.1	2892.4	2729.1	2779.9	2678.9	2785.5	2651.9

RUN NUMBER 428

AVERAGE REYNOLDS NUMBER	= 0.528E+04	
AVERAGE PRANDTL NUMBER	= 0.597E+01	
MASS FLUX	= 0.172E+06	LBM/(SQ.FT-HR)
AVERAGE HEAT FLUX	= 0.268E+04	BTU/(SQ.FT-HR)
Q=AMP*VOLT	= 0.588E+04	BTU/HR
Q=M*C*(T2-T1)	= 0.594E+04	BTU/HR
HEAT LOST	=-0.175E+02	BTU/HR
HEAT BALANCE ERROR %	=-0.678E+00	

PERIPHERAL HEAT TRANSFER COEFFICIENT BTU/(SQ.FT-HR-DEG.F)

	1	2	3	4	5	6	7	8	9	10	11
1	222.1	196.3	320.8	680.5	536.3	636.8	555.6	373.1	367.1	379.2	266.3
2	213.9	247.7	184.6	544.4	499.2	485.6	547.0	413.0	356.5	421.5	292.6
3	212.2	209.2	201.8	409.4	332.8	363.3	488.8	472.9	328.1	335.9	314.4
4	214.4	250.5	224.9	175.3	190.0	176.4	245.8	258.4	228.2	224.2	221.5
5	214.5	294.4	197.0	123.5	123.6	109.1	121.0	188.4	191.2	214.8	212.2
6	244.6	210.6	244.6	193.9	218.4	230.3	220.5	220.9	214.2	219.1	277.2
7	233.6	207.4	189.8	448.3	358.7	399.1	414.1	361.4	329.3	280.7	329.3
8	214.5	220.6	186.4	563.2	493.1	477.5	497.1	428.1	333.5	380.3	280.7

AVERAGE HEAT TRANSFER COEFFICIENT-BTU/(SQ.FT.HR-DEG.F)

	1	2	3	4	5	6	7	8	9	10	11
(H1)	221.2	229.6	218.7	392.3	344.0	359.8	386.2	339.5	293.5	307.0	274.3
(H2)	220.8	227.0	214.5	304.8	287.1	293.1	312.4	312.3	279.2	289.3	269.9

RATIO OF CALCULATED HEAT TRANSFER COEFFICIENT TO THOSE PREDICTED BY LITERATURE

	1	2	3	4	5	6	7	8	9	10	11
LIT(1)	1.04	1.05	0.99	1.79	1.56	1.63	1.75	1.53	1.32	1.38	1.21
LIT(2)	0.93	0.95	0.90	1.61	1.41	1.47	1.58	1.38	1.19	1.24	1.09
LIT(3)	0.98	0.99	0.94	1.69	1.48	1.55	1.66	1.45	1.25	1.30	1.15

RUN NUMBER 514

INSIDE SURFACE TEMPERATURES - DEGREES F

	1	2	3	4	5	6	7	8	9	10	11
1	95.4	97.1	96.6	93.5	93.4	93.0	94.7	96.5	98.1	99.6	103.4
2	95.9	97.5	97.7	94.3	93.9	93.9	96.3	98.4	100.0	101.1	105.0
3	95.4	98.2	98.8	96.2	97.3	97.4	99.5	101.8	102.8	103.7	106.5
4	95.5	98.8	100.1	100.6	103.5	104.6	104.3	105.9	106.5	107.3	108.6
5	94.8	99.0	100.8	106.3	110.8	112.9	111.5	108.3	109.0	109.0	109.3
6	93.4	98.9	100.2	100.7	103.1	104.5	102.7	102.7	104.3	104.6	106.0
7	92.4	97.4	98.2	96.8	98.0	98.1	97.0	99.0	100.1	100.4	102.9
8	93.6	97.3	97.3	94.8	94.7	94.7	95.0	96.8	98.2	99.2	102.6

INSIDE SURFACES HEAT FLUXES BTU/HR/FT2

	1	2	3	4	5	6	7	8	9	10	11
1	12853.8	12952.1	13021.5	13677.1	13584.6	13913.5	13035.4	13053.6	13042.8	12991.9	12971.2
2	12870.0	12935.5	12931.2	13391.2	13347.1	13466.0	13017.4	13012.3	12979.3	12991.2	12929.9
3	12944.4	12924.4	12935.7	13037.8	13051.3	13114.0	13015.8	12959.8	12972.7	12978.3	12963.4
4	12881.3	12900.8	12889.9	12586.0	12707.8	12571.0	13044.1	12829.0	12859.1	12825.1	12849.7
5	12887.1	12906.9	12850.2	11518.2	11551.9	11215.4	12048.3	12487.6	12528.1	12580.3	12702.2
6	12938.6	12850.0	12850.7	12608.2	12782.6	12622.2	13084.7	13023.2	12955.2	12944.8	12946.8
7	13046.1	12992.3	12980.7	13004.2	13000.7	13067.7	13134.6	13011.9	13052.5	13093.0	13083.4
8	12949.5	12929.6	12936.0	13368.6	13297.3	13427.0	13024.0	13035.6	13031.3	13020.2	12993.3

RUN NUMBER 514

AVERAGE REYNOLDS NUMBER	= 0.239E+05	
AVERAGE PRANDTL NUMBER	= 0.570E+01	
MASS FLUX	= 0.748E+06	LBM/(SQ.FT-HR)
AVERAGE HEAT FLUX	= 0.138E+05	BTU/(SQ.FT-HR)
Q=AMP*VOLT	= 0.282E+05	BTU/HR
Q=M*C*(T2-T1)	= 0.289E+05	BTU/HR
HEAT LOST	= 0.790E+01	BTU/HR
HEAT BALANCE ERROR %	=-0.252E+01	

PERIPHERAL HEAT TRANSFER COEFFICIENT BTU/(SQ.FT-HR-DEG.F)

	1	2	3	4	5	6	7	8	9	10	11
1	702.7	775.3	834.1	1184.5	1246.3	1432.2	1215.6	1092.9	1005.4	934.0	836.4
2	685.0	756.0	777.4	1071.1	1171.1	1259.3	1055.8	939.1	871.7	842.9	759.7
3	704.6	729.6	729.4	901.5	881.0	926.5	837.9	750.3	733.1	720.3	700.2
4	700.6	704.2	676.7	667.8	606.8	588.4	641.5	602.0	603.0	594.9	622.5
5	728.8	697.0	650.4	468.6	408.6	378.0	438.5	527.1	526.2	539.5	594.2
6	790.4	697.2	670.8	665.6	619.7	593.9	698.3	717.1	678.2	687.5	718.6
7	850.3	764.4	753.7	862.9	837.3	879.0	1010.1	900.0	871.7	891.5	873.3
8	781.7	769.1	792.0	1027.7	1089.0	1177.5	1181.2	1064.2	996.6	964.3	883.8

AVERAGE HEAT TRANSFER COEFFICIENT-BTU/(SQ.FT.HR-DEG.F)

	1	2	3	4	5	6	7	8	9	10	11
(H1)	743.0	736.6	735.6	856.2	857.5	904.4	884.9	824.1	785.8	771.9	748.6
(H2)	739.4	735.3	730.7	800.7	767.1	776.7	800.7	777.9	750.3	742.8	734.8

RATIO OF CALCULATED HEAT TRANSFER COEFFICIENT TO THOSE PREDICTED BY LITERATURE

	1	2	3	4	5	6	7	8	9	10	11
LIT(1)	1.04	1.01	1.01	1.17	1.16	1.22	1.19	1.10	1.05	1.03	0.98
LIT(2)	0.95	0.93	0.92	1.07	1.06	1.12	1.09	1.01	0.96	0.94	0.90
LIT(3)	1.00	0.97	0.97	1.12	1.12	1.17	1.14	1.06	1.01	0.99	0.95

RUN NUMBER 515

INSIDE SURFACE TEMPERATURES - DEGREES F

	1	2	3	4	5	6	7	8	9	10	11
1	99.7	101.7	100.7	96.6	96.5	95.8	97.5	99.3	101.3	103.5	107.9
2	100.5	102.0	101.7	97.5	97.0	96.5	99.5	101.5	103.8	105.4	109.7
3	99.7	102.5	103.0	100.0	100.8	100.7	103.1	105.6	107.1	108.4	111.5
4	99.8	103.2	104.8	103.8	107.9	109.0	108.6	110.6	111.8	112.9	114.6
5	98.8	103.6	105.5	111.7	116.8	119.6	117.0	113.7	115.1	115.5	116.0
6	97.2	103.3	104.7	104.6	107.7	109.3	106.7	106.9	109.2	109.8	111.4
7	95.7	101.4	102.4	100.4	101.8	101.9	99.8	102.4	103.9	104.2	106.9
8	97.4	101.6	101.2	98.2	97.9	97.4	97.5	99.7	101.5	102.8	106.8

INSIDE SURFACES HEAT FLUXES BTU/HR/FT2

	1	2	3	4	5	6	7	8	9	10	11
1	16504.1	16604.3	16668.7	17798.4	17420.1	17802.9	16711.9	16746.7	16748.4	16675.6	16643.3
2	16497.3	16604.5	16616.8	17202.2	17114.2	17306.5	16687.4	16699.1	16650.4	16662.6	16601.6
3	16639.6	16604.1	16622.2	16644.0	16741.3	16800.1	16701.2	16651.9	16676.7	16683.4	16674.2
4	16525.7	16575.0	16530.2	16288.1	16337.7	16186.4	16740.7	16479.5	16509.5	16482.4	16496.9
5	16556.0	16552.9	16507.0	14759.7	14891.2	14425.8	15568.0	16045.5	16081.0	16133.7	16268.0
6	16601.4	16507.3	16508.2	16224.1	16407.1	16221.2	16770.6	16714.7	16630.9	16603.6	16606.7
7	16760.3	16701.0	16656.5	16672.5	16673.4	16731.2	16855.6	16699.2	16756.7	16832.3	16841.6
8	16628.6	16593.4	16640.1	17150.5	17068.7	17272.1	16728.4	16729.2	16724.7	16714.2	16676.8

RUN NUMBER 515

AVERAGE REYNOLDS NUMBER	= 0.272E+05	
AVERAGE PRANDTL NUMBER	= 0.560E+01	
MASS FLUX	= 0.840E+06	LBM/(SQ.FT-HR)
AVERAGE HEAT FLUX	= 0.179E+05	BTU/(SQ.FT-HR)
Q=AMP*VOLT	= 0.364E+05	BTU/HR
Q=M*C*(T2-T1)	= 0.377E+05	BTU/HR
HEAT LOST	= 0.152E+01	BTU/HR
HEAT BALANCE ERROR %	=-0.357E+01	

PERIPHERAL HEAT TRANSFER COEFFICIENT BTU/(SQ.FT-HR-DEG.F)

	1	2	3	4	5	6	7	8	9	10	11
1	744.6	818.9	891.6	1295.7	1366.7	1586.9	1386.8	1270.4	1153.3	1043.6	932.3
2	718.3	807.0	847.4	1183.0	1292.3	1454.3	1186.9	1084.6	982.4	931.6	844.2
3	751.8	787.8	794.9	976.6	981.1	1043.9	945.6	857.7	823.6	798.8	777.3
4	742.4	760.8	727.1	779.4	678.1	662.9	722.7	673.6	660.5	647.9	670.7
5	779.1	745.9	704.2	511.8	450.2	412.0	493.1	582.0	568.2	575.7	626.8
6	845.4	753.7	729.2	747.1	684.2	656.5	739.1	803.4	743.7	744.3	777.2
7	921.0	832.8	820.5	950.7	922.1	966.5	1177.0	1024.6	978.5	1005.2	996.3
8	838.5	822.4	871.1	1124.3	1205.3	1348.3	1388.7	1231.3	1135.6	1087.5	996.1

AVERAGE HEAT TRANSFER COEFFICIENT-BTU/(SQ.FT.HR-DEG.F)

	1	2	3	4	5	6	7	8	9	10	11
(H1)	792.6	791.2	798.2	946.1	947.6	1016.4	1011.2	940.9	880.7	854.3	827.6
(H2)	787.9	790.0	792.8	887.5	847.9	865.0	908.6	880.9	833.9	816.5	807.2

RATIO OF CALCULATED HEAT TRANSFER COEFFICIENT TO THOSE PREDICTED BY LITERATURE

	1	2	3	4	5	6	7	8	9	10	11
LIT(1)	1.01	0.98	0.99	1.17	1.16	1.24	1.23	1.14	1.06	1.02	0.97
LIT(2)	0.92	0.90	0.91	1.07	1.07	1.14	1.13	1.04	0.97	0.94	0.90
LIT(3)	0.97	0.95	0.95	1.12	1.12	1.19	1.18	1.09	1.02	0.99	0.94

RUN NUMBER 522

INSIDE SURFACE TEMPERATURES - DEGREES F

	1	2	3	4	5	6	7	8	9	10	11
1	77.5	80.6	79.6	76.7	77.3	77.6	79.3	88.0	84.0	84.9	89.0
2	77.1	79.2	79.4	77.5	78.6	77.6	79.9	89.2	84.7	86.0	89.7
3	79.2	79.6	78.8	79.5	82.5	80.9	81.5	89.0	85.8	87.2	90.5
4	81.2	79.5	78.6	88.2	88.7	89.0	88.0	89.9	86.9	88.0	90.2
5	81.6	77.9	78.1	86.2	98.7	101.8	103.9	91.4	88.4	88.4	89.2
6	82.2	78.9	78.3	81.8	87.9	90.0	96.2	90.2	87.1	87.1	88.2
7	80.5	79.1	79.4	78.6	80.1	80.9	82.7	87.2	85.1	85.8	87.4
8	78.6	80.5	80.6	76.9	77.4	78.0	79.9	87.2	84.1	85.1	87.9

INSIDE SURFACES HEAT FLUXES BTU/HR/FT2

	1	2	3	4	5	6	7	8	9	10	11
1	3400.7	3272.4	3401.5	3630.6	3587.9	3598.5	3430.3	3381.8	3402.0	3430.5	3336.6
2	3483.3	3456.1	3333.6	3524.5	3561.3	3642.6	3418.8	3280.4	3380.1	3363.9	3364.6
3	3356.2	3327.8	3378.9	3715.4	3478.3	3618.0	3624.3	3420.0	3358.4	3335.9	3297.6
4	3266.8	3277.9	3339.5	2664.6	3484.8	3501.0	3867.8	3392.5	3380.6	3335.9	3319.9
5	3367.8	3490.4	3395.2	3015.3	2059.0	1790.3	2067.9	3207.8	3202.1	3263.7	3359.3
6	3228.5	3316.6	3406.2	3319.1	3438.7	3399.6	3044.0	3264.4	3319.3	3358.1	3370.0
7	3344.7	3423.3	3361.8	3439.3	3634.5	3691.4	3934.4	3515.6	3413.7	3391.4	3431.1
8	3401.2	3283.6	3233.3	3536.7	3559.7	3597.6	3478.3	3408.4	3407.9	3386.1	3392.6

RUN NUMBER 522

AVERAGE REYNOLDS NUMBER	= 0.528E+04	
AVERAGE PRANDTL NUMBER	= 0.696E+01	
MASS FLUX	= 0.198E+06	LBM/(SQ.FT-HR)
AVERAGE HEAT FLUX	= 0.354E+04	BTU/(SQ.FT-HR)
Q=AMP*VOLT	= 0.719E+04	BTU/HR
Q=M*C*(T2-T1)	= 0.756E+04	BTU/HR
HEAT LOST	=-0.257E+02	BTU/HR
HEAT BALANCE ERROR %	=-0.485E+01	

PERIPHERAL HEAT TRANSFER COEFFICIENT BTU/(SQ.FT-HR-DEG.F)

	1	2	3	4	5	6	7	8	9	10	11
1	240.3	233.3	273.4	408.9	413.2	431.3	370.9	194.3	264.9	260.3	220.1
2	251.8	274.6	272.0	363.5	353.5	437.5	347.0	176.1	249.5	235.3	212.2
3	211.6	255.7	290.2	319.0	248.8	311.2	315.0	185.9	229.2	215.2	197.8
4	182.7	253.6	291.5	130.7	172.8	177.3	215.5	175.7	214.7	204.6	202.8
5	184.4	306.8	310.3	163.9	68.4	55.0	61.0	153.9	185.2	195.2	218.7
6	170.9	269.3	305.3	238.2	177.5	164.4	116.4	166.3	207.9	218.1	234.8
7	194.9	274.0	274.4	321.1	314.9	318.0	309.0	210.8	244.9	240.7	253.4
8	223.0	235.3	239.9	388.9	401.1	411.6	350.0	205.3	263.4	252.9	241.5

AVERAGE HEAT TRANSFER COEFFICIENT-BTU/(SQ.FT.HR-DEG.F)

	1	2	3	4	5	6	7	8	9	10	11
(H1)	207.4	262.9	282.2	291.8	268.8	288.3	260.6	183.5	232.5	227.8	222.7
(H2)	204.5	261.5	280.8	261.3	218.3	220.7	204.7	182.2	229.8	226.0	221.4

RATIO OF CALCULATED HEAT TRANSFER COEFFICIENT TO THOSE PREDICTED BY LITERATURE

	1	2	3	4	5	6	7	8	9	10	11
LIT(1)	0.93	1.16	1.24	1.28	1.17	1.24	1.12	0.78	0.99	0.97	0.93
LIT(2)	0.84	1.04	1.11	1.15	1.05	1.12	1.01	0.71	0.90	0.87	0.84
LIT(3)	0.88	1.10	1.17	1.21	1.11	1.18	1.06	0.75	0.94	0.92	0.89

RUN NUMBER 528

INSIDE SURFACE TEMPERATURES - DEGREES F

	1	2	3	4	5	6	7	8	9	10	11
1	73.4	77.3	75.9	76.8	87.0	97.5	102.8	106.7	106.5	106.7	110.7
2	73.5	80.1	79.8	78.3	86.6	97.7	102.0	101.9	106.7	107.5	105.1
3	76.9	90.1	88.8	81.2	87.5	94.4	95.8	94.9	97.7	99.4	100.5
4	83.2	101.1	102.1	95.2	90.6	92.4	91.9	90.5	92.8	93.4	95.3
5	91.7	103.9	105.7	94.9	92.8	92.0	89.8	89.2	89.9	90.8	94.1
6	84.5	90.4	99.2	85.4	89.0	91.3	90.2	89.1	89.7	90.5	97.7
7	78.5	82.1	86.4	79.6	86.1	92.6	92.5	91.0	92.6	92.9	102.0
8	75.5	78.0	79.1	77.4	86.1	96.8	96.2	98.1	101.7	100.3	104.8

INSIDE SURFACES HEAT FLUXES BTU/HR/FT2

	1	2	3	4	5	6	7	8	9	10	11
1	1238.9	1316.1	1500.1	1305.1	1096.6	1155.6	710.9	384.7	864.7	813.7	495.6
2	1299.5	1508.2	1407.3	1232.7	1212.5	971.1	824.2	999.9	609.4	626.7	1168.7
3	1278.5	1177.5	1352.1	1716.7	1239.1	1185.3	1243.7	1259.7	1346.5	1234.4	1085.7
4	1233.4	664.4	590.0	294.2	1039.9	1175.2	1219.6	1291.6	1230.7	1309.8	1343.7
5	264.2	223.9	561.5	541.9	737.9	1034.6	1258.4	1185.6	1269.1	1246.9	1388.2
6	1177.2	1403.9	769.8	1283.0	1141.5	1196.5	1224.8	1229.4	1296.2	1269.1	1159.9
7	1284.4	1351.0	1423.5	1315.9	1278.1	1275.0	1197.1	1409.4	1451.5	1399.6	1035.8
8	1166.8	1305.9	1350.3	1239.5	1189.8	970.7	1278.8	1195.3	890.9	1059.6	1286.8

RUN NUMBER 528

AVERAGE REYNOLDS NUMBER	= 0.768E+03	
AVERAGE PRANDTL NUMBER	= 0.619E+01	
MASS FLUX	= 0.259E+05	LBM/(SQ.FT-HR)
AVERAGE HEAT FLUX	= 0.121E+04	BTU/(SQ.FT-HR)
Q=AMP*VOLT	= 0.244E+04	BTU/HR
Q=M*C*(T2-T1)	= 0.243E+04	BTU/HR
HEAT LOST	=-0.145E+02	BTU/HR
HEAT BALANCE ERROR %	= 0.965E+00	

PERIPHERAL HEAT TRANSFER COEFFICIENT BTU/(SQ.FT-HR-DEG.F)

	1	2	3	4	5	6	7	8	9	10	11
1	118.0	222.4	480.5	622.5	104.7	60.6	31.6	15.4	37.2	36.9	24.3
2	122.7	171.9	202.7	341.4	120.7	50.5	38.0	49.8	25.9	27.4	78.5
3	91.4	62.8	84.7	264.3	113.3	74.2	80.3	96.0	93.2	83.8	105.4
4	60.7	22.3	20.2	14.3	73.9	84.1	105.3	148.2	128.5	150.4	266.8
5	9.2	6.9	17.1	26.9	45.4	76.1	132.8	159.4	190.3	203.6	362.8
6	54.5	73.9	29.2	120.0	91.7	93.0	123.9	167.7	200.6	218.1	155.1
7	82.4	126.1	105.1	269.1	134.2	90.1	98.2	153.4	154.0	170.9	87.7
8	92.5	197.3	215.8	457.5	124.6	53.0	80.6	73.2	48.3	67.6	88.4

AVERAGE HEAT TRANSFER COEFFICIENT-BTU/(SQ.FT.HR-DEG.F)

	1	2	3	4	5	6	7	8	9	10	11
(H1)	78.9	110.5	144.4	264.5	101.1	72.7	86.3	107.9	109.7	119.9	146.1
(H2)	66.7	67.8	66.7	125.4	95.8	70.5	75.5	83.6	80.1	86.0	101.5

RATIO OF CALCULATED HEAT TRANSFER COEFFICIENT TO THOSE PREDICTED BY LITERATURE

	1	2	3	4	5	6	7	8	9	10	11
LIT(1)	1.06	1.33	1.70	3.76	1.29	0.82	0.98	1.24	1.23	1.36	1.67
LIT(2)	0.89	0.81	0.78	1.78	1.22	0.79	0.85	0.96	0.90	0.98	1.16

RUN NUMBER 203

	1	2	3	4	5	6	7	8	9	10	11
X/D	-0.968E+02	-0.242E+02	0.0	0.190E+01	0.380E+01	0.570E+01	0.760E+01	0.318E+02	0.560E+02	0.104E+03	0.153E+03
TB,F	0.881E+02	0.904E+02	0.911E+02	0.912E+02	0.912E+02	0.913E+02	0.913E+02	0.921E+02	0.928E+02	0.943E+02	0.958E+02
JHC	0.118E+02	0.118E+02	0.160E+02	0.170E+02	0.204E+02	0.205E+02	0.231E+02	0.116E+02	0.114E+02	0.121E+02	0.141E+02
RE.NO.	0.348E+04	0.357E+04	0.360E+04	0.361E+04	0.361E+04	0.361E+04	0.361E+04	0.364E+04	0.368E+04	0.374E+04	0.380E+04
PR.NO.	0.529E+01	0.514E+01	0.509E+01	0.508E+01	0.508E+01	0.508E+01	0.507E+01	0.502E+01	0.498E+01	0.488E+01	0.479E+01
GR.NO.	0.633E+05	0.697E+05	0.595E+05	0.537E+05	0.468E+05	0.477E+05	0.493E+05	0.766E+05	0.802E+05	0.806E+05	0.102E+06
HT/HB	0.920E+00	0.104E+01	0.309E+00	0.137E+01	0.194E+01	0.214E+01	0.101E+02	0.100E+01	0.948E+00	0.905E+00	0.366E-01
DE.NO.	0.158E+04	0.162E+04	0.164E+04	0.164E+04	0.164E+04	0.164E+04	0.164E+04	0.166E+04	0.167E+04	0.170E+04	0.173E+04
GR/RE2	0.523E-02	0.546E-02	0.458E-02	0.413E-02	0.359E-02	0.366E-02	0.378E-02	0.577E-02	0.594E-02	0.577E-02	0.704E-02
NU.NO.	0.232E+02	0.230E+02	0.309E+02	0.327E+02	0.394E+02	0.395E+02	0.444E+02	0.223E+02	0.219E+02	0.230E+02	0.267E+02
PW	0.949E+01	0.941E+01	0.113E+02	0.128E+02	0.145E+02	0.144E+02	0.138E+02	0.914E+01	0.898E+01	0.945E+01	0.790E+01

RUN NUMBER 205

	1	2	3	4	5	6	7	8	9	10	11
X/D	-0.968E+02	-0.242E+02	0.0	0.190E+01	0.380E+01	0.570E+01	0.760E+01	0.318E+02	0.560E+02	0.104E+03	0.153E+03
TB,F	0.898E+02	0.918E+02	0.925E+02	0.926E+02	0.926E+02	0.927E+02	0.927E+02	0.934E+02	0.941E+02	0.955E+02	0.968E+02
JHC	0.192E+02	0.193E+02	0.246E+02	0.254E+02	0.271E+02	0.270E+02	0.298E+02	0.180E+02	0.187E+02	0.185E+02	0.186E+02
RE.NO.	0.543E+04	0.556E+04	0.560E+04	0.561E+04	0.561E+04	0.561E+04	0.562E+04	0.566E+04	0.570E+04	0.579E+04	0.588E+04
PR.NO.	0.517E+01	0.504E+01	0.500E+01	0.499E+01	0.499E+01	0.499E+01	0.498E+01	0.494E+01	0.490E+01	0.482E+01	0.474E+01
GR.NO.	0.590E+05	0.642E+05	0.581E+05	0.538E+05	0.508E+05	0.520E+05	0.538E+05	0.732E+05	0.729E+05	0.776E+05	0.812E+05
HT/HB	0.939E+00	0.110E+01	0.301E+00	0.121E+01	0.145E+01	0.162E+01	0.654E+01	0.104E+01	0.112E+01	0.110E+01	0.992E+00
DE.NO.	0.247E+04	0.253E+04	0.255E+04	0.255E+04	0.255E+04	0.255E+04	0.255E+04	0.257E+04	0.259E+04	0.263E+04	0.267E+04
GR/RE2	0.200E-02	0.208E-02	0.185E-02	0.171E-02	0.162E-02	0.165E-02	0.171E-02	0.228E-02	0.224E-02	0.231E-02	0.235E-02
NU.NO.	0.374E+02	0.371E+02	0.472E+02	0.486E+02	0.518E+02	0.516E+02	0.571E+02	0.345E+02	0.355E+02	0.350E+02	0.350E+02
PW	0.153E+02	0.152E+02	0.172E+02	0.189E+02	0.199E+02	0.196E+02	0.188E+02	0.142E+02	0.146E+02	0.144E+02	0.144E+02

RUN NUMBER 213

	1	2	3	4	5	6	7	8	9	10	11
X/D	-C.968E+02	-0.242E+02	0.0	0.190E+01	0.380E+01	0.570E+01	0.760E+01	0.318E+02	0.560E+02	0.104E+03	0.153E+03
TB,F	0.101E+03	0.104E+03	0.105E+03	0.105E+03	0.105E+03	0.105E+03	0.105E+03	0.106E+03	0.107E+03	0.109E+03	0.111E+03
JHC	0.658E+02	0.660E+02	0.841E+02	0.779E+02	0.825E+02	0.862E+02	0.110E+03	0.702E+02	0.713E+02	0.746E+02	0.735E+02
RE.NC.	0.235E+05	0.243E+05	0.245E+05	0.245E+05	0.245E+05	0.246E+05	0.246E+05	0.248E+05	0.251E+05	0.255E+05	0.260E+05
PR.NO.	0.450E+01	0.435E+01	0.430E+01	0.430E+01	0.430E+01	0.429E+01	0.429E+01	0.424E+01	0.420E+01	0.411E+01	0.402E+01
GR.NC.	0.142E+06	0.157E+06	0.150E+06	0.144E+06	0.137E+06	0.133E+06	0.128E+06	0.160E+06	0.163E+06	0.167E+06	0.181E+06
HT/HB	0.984E+00	0.103E+01	0.282E+00	0.104E+01	0.111E+01	0.122E+01	0.511E+01	0.998E+00	0.102E+01	0.100E+01	0.104E+01
DE.NC.	0.107E+05	0.110E+05	0.111E+05	0.111E+05	0.112E+05	0.112E+05	0.112E+05	0.113E+05	0.114E+05	0.116E+05	0.118E+05
GR/RE2	0.256E-03	0.268E-03	0.249E-03	0.239E-03	0.228E-03	0.221E-03	0.212E-03	0.260E-03	0.260E-03	0.255E-03	0.266E-03
NU.NC.	0.121E+03	0.120E+03	0.152E+03	0.141E+03	0.149E+03	0.156E+03	0.198E+03	0.127E+03	0.128E+03	0.133E+03	0.130E+03
PW	0.501E+02	0.496E+02	0.538E+02	0.570E+02	0.595E+02	0.618E+02	0.636E+02	0.523E+02	0.530E+02	0.550E+02	0.538E+02

RUN NUMBER 215

	1	2	3	4	5	6	7	8	9	10	11
X/D	-C.968E+02	-0.242E+02	0.0	0.190E+01	0.380E+01	0.570E+01	0.760E+01	0.318E+02	0.560E+02	0.104E+03	0.153E+03
TB,F	C.937E+02	0.101E+03	0.103E+03	0.104E+03	0.104E+03	0.104E+03	0.104E+03	0.107E+03	0.109E+03	0.114E+03	0.119E+03
JHC	C.876E+01	C.984E+01	0.867E+04	-0.253E+03	-0.290E+02	0.241E+02	0.148E+02	0.992E+01	0.976E+01	0.104E+02	0.108E+02
RE.NO.	C.118E+04	0.128E+04	0.131E+04	0.131E+04	0.132E+04	0.132E+04	0.132E+04	0.136E+04	0.139E+04	0.146E+04	0.153E+04
PR.NC.	0.493E+01	0.450E+01	0.437E+01	0.436E+01	0.435E+01	0.434E+01	0.434E+01	0.421E+01	0.410E+01	0.388E+01	0.368E+01
GR.NO.	C.147E+06	0.152E+06	0.961E+05	0.732E+05	0.490E+05	0.823E+05	0.116E+06	0.209E+06	0.231E+06	0.272E+06	0.318E+06
HT/HB	C.109E+00	0.973E-01	-0.409E-05	-0.269E+02	-0.672E+01	0.436E+01	0.518E+01	0.137E+00	0.875E-01	0.112E+00	0.943E-01
DE.NO.	C.536E+03	0.581E+03	0.596E+03	0.598E+03	0.599E+03	0.600E+03	0.601E+03	0.617E+03	0.632E+03	0.664E+03	0.696E+03
GR/RE2	C.106E+00	0.117E+00	0.558E-01	0.424E-01	0.232E-01	0.473E-01	0.665E-01	0.114E+00	0.120E+00	0.128E+00	0.136E+00
NU.NO.	0.169E+02	0.183E+02	0.158E+05	-0.458E+03	-0.525E+02	0.436E+02	0.269E+02	0.179E+02	0.174E+02	0.181E+02	0.184E+02
PW	C.554E+01	0.583E+01	0.463E+01	0.426E+01	0.378E+01	0.440E+01	0.490E+01	0.585E+01	0.598E+01	0.618E+01	0.637E+01

RUN NUMBER 252

	1	2	3	4	5	6	7	8	9	10	11
X/D	-C.968E+02	-0.242E+02	0.0	0.190E+01	0.380E+01	0.570E+01	0.760E+01	0.318E+02	0.560E+02	0.104E+03	0.153E+03
TB.F	C.969E+02	0.983E+02	C.988E+02	0.988E+02	0.988E+02	0.989E+02	0.989E+02	0.994E+02	0.999E+02	0.101E+03	0.102E+03
JHC	C.223E+01	0.197E+01	0.471E+01	0.701E+01	0.266E+02	0.292E+02	0.470E+02	0.410E+01	0.281E+01	0.212E+01	0.219E+01
RE.NO.	C.120E+04	0.123E+04	0.124E+04	0.124E+04	0.124E+04	0.124E+04	0.124E+04	0.125E+04	0.126E+04	0.129E+04	0.131E+04
PR.NO.	C.978E+02	0.956E+02	0.949E+02	0.948E+02	0.948E+02	0.947E+02	0.947E+02	0.940E+02	0.933E+02	0.920E+02	0.906E+02
GR.NO.	C.507E+04	0.610E+04	0.349E+04	0.235E+04	0.120E+04	0.104E+04	0.877E+03	0.322E+04	0.464E+04	0.632E+04	0.650E+04
HT/HB	C.652E+00	0.516E+00	0.195E-01	0.756E+01	0.833E+02	0.283E+02	0.102E+03	0.167E+01	0.123E+01	0.723E+00	0.417E+00
DE.NO.	C.544E+03	0.558E+03	0.563E+03	0.564E+03	0.564E+03	0.564E+03	0.565E+03	0.570E+03	0.574E+03	0.584E+03	0.594E+03
GR/RE2	C.354E-02	0.404E-02	0.227E-02	0.153E-02	0.781E-03	0.675E-03	0.568E-03	0.205E-02	0.291E-02	0.383E-02	0.380E-02
NU.NO.	0.153E+02	0.136E+02	C.309E+02	0.451E+02	0.168E+03	0.184E+03	0.295E+03	0.266E+02	0.186E+02	0.143E+02	0.147E+02
PW	C.326E+01	0.342E+01	0.284E+01	0.250E+01	0.202E+01	0.193E+01	0.184E+01	0.275E+01	0.309E+01	0.339E+01	0.339E+01

RUN NUMBER 253

	1	2	3	4	5	6	7	8	9	10	11
X/D	-C.968E+02	-0.242E+02	0.0	0.190E+01	0.380E+01	0.570E+01	0.760E+01	0.318E+02	0.560E+02	0.104E+03	0.153E+03
TB.F	0.991E+02	0.100E+03	0.101E+03	0.101E+03	0.101E+03	0.101E+03	0.101E+03	0.101E+03	0.101E+03	0.102E+03	0.103E+03
JHC	C.198E+01	0.177E+01	0.381E+01	0.529E+01	0.219E+02	0.239E+02	0.365E+02	0.338E+01	0.236E+01	0.193E+01	0.195E+01
RE.NO.	0.931E+03	0.950E+03	0.957E+03	0.958E+03	0.958E+03	0.959E+03	0.959E+03	0.966E+03	0.972E+03	0.986E+03	0.999E+03
PR.NO.	C.944E+02	0.923E+02	0.922E+02	0.922E+02	0.922E+02	0.921E+02	0.921E+02	0.915E+02	0.910E+02	0.899E+02	0.889E+02
GR.NO.	0.388E+04	0.458E+04	0.282E+04	0.192E+04	0.910E+03	0.783E+03	0.654E+03	0.254E+04	0.362E+04	0.459E+04	0.477E+04
HT/HB	0.653E+00	0.474E+00	0.265E-01	0.689E+01	0.142E+03	0.282E+02	0.906E+02	0.134E+01	0.996E+00	0.615E+00	0.401E+00
DE.NO.	C.423E+03	0.432E+03	0.435E+03	0.435E+03	0.436E+03	0.436E+03	0.436E+03	0.439E+03	0.442E+03	0.448E+03	0.454E+03
GR/RE2	0.448E-02	0.507E-02	0.308E-02	0.209E-02	0.992E-03	0.853E-03	0.711E-03	0.272E-02	0.383E-02	0.473E-02	0.478E-02
NU.NO.	C.130E+02	0.117E+02	0.244E+02	0.333E+02	0.135E+03	0.148E+03	0.225E+03	0.214E+02	0.152E+02	0.125E+02	0.126E+02
PW	0.293E+01	0.307E+01	0.261E+01	0.231E+01	0.183E+01	0.175E+01	0.166E+01	0.251E+01	0.281E+01	0.302E+01	0.303E+01

RUN NUMBER 202

	1	2	3	4	5	6	7	8	9	10	11
X/D	-0.968E+02	-0.242E+02	0.0	0.190E+01	0.380E+01	0.570E+01	0.760E+01	0.318E+02	0.560E+02	0.104E+03	0.153E+03
TB,F	0.913E+02	0.951E+02	0.963E+02	0.964E+02	0.965E+02	0.966E+02	0.967E+02	0.980E+02	0.992E+02	0.102E+03	0.104E+03
JHC	0.164E+01	0.183E+01	0.258E+01	0.462E+01	-0.770E+00	0.647E+01	0.375E+01	0.166E+01	0.185E+01	0.203E+01	0.215E+01
RE.NO.	0.167E+03	0.179E+03	0.184E+03	0.184E+03	0.184E+03	0.185E+03	0.185E+03	0.189E+03	0.194E+03	0.203E+03	0.212E+03
PR.NO.	0.107E+03	0.101E+03	0.986E+02	0.985E+02	0.983E+02	0.982E+02	0.980E+02	0.961E+02	0.942E+02	0.906E+02	0.872E+02
GR.NO.	0.231E+04	0.255E+04	0.206E+04	0.122E+04	0.355E+03	0.833E+03	0.131E+04	0.306E+04	0.298E+04	0.311E+04	0.331E+04
HT/HB	0.300E+00	0.261E+00	-0.496E-02	0.455E+01	-0.837E+01	0.216E+01	0.196E+01	0.485E+00	0.270E+00	0.223E+00	0.217E+00
DE.NO.	0.759E+02	0.815E+02	0.835E+02	0.836E+02	0.838E+02	0.839E+02	0.841E+02	0.860E+02	0.880E+02	0.921E+02	0.964E+02
GR/RE2	0.830E-01	0.794E-01	0.612E-01	0.360E-01	0.105E-01	0.245E-01	0.383E-01	0.855E-01	0.794E-01	0.756E-01	0.736E-01
NU.NO.	0.112E+02	0.122E+02	0.168E+02	0.296E+02	-0.486E+01	0.412E+02	0.241E+02	0.109E+02	0.120E+02	0.129E+02	0.134E+02
PW	0.266E+01	0.265E+01	0.245E+01	0.207E+01	0.145E+01	0.184E+01	0.212E+01	0.274E+01	0.269E+01	0.267E+01	0.266E+01

RUN NUMBER 402

	1	2	3	4	5	6	7	8	9	10	11
X/D	-0.700E+02	-0.778E+01	0.0	0.484E+01	0.968E+01	0.145E+02	0.194E+02	0.271E+02	0.349E+02	0.427E+02	0.894E+02
TB,F	0.855E+02	0.896E+02	0.901E+02	0.904E+02	0.907E+02	0.911E+02	0.914E+02	0.919E+02	0.924E+02	0.929E+02	0.960E+02
JHC	0.593E+01	0.829E+01	0.889E+01	0.496E+02	0.116E+02	0.568E+01	0.485E+01	0.729E+01	0.662E+01	0.752E+01	0.798E+01
RE.NO.	0.721E+03	0.756E+03	0.760E+03	0.763E+03	0.766E+03	0.769E+03	0.771E+03	0.776E+03	0.780E+03	0.785E+03	0.812E+03
PR.NO.	0.547E+01	0.519E+01	0.515E+01	0.513E+01	0.511E+01	0.509E+01	0.507E+01	0.504E+01	0.500E+01	0.497E+01	0.479E+01
GR.NO.	0.113E+06	0.133E+06	0.133E+06	0.684E+05	0.863E+05	0.152E+06	0.176E+06	0.136E+06	0.150E+06	0.148E+06	0.170E+06
HT/HB	0.609E+00	0.843E-01	0.791E-01	-0.771E+03	0.730E+01	0.223E+01	0.112E+01	0.186E+00	0.156E+00	0.143E+00	0.119E+00
DE.NO.	0.205E+03	0.215E+03	0.217E+03	0.217E+03	0.218E+03	0.219E+03	0.220E+03	0.221E+03	0.222E+03	0.224E+03	0.231E+03
GR/RE2	0.217E+00	0.232E+00	0.231E+00	0.117E+00	0.147E+00	0.258E+00	0.296E+00	0.226E+00	0.246E+00	0.240E+00	0.258E+00
NU.NO.	0.118E+02	0.162E+02	0.173E+02	0.958E+02	0.224E+02	0.110E+02	0.940E+01	0.140E+02	0.127E+02	0.144E+02	0.151E+02
PW	0.761E+01	0.787E+01	0.786E+01	0.637E+01	0.683E+01	0.817E+01	0.856E+01	0.785E+01	0.808E+01	0.803E+01	0.828E+01

RUN NUMBER 419

	1	2	3	4	5	6	7	8	9	10	11
X/D	-0.700E+02	-0.778E+01	0.0	0.484E+01	0.968E+01	0.145E+02	0.194E+02	0.271E+02	0.349E+02	0.427E+02	0.894E+02
TB,F	0.903E+02	0.953E+02	0.959E+02	0.962E+02	0.966E+02	0.969E+02	0.973E+02	0.978E+02	0.984E+02	0.989E+02	0.102E+03
JHC	0.649E+02	0.660E+02	0.652E+02	0.863E+02	0.977E+02	0.984E+02	0.867E+02	0.812E+02	0.787E+02	0.763E+02	0.747E+02
RE.NO.	0.231E+05	0.243E+05	0.244E+05	0.245E+05	0.246E+05	0.247E+05	0.248E+05	0.250E+05	0.251E+05	0.253E+05	0.262E+05
PR.NO.	0.510E+01	0.482E+01	0.479E+01	0.477E+01	0.475E+01	0.473E+01	0.471E+01	0.468E+01	0.465E+01	0.462E+01	0.443E+01
GR.NO.	0.375E+06	0.440E+06	0.456E+06	0.401E+06	0.367E+06	0.402E+06	0.396E+06	0.420E+06	0.438E+06	0.455E+06	0.514E+06
HT/HB	0.123E+01	0.102E+01	0.889E+00	0.394E+01	0.391E+01	0.591E+01	0.263E+01	0.205E+01	0.196E+01	0.179E+01	0.137E+01
DE.NO.	0.658E+04	0.691E+04	0.696E+04	0.698E+04	0.701E+04	0.704E+04	0.706E+04	0.711E+04	0.715E+04	0.719E+04	0.746E+04
GR/RE2	0.704E-03	0.748E-03	0.764E-03	0.667E-03	0.606E-03	0.658E-03	0.644E-03	0.675E-03	0.695E-03	0.713E-03	0.751E-03
NU.NO.	0.128E+03	0.127E+03	0.125E+03	0.165E+03	0.186E+03	0.187E+03	0.164E+03	0.154E+03	0.149E+03	0.144E+03	0.138E+03
PW	0.768E+02	0.770E+02	0.759E+02	0.877E+02	0.971E+02	0.897E+02	0.917E+02	0.883E+02	0.863E+02	0.847E+02	0.837E+02

RUN NUMBER 428

	1	2	3	4	5	6	7	8	9	10	11
X/D	-0.700E+02	-0.778E+01	0.0	0.484E+01	0.968E+01	0.145E+02	0.194E+02	0.271E+02	0.349E+02	0.427E+02	0.894E+02
TB,F	0.742E+02	0.781E+02	0.785E+02	0.788E+02	0.791E+02	0.794E+02	0.797E+02	0.802E+02	0.807E+02	0.812E+02	0.841E+02
JHC	0.190E+02	0.201E+02	0.191E+02	0.346E+02	0.303E+02	0.318E+02	0.342E+02	0.301E+02	0.261E+02	0.273E+02	0.247E+02
RE.NO.	0.496E+04	0.521E+04	0.524E+04	0.526E+04	0.528E+04	0.530E+04	0.532E+04	0.535E+04	0.538E+04	0.542E+04	0.561E+04
PR.NO.	0.641E+01	0.606E+01	0.602E+01	0.599E+01	0.597E+01	0.594E+01	0.592E+01	0.588E+01	0.584E+01	0.580E+01	0.558E+01
GR.NO.	0.134E+06	0.157E+06	0.170E+06	0.121E+06	0.130E+06	0.130E+06	0.123E+06	0.126E+06	0.144E+06	0.142E+06	0.172E+06
HT/HB	0.966E+00	0.150E+01	0.614E+00	0.551E+01	0.434E+01	0.584E+01	0.459E+01	0.198E+01	0.192E+01	0.177E+01	0.126E+01
DE.NO.	0.141E+04	0.148E+04	0.149E+04	0.150E+04	0.150E+04	0.151E+04	0.152E+04	0.152E+04	0.153E+04	0.154E+04	0.160E+04
GR/RE2	0.546E-02	0.578E-02	0.618E-02	0.438E-02	0.468E-02	0.461E-02	0.434E-02	0.439E-02	0.495E-02	0.482E-02	0.545E-02
NU.NO.	0.408E+02	0.421E+02	0.401E+02	0.719E+02	0.630E+02	0.659E+02	0.707E+02	0.621E+02	0.536E+02	0.560E+02	0.499E+02
PW	0.243E+02	0.250E+02	0.236E+02	0.336E+02	0.316E+02	0.323E+02	0.344E+02	0.344E+02	0.307E+02	0.318E+02	0.296E+02

RUN NUMBER 420

	1	2	3	4	5	6	7	8	9	10	11
X/D	-0.700E+02	-0.778E+01	0.0	0.484E+01	0.968E+01	0.145E+02	0.194E+02	0.271E+02	0.349E+02	0.427E+02	0.894E+02
TB.F	0.947E+02	0.993E+02	0.998E+02	0.100E+03	0.101E+03	0.101E+03	0.101E+03	0.102E+03	0.102E+03	0.103E+03	0.106E+03
JHC	0.777E+02	0.769E+02	0.749E+02	0.974E+02	0.109E+03	0.122E+03	0.105E+03	0.951E+02	0.898E+02	0.865E+02	0.840E+02
RE.NO.	0.276E+05	0.290E+05	0.291E+05	0.292E+05	0.294E+05	0.295E+05	0.296E+05	0.298E+05	0.299E+05	0.301E+05	0.312E+05
PR.NO.	0.486E+01	0.460E+01	0.457E+01	0.455E+01	0.453E+01	0.451E+01	0.449E+01	0.446E+01	0.443E+01	0.440E+01	0.423E+01
GR.NO.	0.428E+06	0.512E+06	0.537E+06	0.485E+06	0.444E+06	0.453E+06	0.450E+06	0.488E+06	0.519E+06	0.543E+06	0.615E+06
HT/HB	0.124E+01	0.104E+01	0.876E+00	0.421E+01	0.389E+01	0.666E+01	0.286E+01	0.215E+01	0.199E+01	0.184E+01	0.139E+01
DE.NC.	0.785E+04	0.825E+04	0.830E+04	0.833E+04	0.836E+04	0.839E+04	0.843E+04	0.848E+04	0.853E+04	0.858E+04	0.889E+04
GR/RE2	0.563E-03	0.610E-03	0.632E-03	0.567E-03	0.515E-03	0.522E-03	0.514E-03	0.551E-03	0.579E-03	0.598E-03	0.632E-03
NU.NO.	0.150E+03	0.145E+03	0.141E+03	0.182E+03	0.203E+03	0.228E+03	0.195E+03	0.177E+03	0.166E+03	0.160E+03	0.153E+03
PW	0.902E+02	0.882E+02	0.858E+02	0.965E+02	0.107E+03	0.106E+03	0.107E+03	0.101E+03	0.967E+02	0.941E+02	0.925E+02

RUN NUMBER 514

	1	2	3	4	5	6	7	8	9	10	11
X/D	-0.532E+02	-0.778E+01	0.0	0.101E+02	0.201E+02	0.302E+02	0.402E+02	0.480E+02	0.558E+02	0.636E+02	0.934E+02
TB,F	0.771E+02	0.804E+02	0.810E+02	0.816E+02	0.825E+02	0.833E+02	0.840E+02	0.846E+02	0.852E+02	0.857E+02	0.879E+02
JHC	0.641E+02	0.645E+02	0.646E+02	0.756E+02	0.758E+02	0.803E+02	0.788E+02	0.735E+02	0.702E+02	0.691E+02	0.676E+02
RE.NO.	0.223E+05	0.233E+05	0.235E+05	0.237E+05	0.239E+05	0.241E+05	0.243E+05	0.245E+05	0.247E+05	0.248E+05	0.255E+05
PR.NO.	0.615E+01	0.586E+01	0.582E+01	0.576E+01	0.570E+01	0.564E+01	0.558E+01	0.554E+01	0.550E+01	0.546E+01	0.530E+01
GR.NO.	0.222E+06	0.260E+06	0.268E+06	0.253E+06	0.272E+06	0.278E+06	0.278E+06	0.293E+06	0.311E+06	0.322E+06	0.356E+06
HT/HB	0.104E+01	0.899E+00	0.780E+00	0.253E+01	0.305E+01	0.379E+01	0.277E+01	0.207E+01	0.191E+01	0.173E+01	0.141E+01
DE.NO.	0.441E+04	0.460E+04	0.464E+04	0.468E+04	0.472E+04	0.476E+04	0.481E+04	0.484E+04	0.487E+04	0.491E+04	0.504E+04
GR/RE2	0.445E-03	0.479E-03	0.487E-03	0.451E-03	0.477E-03	0.478E-03	0.470E-03	0.488E-03	0.512E-03	0.522E-03	0.547E-03
NU.NO.	0.136E+03	0.135E+03	0.134E+03	0.156E+03	0.156E+03	0.165E+03	0.161E+03	0.150E+03	0.143E+03	0.140E+03	0.135E+03
PW	0.812E+02	0.806E+02	0.801E+02	0.878E+02	0.840E+02	0.851E+02	0.877E+02	0.851E+02	0.821E+02	0.812E+02	0.803E+02

RUN NUMBER 515

	1	2	3	4	5	6	7	8	9	10	11
X/D	-0.532E+02	-0.778E+01	0.0	0.101E+02	0.201E+02	0.302E+02	0.402E+02	0.480E+02	0.558E+02	0.636E+02	0.934E+02
TB,F	0.775E+02	0.814E+02	0.821E+02	0.829E+02	0.838E+02	0.846E+02	0.855E+02	0.861E+02	0.868E+02	0.875E+02	0.900E+02
JHC	0.682E+02	0.692E+02	0.700E+02	0.836E+02	0.839E+02	0.904E+02	0.904E+02	0.842E+02	0.789E+02	0.767E+02	0.751E+02
RE.NO.	0.252E+05	0.265E+05	0.267E+05	0.270E+05	0.272E+05	0.275E+05	0.278E+05	0.280E+05	0.282E+05	0.285E+05	0.293E+05
PR.NO.	0.611E+01	0.579E+01	0.573E+01	0.567E+01	0.560E+01	0.554E+01	0.547E+01	0.543E+01	0.538E+01	0.533E+01	0.516E+01
GR.NO.	0.273E+06	0.324E+06	0.332E+06	0.307E+06	0.333E+06	0.339E+06	0.334E+06	0.354E+06	0.384E+06	0.403E+06	0.451E+06
HT/HB	0.105E+01	0.911E+00	0.790E+00	0.253E+01	0.304E+01	0.385E+01	0.281E+01	0.218E+01	0.203E+01	0.181E+01	0.149E+01
DE.NO.	0.498E+04	0.523E+04	0.527E+04	0.533E+04	0.536E+04	0.544E+04	0.549E+04	0.554E+04	0.558E+04	0.562E+04	0.579E+04
GR/RE2	0.429E-03	0.462E-03	0.466E-03	0.423E-03	0.450E-03	0.448E-03	0.433E-03	0.451E-03	0.482E-03	0.498E-03	0.525E-03
NU.NO.	0.145E+03	0.144E+03	0.146E+03	0.172E+03	0.172E+03	0.185E+03	0.184E+03	0.171E+03	0.160E+03	0.155E+03	0.149E+03
PW	0.863E+02	0.864E+02	0.867E+02	0.971E+02	0.927E+02	0.946E+02	0.993E+02	0.963E+02	0.911E+02	0.891E+02	0.880E+02

RUN NUMBER 522

	1	2	3	4	5	6	7	8	9	10	11
X/D	-0.532E+02	-0.778E+01	0.0	0.101E+02	0.201E+02	0.302E+02	0.402E+02	0.480E+02	0.558E+02	0.636E+02	0.934E+02
TB.F	0.633E+02	0.666E+02	0.671E+02	0.678E+02	0.686E+02	0.693E+02	0.700E+02	0.706E+02	0.711E+02	0.717E+02	0.738E+02
JHC	0.188E+02	0.218E+02	0.235E+02	0.240E+02	0.224E+02	0.241E+02	0.218E+02	0.154E+02	0.196E+02	0.193E+02	0.190E+02
RE.NO.	0.491E+04	0.514E+04	0.518E+04	0.523E+04	0.528E+04	0.533E+04	0.539E+04	0.543E+04	0.547E+04	0.551E+04	0.566E+04
PR.NO.	0.755E+01	0.718E+01	0.712E+01	0.704E+01	0.696E+01	0.689E+01	0.681E+01	0.676E+01	0.670E+01	0.664E+01	0.644E+01
GR.NO.	0.101E+06	0.952E+05	0.915E+05	0.102E+06	0.127E+06	0.131E+06	0.147E+06	0.170E+06	0.139E+06	0.145E+06	0.165E+06
HT/HB	0.767E+00	0.132E+01	0.113E+01	0.250E+01	0.604E+01	0.784E+01	0.608E+01	0.126E+01	0.143E+01	0.133E+01	0.101E+01
DE.NO.	0.971E+03	0.102E+04	0.102E+04	0.103E+04	0.104E+04	0.105E+04	0.106E+04	0.107E+04	0.108E+04	0.109E+04	0.112E+04
GR/RE2	0.417E-02	0.360E-02	0.341E-02	0.374E-02	0.456E-02	0.461E-02	0.507E-02	0.577E-02	0.464E-02	0.479E-02	0.514E-02
NU.NC.	0.389E+02	0.491E+02	0.526E+02	0.543E+02	0.500E+02	0.536E+02	0.484E+02	0.340E+02	0.431E+02	0.422E+02	0.411E+02
PW	0.226E+02	0.289E+02	0.310E+02	0.289E+02	0.241E+02	0.243E+02	0.226E+02	0.201E+02	0.253E+02	0.249E+02	0.244E+02

RUN NUMBER 528

	1	2	3	4	5	6	7	8	9	10	11
X/D	-0.532E+02	-0.778E+01	0.0	0.101E+02	0.201E+02	0.302E+02	0.402E+02	0.480E+02	0.558E+02	0.636E+02	0.934E+02
TB.F	0.629E+02	0.714E+02	0.728E+02	0.747E+02	0.766E+02	0.784E+02	0.803E+02	0.818E+02	0.832E+02	0.847E+02	0.902E+02
JHC	0.638E+01	0.930E+01	0.122E+02	0.229E+02	0.878E+01	0.633E+01	0.759E+01	0.956E+01	0.978E+01	0.108E+02	0.135E+02
RE.NO.	0.640E+03	0.718E+03	0.732E+03	0.750E+03	0.768E+03	0.787E+03	0.805E+03	0.820E+03	0.834E+03	0.849E+03	0.906E+03
PR.NO.	0.760E+01	0.668E+01	0.653E+01	0.636E+01	0.619E+01	0.603E+01	0.587E+01	0.576E+01	0.564E+01	0.553E+01	0.514E+01
GR.NO.	0.100E+06	0.159E+06	0.174E+06	0.101E+06	0.145E+06	0.215E+06	0.218E+06	0.210E+06	0.233E+06	0.230E+06	0.244E+06
HT/HB	0.777E-01	0.309E-01	0.356E-01	0.232E+02	0.230E+01	0.796E+00	0.238E+00	0.968E-01	0.195E+00	0.181E+00	0.668E-01
DE.NO.	0.126E+03	0.142E+03	0.145E+03	0.148E+03	0.152E+03	0.155E+03	0.159E+03	0.162E+03	0.165E+03	0.168E+03	0.179E+03
GR/RE2	0.245E+00	0.308E+00	0.324E+00	0.179E+00	0.245E+00	0.347E+00	0.336E+00	0.312E+00	0.335E+00	0.320E+00	0.297E+00
NU.NC.	0.148E+02	0.205E+02	0.267E+02	0.487E+02	0.186E+02	0.133E+02	0.158E+02	0.197E+02	0.200E+02	0.218E+02	0.263E+02
PW	0.825E+01	0.916E+01	0.936E+01	0.776E+01	0.864E+01	0.975E+01	0.971E+01	0.951E+01	0.978E+01	0.967E+01	0.959E+01

APPENDIX G

ERROR ANALYSIS

To determine the error in the calculated heat transfer coefficient, an error analysis (in the pattern suggested by Singh (7)) originally was performed. The analysis is as follows:

From Chapter V

$$h = \frac{\dot{q}''}{T_w - T_b} = f(\dot{q}'', T_w, T_b) \qquad (G\text{-}1)$$

or

$$dh = \frac{\partial f}{\partial \dot{q}''} \cdot d\dot{q}'' + \frac{\partial f}{\partial T_w} \cdot dT_w + \frac{\partial f}{\partial T_b} \cdot dT_b \qquad (G\text{-}2)$$

From Equation (G.1)

$$\frac{\partial f}{\partial \dot{q}''} = \frac{1}{T_w - T_n} \quad ; \quad \frac{\partial f}{\partial T_w} = -\frac{\dot{q}''}{(T_w - T_b)^2} \quad ; \quad \frac{\partial f}{\partial T_b} = \frac{\dot{q}''}{(T_w - T_b)^2}$$

Substituting in Equation (G-2)

$$dh = \frac{d\dot{q}''}{(T_w - T_b)} - \frac{\dot{q}'' dT_w}{(T_w - T_b)^2} + \frac{\dot{q}'' dT_b}{(T_w - T_b)^2}$$

or

$$\frac{dh}{h} = \frac{d\dot{q}''}{\dot{q}''} - \frac{dT_w}{(T_w - T_b)} + \frac{dT_b}{(T_w - T_b)}$$

To estimate the error in h, the error in the measurement of $\dot{q}''$, T_w and T_b will be estimated.

The error in the heat flux, $\dot{q}''$, depends upon the error associated with the primary measurements used to determine the heat flux. These measurements together with an estimate of their error are:

1. Test section current ± 1.0%
2. Test section voltage ± 1.0%
3. Test section dimensions ± 0.1%
4. Inside wall temperature ± 1.0%
5. Room temperature ± 0.5%

If all of the above mentioned measurements were in error to the extent indicated and in the same direction, Singh (7) reported a maximum error of 3.6% in heat flux.

From Appendix B, the calibration data on the bulk fluid and the wall thermocouples indicate that at an average temperature of 210^{o}F:

1. The bulk fluid thermocouples had an average correction of -0.8^{o}F.

2. The surface thermocouples on the test sections had an average correction of -0.25^{o}F.

The calibrations were performed using the Leeds and Northrup Numatron (with a digital readout) to measure the thermocouple outputs. The Numatron had a stated accuracy of ± 0.26^{o}F for the 0 to 300^{o}F range. Since the calibrations were made in-situ, the above mentioned corrections reflect the inaccuracies of Numatron and the associated thermocouples wires.

Based on the above data, the average error in the bulk fluid temperature and the surface of the test sections was estimated to be -0.38 and 0.18 percent, respectively.

Now, since the inside wall temperature was determined by a numerical solution, the average error in the wall temperature would be affected by the errors in the test section dimensions, the room

temperature, the flow rate and any computational errors. Taking all the errors into account, Singh (7) reported the combined total error in the inside wall temperature to be 1 percent.

Rewriting Equation (G-3)

$$\frac{dh}{h} = \frac{d\dot{q}''}{\dot{q}''} - \frac{(dT_w)/T_w}{[1-(T_b/T_w)]} + \frac{(dT_b)/T_b}{[(T_w/T_b)-1]} \qquad \text{(G-4)}$$

The average bulk fluid and inside wall temperature were estimated to $80^{o}F$ and $120^{o}F$, respectively.

The maximum error in the heat transfer coefficient would occur when the error in the independent variables are all additive.

Therefore,

$$\frac{dh}{h} = 0.036 + \frac{0.01}{[1-(80/120)]} + \frac{0.0038}{[(120/80)-1]} \qquad \text{(G-5)}$$

$$\frac{dh}{h} = 0.036 + 0.030 + 0.008$$

$$= 0.074$$

$$= 7.4\%$$

However, the most likely error in heat transfer coefficient is estimated to be about 3 percent.

In addition, a heat balance was made around the test sections for each experimental run. The average absolute percent error for runs with Reynolds number greater than 2100 was 3.06. However, for runs with Reynolds number less than 2100, the average absolute percent deviation was 18.73. The higher heat balance error for laminar flow

is due to error in measuring the exit bulk fluid temperature. As mentioned in Chapter III, the exit bulk fluid temperature was measured only at the center of pipe cross section. For laminar flow where there is no turbulent mixing the fluid temperature is highly nonuniform.

To verify that the measurement of the exit bulk fluid temperature is the source of error in heat balance, one of the experimental runs was repeated at the same condition (the same fluid, the same heat flux and the same room temperature) after a motionless mixer (for detail regarding the motionless mixers, see reference (23)) was placed upstream of the exit bulk fluid thermocouple. The motionless mixer reduced the heat balance error percent to 2.80%. Because the motionless mixer increased the pressure drop, it was removed from the test section. As a result of this test, the exit bulk fluid temperature was calculated from the measured inlet bulk fluid temperature, mass flow rate of test fluid, and the rate of electrical heat input through a heat balance. The calculated exit bulk temperature then was used for further calculations.

VITA 2

Mahmood Moshfeghian

Candidate for the Degree of

Doctor of Philosophy

Thesis: FLUID FLOW AND HEAT TRANSFER IN U-BENDS

Major Field: Chemical Engineering

Biographical:

Personal Data: Born in Shiraz, Iran, June 2, 1951, the son of Ali Akbahr and Johnbibi Moshfeghian.

Education: Granduated from Saadat High School, Bushehr and Razi High School, Shiraz, Iran, in 1970; received the Bachelor of Science degree in Chemical Engineering from Oklahoma State University in May, 1974; received the Master of Science degree in Chemical Engineering from Oklahoma State University in July, 1975; completed the requirements for Doctor of Philosophy degree at Oklahoma State University in May, 1978.

Professional Experience: Graduate teaching assistant; taught both graduate and undergraduate transport phenomena course and undergraduate course in chemical reaction engineering, School of Chemical Engineering, Oklahoma State University, 1974-78.

Professional Membership and Honors: Associate Member, American Institute of Chemical Engineers; member of Phi Eta Sigma; member of Tau Beta Pi (Sigma Tau); member of Omega Chi Epsilon; Oklahoma State University International Graduate Student-of-the-Year 1977-1978.